

**COMMERCIAL BUILDING FENESTRATION  
PERFORMANCE INDICES PROJECT**

**PHASE 1: DEVELOPMENT OF METHODOLOGY**

Prepared by

**Windows and Lighting Program  
Applied Science Division  
Lawrence Berkeley Laboratory  
University of California  
Berkeley, California 94720**

and

**Florida Solar Energy Center  
300 State Road 401  
Cape Canaveral, Florida 32920**

**December 30, 1988**

**Project Management by  
Lighting Research Institute  
345 East 47th Street  
New York, New York 10007**

This work was supported by the Electric Power Research Institute and the New York State Energy Research and Development Administration. Project Management was provided by the Lighting Research Institute. This work was also supported by the Assistant Secretary for Conservation and Renewable Energy, Office of Buildings and Community Systems, Building Systems Division of the U.S. Department of Energy under Contract No. DE-AC03-76SF00098.



## CONTENTS

1. Executive Summary .....	i
2. Introduction and Overview .....	1
2.1 Statement of Problem .....	1
2.2 Phase 1 Objective.....	1
2.3 Overall Project Goals.....	2
3. Fenestration Performance Analysis: Methodology.....	3
3.1 Background.....	3
3.2 Analysis and Experimental Procedures.....	4
3.2.1 Fenestration Systems.....	4
3.2.2 Measurement Systems.....	5
3.2.3 Solar Optical Properties.....	9
3.2.4 Thermal Comfort.....	19
3.2.5 Visual Comfort .....	22
3.2.6 Simulation .....	26
3.2.7 Performance Indices.....	31
3.2.8 Figure of Merit .....	40
4. Prototype Micro-Computer Design Tool.....	58
5. Phase 2 Recommendations .....	58
6. Summary and Conclusions.....	59
7. References .....	61
Appendix A: Thermal Comfort Analysis.....	62
Appendix B: Prototype Micro-Computer Design Tool.....	99



# COMMERCIAL BUILDING FENESTRATION PERFORMANCE INDICES PROJECT

## PHASE 1: DEVELOPMENT OF METHODOLOGY

### 1. Executive Summary Background/Problem statement

Many of our current national concerns are linked to the quality of our built environment. Energy use in buildings accounts for almost 40% of total U.S. consumption, a much higher fraction of U.S. electricity use, and requires expenditures of \$140 billion/year. Although we have made significant advances since the energy shocks of the early 1970s, if we compare our energy use to other industrialized nations we find that much of our energy consumption today is still unnecessarily wasteful. Energy waste has other unfortunate economic and environmental consequences. It diverts scarce economic capital to pay fuel bills or to invest in new energy supply infrastructure and it contributes directly to serious long-term adverse environmental effects such as global warming due to CO<sub>2</sub> emissions.

Substantial energy reductions can be achieved in the building sector. However, this will require the concerted action of tens of thousands of individual designers and decision makers, rather than a small number of centralized actions. It is clear that this can be achieved only if each decision maker is well informed, well equipped with proper tools to support the design process, and is strongly motivated to take effective action. Fortunately there are other sound reasons to pursue such strategies. Building design issues that influence energy use also affect the habitability of buildings. Many energy-related elements of the work environment (e.g. air quality, thermal and visual comfort) can raise or lower the level of satisfaction and productivity in our workplaces. In the increasingly competitive global markets, the resourcefulness and productivity of our workforce is important.

The design of buildings can be viewed as a complex, costly and risky undertaking. Unlike many other major industrial "products," such as automobiles and airplanes, which are designed, tested, refined and then mass-produced, most buildings are "one-of-a-kind" products. Numerous design decisions are needed to resolve the contradictory and conflicting criteria that influence building form and function. For example, to select glass transmittance in a curtain wall of an office building, one should consider the following important factors: view, privacy, thermal comfort from absorbed and transmitted sunlight, fixed and operable shading systems, the value of daylight in terms of color temperature and modeling effects, potential glare problems, electric lighting controls, acoustics, annual energy effects, peak demand and load shape, chiller size, etc. Furthermore, these

trade-offs must be considered not only in terms of instantaneous effects but over a full range of annual climatic conditions.

With unlimited time and resources a designer might be able to properly address many of these complex trade-offs. However, to meet deadlines, schedules and budgets, designers are frequently forced to make decisions on these issues without access to the proper expertise or analysis tools. Sometimes past experience is adequate to ensure at least a satisfactory, if not an optimal, solution to the problem at hand. However, far too frequently omissions and mistakes occur. Some are caught in later stages of design and are corrected at great cost; others are not uncovered until after the building is occupied and impose even higher costs on the building managers and occupants in terms of operating costs and/or productivity. Interestingly, one consistently hears of these problems in anecdotal form; there is little organized effort within the profession to critically examine both the successes and failures in occupied buildings and formally report the results back to practitioners. This virtually guarantees that many of these mistakes will be repeated in the future.

Over the last decade building designers have used many of the simplest approaches to replace inefficient design components with more efficient substitutes. Further significant reductions in energy use in buildings will occur only if more complex design strategies and more sophisticated hardware is specified and implemented. This approach, while potentially promising, raises the concerns described above in terms of the risks and the uncertainties of innovation with new building technology.

These risks and opportunities for building designers exist today in the design of fenestration and lighting systems. Lighting and cooling are identified as the most significant energy-related issues in new commercial buildings. The envelope of the building is a crucial contributor, both directly and indirectly, to lighting and cooling performance. Daylighting has emerged as a major design strategy that could lead to significant reductions in unnecessary energy use and also provide load shaping and demand reduction opportunities. However, the design of the envelope of a building is a complex task involving many trade-offs between competing alternatives. Furthermore, more detailed investigations of the overall impacts of daylighting strategies confirms that the non-energy impacts on design must also be carefully considered. Thermal and visual comfort, view, appearance, etc. are all fundamentally linked to energy-related decisions concerning fenestration and the building envelope. Unfortunately, there are no design tools available today that will allow a designer to address these interrelated concerns with confidence in a cost-effective and timely manner.

## **Project Objectives for Phase 1**

This project addressed the problem of providing better guidance to building designers on the set of complex, interrelated decisions regarding fenestration and its role in the building envelope. The long-term goal is to develop the capability to design a building envelope that is simultaneously responsive to concerns for efficient energy use while maximizing comfort and productivity. A key focus is the linkage between thermal and luminous elements of the interior environment. We expect that this capability would be imbedded in a state-of-the-art computer-based design tool. The immediate objective of this first phase of the project was to develop a methodology to determine the energy and comfort impacts of fenestration selection. This methodology was to address both thermal and daylighting effects as well as thermal and visual comfort, since there are no existing tools that do this today. Furthermore, current analysis procedures and tools allow only the simplest of fenestration systems to be analyzed. Therefore, a second important objective of this project was to develop a procedure for determining fenestration performance that would allow a wide range of glazing and shading systems to be accurately analyzed. These two objectives for the first phase were successfully achieved and are discussed in more detail in the body of the report.

## **Overview of Phase 1 Accomplishments**

In Phase 1 of this project we defined a design tool concept and developed the analytical and experimental methodologies required to achieve the overall project goal. We created five fenestration performance indices, which when combined with user-defined weighting factors yield a single figure of merit. Three indices relate to the effects of fenestration on building energy performance: fuel use, electricity use, and peak electricity demand. The two others relate to issues linked to productivity in work environments: thermal and visual comfort. This project represents one of the first attempts to develop a tool that directly links energy and comfort/productivity issues. The use of user-defined weighting factors to establish the relative importance of these seemingly "incompatible" elements allows the user, not the tool creators, to establish the balance between these issues on each particular project.

We derived index values and correlations to key window and lighting design parameters for each of the five factors from a large data base of building energy simulations. A modified version of the DOE-2 building energy simulation program was used to analyse a prototypical office building module to create the performance data base. Four glazing types and two shading devices were combined in several ways so that a representative sampling of realistic fenestration systems was analyzed.

Single-, double-, and triple-glazed windows incorporating clear, bronze-tinted absorptive, reflective and low-E glazings were studied both unshaded and with use of diffusing shades and venetian blinds. We used a recently developed scanning radiometer to measure the solar-optical properties of the angle-selective shading systems. Experimental data was collected and processed into a form that could be used in a modified version of the DOE-2 program for the hourly simulation process. Multiple regression procedures were then used to develop simplified algebraic expressions that related DOE-2 annual energy results to various fenestration and lighting configuration variables.

The complete methodology appears to provide a useful and powerful technique for architects, engineers and lighting designers to make quick yet accurate assessments of the benefits and costs of building envelope design decisions. Building owners, utilities, and state and local agencies with energy responsibilities will also eventually benefit from the new capabilities that this tool will provide to designers. However, the methodology developed in this project must first be extended into a practical, computer-based tool. We prepared a simple computerized mock-up of such a tool using preliminary results obtained in the study and demonstrated it to a number of potential users. This has helped clarify the needs and interests of tool users.

### **Directions for Phase 2 Tool Development**

In conjunction with other DOE-supported research on advanced computer-based design tools, we now have a much clearer concept for the future development of such a tool in Phase 2 of this project. The technical heart of the tool would be based on the experimental and analysis methodologies developed in Phase 1. The preferred implementation of the procedure would be a software package using a hypermedia-based user interface, using text, data, graphics, animation and sound. Hypermedia software implementation would allow a very large body of supporting information and data on fenestration design to be accessed in a nonlinear fashion as needed by the tool user. The tool would emphasize visually based approaches for its interface with the user (e.g., graphics and animation, and possibly video) as well as using the more traditional text and numerically based approaches of existing tools. In parallel with this project we have developed and tested prototype hypermedia-based design tools for other projects and are convinced that this approach offers new opportunities to capture the attention and interest of designers, to communicate results more efficiently, and to allow both quantitative and qualitative aspects of fenestration performance to be fully explored and understood. Development of such a tool should be a difficult, but highly rewarding challenge.

# COMMERCIAL BUILDING FENESTRATION PERFORMANCE INDICES PROJECT

## PHASE 1: DEVELOPMENT OF METHODOLOGY

### **2. Introduction and Overview**

#### **2.1 Statement of Problem**

The introduction of energy consumption as a major issue in the design of fenestration in today's office buildings brings about new complications and opportunities for lighting designers and architects. Daylighting can substantially reduce electric lighting requirements but solar gains must be carefully controlled to prevent cooling load penalties. Traditional design tools and design approaches are inadequate for the complexity of the problem. The energy interactions of fenestration are complex and very over time of day and time of year, often involving simultaneous beneficial and detrimental energy flows. Single design day methodologies may lead to poorly performing solutions, and traditional design experience does not always provide an intuitive sense of correct solutions. New analysis tools, from simple nomographs to detailed computer energy simulation codes that are now available to assist designers have shortcomings in practical design application. The simple tools, while convenient to use, do not account for all design parameters and generally provide rather crude answers. The more rigorous computer codes can account for all parameters and interactions, but their use is too time consuming and costly to be practical in most situations for comparing a number of options during conceptual design. Additionally, many fenestration options cannot be properly treated by computer simulation because solar-optical performance is either inadequate or non-existent. Designers must then generate designs based on a mix of partial analysis and guesswork. Thus there exists the need for a design tool that offers simplicity, convenience, and flexibility in use so that the designer might compare a number of options at any stage of the design process and have a high degree of predictive reliability.

#### **2.2 Phase 1 Objective**

In the first phase of this project, the objective has been to develop a design tool concept and a technical methodology to produce it and then to prove the concept and the methodology. Two fundamental problems, as previously described, had to be addressed in developing an approach to the problem. The design tool had to be developed so that its technical basis uses the most powerful analysis consistent with the problem and its use be simple, straightforward, and easily accessible to designers. Furthermore, the existing

information gaps relative to fenestration elements performance had to be filled in order for the technical analysis to be valid. The design tool had to give the designer flexibility in not only evaluating energy performance but in being able to assign relative importance to various performance issues. The designer is then able to exercise judgment in making decisions relating to the design objectives of the individual project.

The design tool concept evolved into the form of a series of indices related to specific issues of fenestration performance such as cooling loads, daylighting contributions, and comfort. The basic indices would be generated from results obtained from DOE-2 simulations. Since the first phase is limited to development and proof of concept, we chose to include a limited number of fenestration configurations, but ones sufficiently complex to prove the methodology.

### **2.3 Overall Project Goals**

The overall goal of this project is to produce a working fenestration design tool that allows a designer easily and accurately evaluate the potential performance of any fenestration design option. Phase 1 has developed the concept, demonstrated the viability of the concept and produced a prototype design tool. In subsequent phases the design tool will be revised and refined in response to user reactions and the data base will be expanded to include most fenestration configurations and products. This will require physical measurements of bidirectional transmittance values for a large number of physical configurations, and subsequent DOE-2 simulations and regressions analysis.

### 3. Fenestration Performance Analysis: Methodology

#### 3.1 Background

The development of a system of fenestration performance indices represents the distillation of LBL fenestration research that has been evolving over many years and is based on concurrent analytical and experimental procedures.

The energy performance of fenestration is an inherently complex process involving instantaneous flux variations, time delay phenomena, and interactions with the building lighting and HVAC systems. The multitude of interactive parameters influencing fenestration energy performance in buildings makes an all inclusive analysis formidable if not impossible. In order to isolate and systematically characterize the impacts of fenestration a series of sensitivity studies were made early in our research (Arasteh et al. 1985; Johnson et al 1986). These studies identified levels of importance for the various fenestration energy performance parameters. With this basis we were able to develop a prototypical building module and a parametric analysis procedure to systematically study fenestration and daylighting energy performance. These studies produced interesting and important results with regard to energy performance. Major trends in fenestration and daylighting performance were identified and characterized bringing about a better understanding of the complex issues involved and the existence of design optima peculiar to each specific situation. Through regression analysis the results of many DOE-2 simulations could be fit to functional forms with high degrees of reliability.

These results were of considerable use and importance from a research standpoint but did not yet fully meet the needs of designers for practical application because of certain major shortcomings. The results format did not lend itself to convenient evaluation of tradeoffs among prospective design options. The results encompassed energy performance only and did not evaluate issues of comfort and amenity. Performance data for complex shading systems was non-existent or unreliable and not accounted for. It was thus necessary to undertake new work to overcome these shortcomings and provide designers with a tool based on the most recent research.

A design tool based on a series of performance indices leading to comparative figures of merit was conceived as an approach to encompass the critical issues and allow the designer maximum flexibility in making trade offs and assigning relative levels of importance to each of the design criteria. To reach this objective required that a number of technical problems be resolved. It was necessary to generate hemispherical solar-optical transmittance, reflectance, and absorptance values (t-r-a) for any fenestration layer. These measured results then had to be used to calculate the net t-r-a for any combination

of layers. These values were then used as input to calculate daylight distribution and thermal transfer and building energy use was then simulated. Parametric simulations and subsequent regression analysis were then used to generate each of the various indices. The details of each of these procedures are described in the following sections.

## **3.2 Analysis and Experimental Procedures**

### **3.2.1 Fenestration Systems**

The objective of Phase I of this project was to develop a concept and a corresponding methodology and to prove them out. Therefore, no attempt was made to comprehensively cover the vast range of fenestration options, but rather to select a few options that, by presenting the generic difficulties likely to be found over the broad range of options, would test the limits of the concept and methodology.

Treatment of glazing materials is somewhat straightforward and measurement of their solar-optical properties is a well established procedure. Solar shading devices, however, while appearing to be very simple have very complex solar-optical properties which are highly dependent on incident angle. Depending on physical geometry there may be very abrupt transitions in the performance curves relative to incident angle. Also, transmitted daylight has very distinct directional properties that vary among devices having the same total transmittance. The problem in Phase I of this project was to select the minimum number of shading devices that would adequately test the procedures and uncover the potential problems that might be encountered with any other shading device. Two shading devices were initially selected to satisfy these criteria: a diffusing shade and a venetian blind with slats in a fixed position.

Diffusing shades are widely used and, if assumed to be perfectly diffusing, are relatively straightforward to model. Real shades are not perfectly diffusing. However, they provide a good point of reference in the project because their light output is relatively uniform and not subject to abrupt shifts as a function of incident angle. Measurement of solar optical properties and translation into functional form for subsequent simulations is thus simplified.

Venetian blinds are also widely used and present practically all of the problems that would be encountered with devices having a configuration made up of combinations of opaque and transparent elements. In any fixed slat position the transmittance is a distinct function of incident angle. The slat position can be varied from full open to full closed.

Opaque overhangs have been routinely modeled. Translucent overhangs, however, present problems that are not presently being handled well and are representative of a

variety of other shading devices such as awnings. Translucent overhangs have solar-optical properties related to both diffusing shades and fixed position slats but with unique properties, particularly related to daylight transmittance. We did not, however, model the shading device, but intend to do so during Phase II. diffusing shade and venetian blind.

Glazing materials were selected for Phase I to be representative of glazing characteristics in present use. We chose to include clear glass, tinted glass, reflective glass, and low-E coated glass in order to include the range of solar-optical glazing properties and their interaction with the shading devices.

### 3.2.2 Measurement Systems

A quantitative understanding of the solar-optical properties of fenestration systems is essential for accurate calculation of daylight illuminance levels, glare potential, solar heat gain and thermal comfort. For clear, tinted, or reflective glass, for each direction of incoming radiation there are only two specific directions of outgoing radiant flux: the direction of the transmitted radiation and the direction of the specularly reflected radiation. In this case, the solar-optical properties are expressed as simple functions of the incident angle of the incoming radiation. However, very little is known about the properties of fenestration systems that are optically more complex, such as systems that incorporate diffusing glass, venetian blinds, horizontal or vertical louvers, solar screens, etc. Here, for each direction of incoming radiation, there is a particular  $4\pi$  steradian solid angle distribution of outgoing radiant flux, either transmitted or reflected by the fenestration system. It is necessary to express the solar-optical properties as functions of both the incoming and the outgoing directions of the radiant flux to obtain a complete description of the radiant behavior of such complex fenestration components.

A scanning radiometer has been developed at the Lawrence Berkeley Laboratory for the purposes of determining solar and visible bidirectional transmittance and reflectance of fenestration components and systems of arbitrary complexity (Spitzglas 1986). The design specifications for the operational scanner prototype, as illustrated in Figure 3.2.2.1, are as follows:

1. A high resolution, wide dynamic range, short response time, single movable detector.
2. The detector is mounted inside a protective housing, and it is moved along a vertical arc within a  $180^\circ$  range, which in turn is pivoted to rotate in the horizontal plane to change positions within  $180^\circ$ .

3. The system has a stationary reference light-beam source, located 3.0 to 6.0 m (10 to 20 ft) from the target.
4. The maximum output area of the tested samples, located within the target plane, is 0.75 x 0.75 m (2.5 x 2.5 ft). However, for the purposes of this project, we used a 4 x 4 in output area.
5. Different illumination angles are produced through the rotation of the target frame, around its horizontal axis, combined with a 90° tilt freedom of the whole target plane against the vertical axis passing through the target center point.

The mechanical dynamics of the system and acquisition of the radiometric information are controlled by a microcomputer, using an incremental scanning control methodology with four stepper motors to control the above mentioned movements. In this control mode, the sensor is moved incrementally 15° in the horizontal direction, taking 120 measurements on every vertical scan.

Determining the bidirectional properties of actual fenestration systems through direct measurement allows us to avoid the assumptions about the geometry and the texture of fenestration components that are commonly used in mathematical modeling. However, various combinations of even the most common fenestration components can produce thousands of optically different fenestration systems. Measuring all such combinations is practically impossible; moreover, the scanning radiometer provides no information about the net absorptance of individual layers as they perform as parts of fenestration systems. The layer-by-layer absorption of solar radiation, which ultimately contributes to solar heat gain through re-conduction, is a complicated function of the distribution of the incident radiation and the nature of the interreflections between the fenestration layers.

A mathematical procedure is therefore required to determine the overall optical properties of a fenestration system from the properties of each individual layer. Papamichael and Winkelmann (1986) describes such a procedure. It is based on a matrix representation of the bidirectional properties of fenestration layers and systems. A computer program named TRA (Transmittance Reflectance Absorptance) was developed as an application of the method. The output of TRA serves as input to the daylighting calculation model SUPERLITE (Selkowitz, Kim, Navvab, and Winkelmann 1982; Modest 1982; Windows and Daylighting Group 1985) for determining daylight illuminance and luminance distributions, and as input to a heat transfer calculation program called WINDOW-2.0 (Rubin, Arasteh and Hartman 1986). Outputs from these two program

are then used within DOE-2 (Building Energy Simulation Group 1984 and 1985) for determining solar heat gain and daylighting characteristics. This approach, presented schematically in Figure 3.2.2.2 offers the capability to determine the hourly, seasonal, or annual luminous and thermal performance of fenestration systems of arbitrary complexity under varying environmental conditions, in an accurate and consistent way.

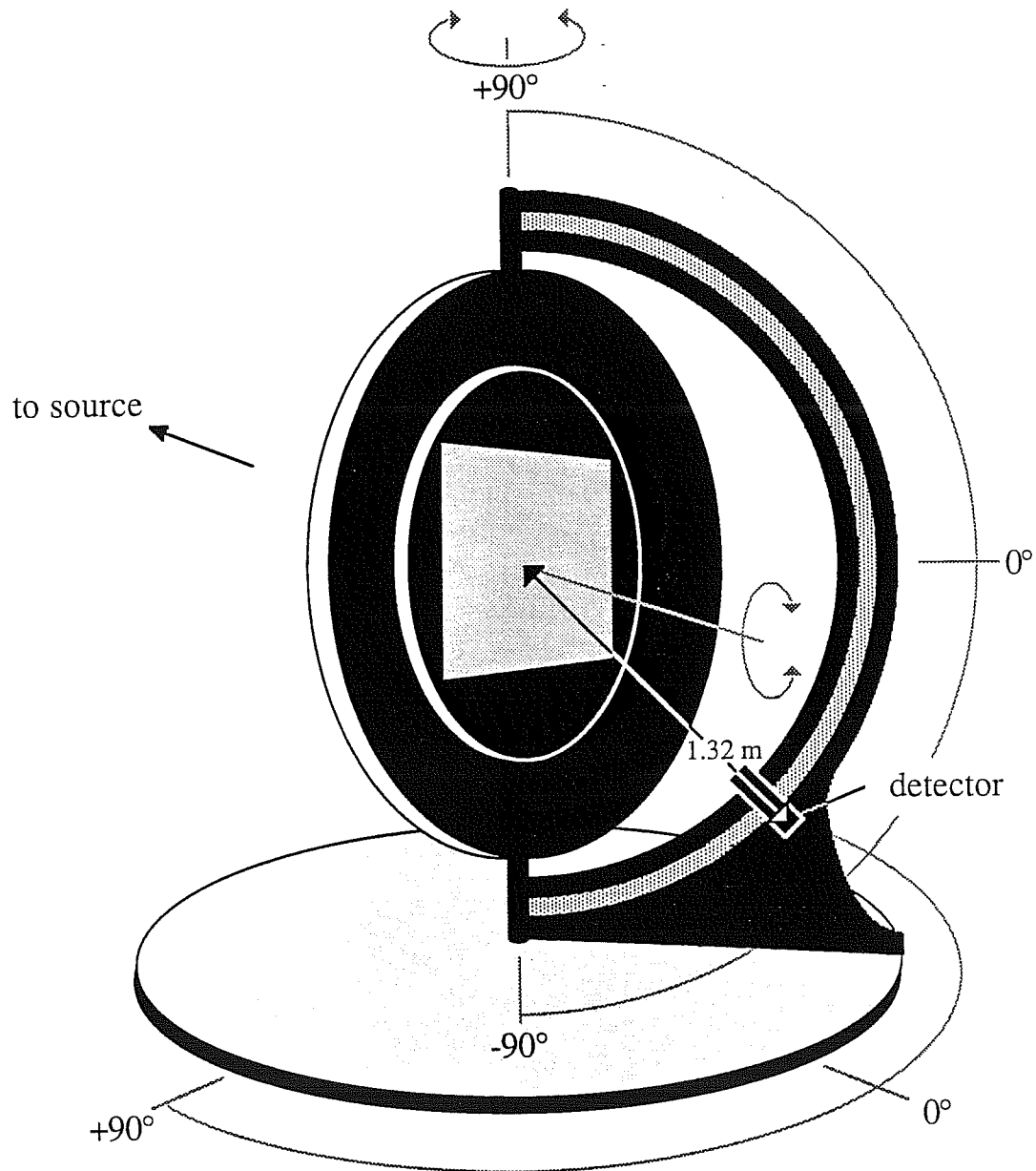


Figure 3.2.2.1. Schematic of the scanning radiometer.



### 3.2.3 Solar Optical and Thermal Properties

We created a revised version of DOE-2.1C specifically for use on this project. The solar optical and thermal conductance data for the shading devices and glass types used in the study were defined in addition to the development of a new procedure for analyzing triple glazing. We also created algorithms for calculating solar heat gain coefficients and visible transmittances that were subsequently used in our regression analysis.

In DOE-2.1C, the user has the option of specifying one of 33 glazing choices (11 glass type codes for single, double, or triple glazing). Of the 11 types, eight correspond to clear and tinted and three to reflective glasses. Each glass type code refers to different thicknesses, both glass and air-gap spacing. The data for the glass types, as presented in the DOE-2.1C User's Manual, consists of the U-value and transmittance of the glazing system at normal incidence. Polynomial expressions are available in the DOE-2.1C Engineer's Manual if users desire to determine the transmittance and absorptance as a function of the angle of incidence.

At the time this project started, these methods were in the process of being updated to take advantage of new experimental and analytical methods in determining the characteristics of glazings. We applied these new techniques to calculate transmittances and absorptances, gap resistances and interior film coefficients for the four glazings discussed in Section 3.2.1. The direct solar optical properties as a function of angle of incidence ( $\eta$ ) were fit to an equation of the form:

$$a_1 * \text{Cos}(\eta) + a_2 * \text{Cos}^2(\eta) + a_3 * \text{Cos}^3(\eta) + a_4 * \text{Cos}^4(\eta)$$

where the a's are regression coefficients that define the polynomial fit. The diffuse component was fixed at a constant value, using coefficient  $a_5$  as its indicator. A similar expression was used for the visible transmittance ( $\tau_v$ ) as a function of angle of incidence. Previously, it was assumed to behave the same as the solar transmittance ( $\tau_s$ ).

We added a third glazing layer, the middle layer, to the calculations involving triple glazing. Outer, middle, and inner pane and absorption coefficients for solar radiation used the same form of polynomial expression as above. Inclusion of the middle layer resulted in the following equation representing energy absorbed by the window:

$$Q_{\text{ABS}} = Q_{\text{DIR}}(N_{i-o}A_{r-o} + N_{i-m}A_{r-m} + N_{i-i}A_{f-i}) + Q_{\text{DIF}}(N_{i-o}A_{f-o} + N_{i-m}A_{f-m} + N_{i-i}A_{f-i})$$

where QDIR and QDIF are the incident direct and diffuse solar radiation components and the A's are the layer absorptances calculated by the polynomial expression with subscripts r and f referring to direct and diffuse components, The N's are inward flowing fractions and subscripts i, o, m referring to inner, middle, and outer layers which were

calculated using the resistance layers of the glazing as follows:

$$N_{i-o} = (R_o \cdot U_g)$$

$$N_{i-m} = (R_o + R_{a1} + R_{a2}) \cdot U_g$$

$$N_{i-i} = (R_o + R_{a2}) \cdot U_g$$

$R_o$  is the resistance of the outer pane,  $R_{a1}$  and  $R_{a2}$  are the resistances of the first and second air gap, and  $U_g$  is the overall U-value of the glazing.

Table 3.2.3.1 shows characteristics at normal incidence for each of the glazing systems and Table 3.2.3.2 presents the winter (cold, no sun) and summer (hot, sun) design conductances, interior film coefficients, and gap resistances. Table 3.2.3.3 through 3.2.3.7 present the above (a) coefficients for the solar and visible transmittance and absorption respectively.

We also revised the DOE-2.1C program to enable the generation of several new bin reports. These included hourly averages for each month of the year and an annual average for the glazing U-value, a solar heat gain coefficient, and visible transmittance. The solar heat gain coefficient was calculated using the following expression:

$$SHG = [(QTRANS + QABS) / (QDIR + QDIF)]$$

where QTRANS and QABS are the transmitted and absorbed solar radiation and QDIR and QDIF are the incident direct and diffuse components. Visible transmittance was determined using:

$$\tau_v = \tau_{\nu_T} [QDIR / (QDIR + QDIF)] + \tau_{\nu_D} [QDIF / (QDIR + QDIF)]$$

where  $\tau_{\nu_T}$  and  $\tau_{\nu_D}$  are the direct and diffuse transmission coefficients that are calculated hourly. Tables 3.2.3.8 and 3.2.3.9 present the annual averages for these parameters for each glazing and geographic location.

The TRA, SUPERLITE, and WINDOW computer programs were to be used for the shading systems as outlined on Figure 3.2.2.2 to develop equations similar to those above. At the time this report was prepared TRA was being revised and checked out and therefore we developed an alternative, although less accurate, method of testing the solar-optical properties of the diffusing shade and venetian blind. We could then proceed with the DOE-2 simulation runs and develop the indices and figures of merit of complete fenestration systems.

For the diffusing shade, we assumed that a shading coefficient and visible transmittance multiplier of the glazing transmittance characteristics would be adequate. The

solar-optical properties of the device therefore varied with angle of incidence in the same manner as did the particular glazing using the shade. A shading coefficient multiplier of 0.65 and visible transmittance multiplier of 0.35 were used in the analysis described in section 3.2.6.

A fixed multiplier, however, could not be used for the venetian blind. Instead, measured transmittances from an integrating sphere were used to derive polynomial expressions as a function of solar altitude and azimuth. Equations were generated for both sun and sky components. We assumed an absorptance level of 5% of the incoming radiation and also generated equations for this component. The following equation form was used:

$$A_1 + A_2 *AZ + A_3 *ALT + A_4 *AZ^2 + A_5 *ALT^2 + A_6 *AZ *ALT + A_7 *AZ^2 *ALT$$

where the A's, presented in Table 3.2.3.10, are the regression coefficients that define the fit and AZ and ALT are solar azimuth and altitude, respectively. This equation can be used to calculate hourly varying multipliers that can be used in a manner similar to that for the diffusing shade (which had a fixed multiplier). We did not make a revision to the DOE-2 program to enable the use of this methodology since changes to the program had already been made to utilize the techniques discussed earlier, which relied on scanning radiometer measurements.

Table 3.2.3.1  
Solar Optical Properties of Glass Types at Normal Incidence

Glass Type	$\tau_s$	$\tau_\nu$	$A_i$	$A_m$	$A_o$
Single Pane					
Clear	.775	.881	.154		
Bronze Tinted	.482	.534	.464		
Reflective	.220	.300	.600		
Pyrolytic Low-e	.690	.830	.210		
Double Pane					
Clear	.604	.781	.159	.120	
Bronze Tinted	.375	.473	.480	.075	
Reflective	.172	.268	.611	.034	
Sputtered Low-e	.480	.630	.169	.095	
Triple Pane					
Clear	.475	.696	.168	.127	.094
Bronze Tinted	.293	.421	.483	.080	.058
Reflective	.134	.239	.617	.036	.027
Sputtered Low-e	.376	.532	.175	.101	.075

Table 3.2.3.2  
Thermal Properties of Glass Types

Glass Type	Single Pane	
	U-Value (Btu/hr-ft <sup>2</sup> °F)	
	Winter	Summer
Clear	$1.46+.003*(0-T_o)$	$1.46-.008*(89-T_o)$
Bronze Tinted	$1.46+.003*(0-T_o)$	$1.59-.005*(89-T_o)$
Reflective	$1.09+.007*(0-T_o)$	$1.14-.004*(89-T_o)$
Pyrolytic Low-e	$1.09+.007*(0-T_o)$	$1.02-.007*(89-T_o)$

Glass Type	Double and Triple Pane							
	U-Value (Btu/hr-ft <sup>2</sup> °F) (with inside film)		$h_i=h_{ci}+h_{ri}$ (Btu/hr-ft <sup>2</sup> °F)		Gap Resistance (hr-ft <sup>2</sup> °F/Btu)		Gap Resistance (hr-ft <sup>2</sup> °F/Btu)	
	Winter	Summer	Winter	Summer	Winter	Summer	Winter	Summer
Double Pane								
Clear	.56	.68	(.60+.79)	(.60+.93)	1.08	.81		
Bronze Tinted	.56	.70	(.60+.79)	(.60+.94)	1.08	.78		
Reflective	.45	.54	(.58+.80)	(.57+.93)	1.50	1.18		
Sputtered Low-e	.37	.40	(.55+.81)	(.56+.92)	2.00	1.82		
Triple Pane								
Clear	.34	.45	(.54+.81)	(.61+.94)	1.14	.78	1.03	.70
Bronze Tinted	.34	.46	(.54+.81)	(.60+.94)	1.14	.75	1.03	.70
Reflective	.30	.38	(.53+.82)	(.56+.93)	1.59	1.15	1.02	.80
Sputtered Low-e	.26	.31	(.51+.82)	(.60+.94)	2.13	1.78	1.00	.70

Table 3.2.3.3

Solar Transmission Coefficients of Glass Types

Glass Type	Direct			Diffuse	
	a <sub>1</sub>	a <sub>2</sub>	a <sub>3</sub>	a <sub>4</sub>	a <sub>5</sub>
Single Pane					
Clear	2.4907	-2.6999	.8822	.1058	.699
Bronze Tinted	1.1852	-.7745	-.2868	.3610	.408
Reflective	1.670	-.4315	4.622	-1.759	.218
Pyrolytic Low-e	2.218	-2.404	.785	.094	.556
Double Pane					
Clear	.750	1.910	-3.924	1.874	.497
Bronze Tinted	.286	1.501	-2.598	1.190	.289
Reflective	.456	-.089	-.596	.402	.154
Sputtered Low-e	.592	1.508	-3.098	1.479	.392
Triple Pane					
Clear	.110	2.808	-4.293	1.850	.357
Bronze Tinted	.0047	1.6485	-2.2597	.8996	.207
Reflective	.126	.658	-1.244	.595	.111
Sputtered Low-e	.088	2.237	-3.420	1.474	.284

Table 3.2.3.4

Visible Transmittance Coefficients of Glass Types

Glass Type	Direct			Diffuse	
	a <sub>1</sub>	a <sub>2</sub>	a <sub>3</sub>	a <sub>4</sub>	a <sub>5</sub>
Single Pane					
Clear	3.086	-3.798	1.759	-.163	.809
Bronze Tinted	1.352	-.915	-.308	.407	.457
Reflective	2.275	-5.865	6.268	-2.381	.297
Pyrolytic Low-e	2.907	-3.578	1.657	-.154	.762
Double Pane					
Clear	1.343	1.484	-4.122	2.081	.668
Bronze Tinted	.454	1.739	-3.214	1.498	.378
Reflective	.826	-.496	-.534	.475	.240
Sputtered Low-e	1.266	1.398	-3.884	1.961	.630
Triple Pane					
Clear	.563	3.261	-5.666	2.543	.568
Bronze Tinted	.118	2.331	-3.566	1.541	.316
Reflective	.353	.870	-1.971	.992	.206
Sputtered Low-e	.535	3.100	-5.387	2.418	.532

Table 3.2.3.6

Inner Pane Absorption Coefficients of Glass Types

Glass Type	Direct				Diffuse
	a <sub>1</sub>	a <sub>2</sub>	a <sub>3</sub>	a <sub>4</sub>	
Double Pane					
Clear	.5661	-.9074	.6449	-.1835	.120
Bronze Tinted	.2413	-.2043	-.02843	.0668	.070
Reflective	.279	-.653	.628	-.220	.037
Sputtered Low-e	.448	-.718	.511	-.146	.095
Triple Pane					
Clear	.2081	.1177	-.4914	.2604	.086
Bronze Tinted	.076	.231	-.505	.257	.050
Reflective	.706	-.086	-.048	.055	.027
Sputtered Low-e	.166	.094	-.392	.207	.009

Table 3.2.3.7

Middle Pane Absorption Coefficients of Glass Types

Glass Type	Direct				Diffuse
	a <sub>1</sub>	a <sub>2</sub>	a <sub>3</sub>	a <sub>4</sub>	
Triple Pane					
Clear	.786	-1.635	1.487	-.512	.133
Bronze Tinted	.335	-.447	.151	.042	.077
Reflective	.366	-.955	.993	-.368	.041
Sputtered Low-e	.625	-1.300	1.183	-.407	.106

Table 3.2.3.5

Outer Pane Absorption Coefficients of Glass Types

Glass Type	Direct				Diffuse
	a <sub>1</sub>	a <sub>2</sub>	a <sub>3</sub>	a <sub>4</sub>	
Single Pane					
Clear	1.4906	-4.1071	4.5734	-1.8075	.169
Bronze Tinted	3.5358	-8.7505	9.1542	-3.4837	.486
Reflective	4.839	-13.346	15.041	-5.951	.591
Pyrolytic Low-e	2.014	-5.547	6.177	-2.442	.228
Double Pane					
Clear	1.8153	-5.1946	5.8349	-2.2986	.185
Bronze Tinted	4.0110	-10.3888	11.1296	-4.2815	.513
Reflective	5.507	-15.804	18.091	-7.204	.611
Sputtered Low-e	1.815	-5.195	5.835	-2.299	.197
Triple Pane					
Clear	1.8961	-5.4199	6.0733	-2.3871	.193
Bronze Tinted	4.1209	-10.628	11.3186	-4.3284	.526
Reflective	5.620	-16.109	18.386	-7.300	.621
Sputtered Low-e	1.975	-5.646	6.326	-2.486	.201

Table 3.2.3.8  
Annual Average Solar Heat Gain Coefficient of Glass Types

Glass Type	Lake Charles				Madison					
	N	S	E	W	N	S	E	W	Avg	
Single Pane										
Clear	.732	.731	.745	.740	.730	.732	.746	.741	.737	
Bronze Tinted	.533	.520	.544	.537	.525	.525	.539	.533	.531	
Reflective	.332	.325	.336	.332	.318	.322	.322	.320	.321	
Pyrolytic Low-e	.590	.604	.624	.618	.586	.619	.626	.620	.613	
Double Pane										
Clear	.588	.580	.607	.601	.587	.592	.610	.604	.598	
Bronze Tinted	.404	.396	.418	.411	.403	.404	.421	.413	.410	
Reflective	.224	.222	.230	.225	.224	.224	.230	.225	.226	
Sputtered Low-e	.410	.403	.424	.419	.409	.412	.427	.422	.418	
Triple Pane										
Clear	.487	.461	.487	.484	.484	.466	.488	.484	.481	
Bronze Tinted	.327	.320	.342	.335	.326	.329	.345	.338	.335	
Reflective	.166	.163	.171	.167	.165	.166	.172	.167	.168	
Sputtered Low-e	.303	.298	.318	.313	.302	.306	.321	.316	.311	

Table 3.2.3.9  
Annual Average Visible Transmittance of Glass Types

Glass Type	Lake Charles				Madison					
	N	S	E	W	N	S	E	W	Avg	
Single Pane										
Clear	.796	.787	.810	.807	.809	.798	.812	.809	.804	
Bronze Tinted	.449	.439	.457	.455	.457	.446	.460	.457	.453	
Reflective	.295	.295	.298	.297	.297	.298	.297	.297	.297	
Pyrolytic Low-e	.750	.741	.763	.760	.762	.752	.764	.762	.757	
Double Pane										
Clear	.655	.647	.675	.671	.675	.660	.679	.675	.667	
Bronze Tinted	.370	.361	.382	.379	.382	.369	.385	.382	.376	
Reflective	.242	.241	.247	.246	.247	.244	.247	.247	.245	
Sputtered Low-e	.617	.610	.636	.632	.636	.623	.640	.636	.629	
Triple Pane										
Clear	.548	.542	.572	.567	.572	.556	.577	.572	.562	
Bronze Tinted	.308	.301	.322	.319	.322	.310	.326	.323	.317	
Reflective	.202	.201	.209	.208	.209	.205	.210	.209	.207	
Sputtered Low-e	.520	.515	.543	.538	.543	.529	.548	.543	.535	

Table 3.2.3.10  
 Transmittance and Absorptance Regression Coefficients  
 for a Venetian Blind with a Fixed Slat Angle of 0°

	Transmittance		Absorptance	
	Sun	Sky	Sun	Sky
A <sub>1</sub>	.9765	.7211	.05297	.0605
A <sub>2</sub>	.001732	-.002525	-6.385 E-4	6.8374 E-4
A <sub>3</sub>	-.023873	-.006175	-6.385 E-4	5.5104 E-4
A <sub>4</sub>	-7.6015 E-5	1.03361 E-5	3.4645 E-5	-2.8570 E-6
A <sub>5</sub>	1.5268 E-4	3.2135 E-5	3.4645 E-5	-1.6266 E-6
A <sub>6</sub>	-2.2878 E-5	3.8124 E-5	-5.7972 E-5	-4.6834 E-6
A <sub>7</sub>	1.6204 E-8	-1.8025 E-9	2.0151 E-8	2.0945 E-10

### 3.2.4 Thermal Comfort

Specific studies relating commercial building fenestration system parameters to levels of thermal comfort have been performed only incidentally to the more general concerns of what defines thermal comfort in different environments. Because such explicit work relative to windows has not been performed, we have developed a new technique using past experimental evidence that will give an indication of expected comfort as a function of various window parameters. Appendix A contains a more exhaustive treatment of thermal comfort that includes an examination of the literature followed by the development of the technique used in the DOE-2 simulation program to calculate a thermal comfort index.

It is shown in Appendix A that the primary thermal comfort issue in commercial office buildings is related to the impact of windows as a source of high intensity direct solar radiation. Windows as a source of cold discomfort, although real under certain conditions, becomes a concern only for windows of a size greater than 60% of the wall area. Since, in our study, 60% represents the largest size window, we have not developed a comfort index for cold discomfort. However, the procedures outlined below which derive a comfort index for a high intensity source could also be used for a cold window. The same is true for warm windows. Experimental evidence on these configurations indicates that further investigations are necessary to verify the extreme temperature asymmetries currently deemed acceptable. This is particularly true because of the increased use of heat absorbing glass in some geographic locations.

For the high intensity solar source, a correlation was made of the magnitude of direct solar radiation coming through a window to the percentage of people dissatisfied, calculated in accordance with methods developed by Per Fanger in Ref. A.5. The amount of solar radiation was binned for the occupied hours during each DOE-2.1C simulation run. These values were then related to level of dissatisfaction. Table 3.2.4.1 shows the relationship between the particular bin and percent dissatisfied and a sample output is shown on Table 3.2.4.2. A comfort index was calculated using the following expression:

$$TC = \frac{\sum_{i=1}^{NB} X_i (1 - PPD_i)}{NB}$$

where X is the fractional percent hours at a solar level and PPD is the fractional percent dissatisfied at that level. Subscript (i) represents a summation over the the number bins (NB). The highest or best index value for thermal comfort is 0.95 since a 5% level of dissatisfaction is always apparent according to Fanger's studies. However, to simplify our analysis, for TC's greater than or equal to 0.95, we use the value 1.0. The lowest or

worst index is 0.0 for the case where 100% of the occupied hours have a solar radiation greater than 473 W/m<sup>2</sup> (150 Btu/hr-ft<sup>2</sup>). This condition, of course never occurs, and is only mentioned to assist in the understanding of the index concept.

A proportional relationship is used to account for window area variations under the assumption that the largest window corresponds to the largest level of discomfort. A relative comparison between fenestration systems is obtained using the minimum TC value and maximum window area as follows:

$$TC_n = 1.0 - \{ [(1-TC)/(1-TC_{min})] [A_g/A_{gmax}] \}$$

where A<sub>g</sub> is the window area and where TC<sub>n</sub> is the normalized comfort index and its value varies between 0.0 and 1.0. The calculated thermal comfort index was subsequently correlated with the solar heat gain coefficient.

The thermal comfort index did not show much variation with changing fenestration system parameters. The calculated TC varied from a low of 0.85 to a high of 1.0. Such a subtle change necessitates that additional indicators should be investigated in Phase 2 of this project.

Table 3.2.4.1  
Transmitted Direct Solar Radiation Bin Data and  
Corresponding Level of Dissatisfaction

Solar Bin W/m <sup>2</sup> (Btu/hr-ft <sup>2</sup> )	Percent Dissatisfied	Percent Dissatisfied *
567- (180- )	>76	100
473-567(150-180)	59-76	100
378-473(120-150)	43-59	70
284-378( 90-120)	28-43	50
189-284( 60-90 )	16-28	40
95-189( 30-60 )	7-16	20
63-95( 20-30 )	6- 7	10
32-63( 10-20 )	5- 6	10
3-32 ( 1-10 )	5	5
Less Than 3(1)	5	5

Note: (\*) The conservative PPD value was used in the analysis.



### 3.2.5 Visual Comfort

It was not necessary to perform as detailed an analysis for visual comfort as was done for thermal comfort. This is because the DOE-2.1C simulation program, as part of its daylighting calculation, already defines a glare index and it was not the intent of this study to develop new methodologies for evaluating glare. However, certain revisions were made to the the DOE-2.1C program to enable the determination of various alternative indices and also to facilitate the derivation of a weighted index similar to the above thermal comfort index. Four glare indices were generated on an hourly basis at two reference points in the space during the DOE-2.1C parametric runs. These indices were binned during the occupied hours and subsequently used to determine an overall glare index which was then defined as a function of fenestration system parameters. Table 3.2.5.1 shows the glare index bins and degrees of discomfort and Table 3.2.5.2 presents a sample output from a DOE-2.1C run. The glare indices calculated were as follows:

1. Cornell Formula (currently used in DOE-2.1C):

$$\text{Glare Index} = 10 \log G$$

where

$$G = \frac{L_s^{1.6} \Omega^{.8}}{L_b + 0.07 \omega .5 L_s}$$

where  $L_s$  is the source luminance;  $\Omega$  is the solid angle of the source modified for the position of its elements in the field of view;  $L_b$  is the luminance of the surroundings; and  $\omega$  is the solid angular subtense of the source at the eye.

2. IES Formula

$$\text{Glare Index} = 1.5 (10 \log G - 14)$$

where

$$G = \frac{L_s^{1.6} \Omega^{.8}}{L_b}$$

where  $L_s$  is the source luminance;  $\Omega$  is the solid angle subtense of the source modified for the position of its elements in the field of view; and  $L_b$  is the luminance of the surroundings.

### 3. MacGowan Formula:

$$\text{Glare Index} = 0.8 (L_s / L_t)$$

where  $L_s$  is the source luminance and  $L_t$  is the luminance of the task. In the DOE-2.1C runs, the task luminance was set equal to the input setpoint value at each reference point unless the calculated daylighting illuminance exceeded this value. In such a situation,  $L_t$  equals the value of daylighting illuminance multiplied by the task reflectance, which was taken to be 0.5.

4. Alternate Cornell Formula: This method uses the same expression as in (a) above, except that the glare index was set to 28 (the most unacceptable value) when the daylighting illuminance at the reference point exceeded 500 footcandles. This procedure was an attempt to take into account the effect of excessive direct solar radiation on the work plane.

DOE-2.1C outputs were examined for various window configurations and the decision was made to use the Cornell formula to define an overall glare index quantity. Since the MacGowan method does not account for window area changes and the alternate Cornell formula has not been widely verified by experiment, they were eliminated from consideration. The Cornell method yielded greater levels of discomfort than the IES formula and therefore represents the more conservative technique. The overall glare index was calculated as follows:

$$G = \sum_{i=1}^{NB} X_i (GI_i)$$

where  $X$  is the percent hours at a glare index level,  $GI$ . Subscript ( $i$ ) represents a summation over the number of bin ( $NB$ ). The glare index was subsequently correlated with the effective aperture of the window.

The visual comfort index, just as the thermal comfort index, did not show much variation for the different fenestration systems analyzed. Binning glare indices over the course of a year has a damping effect so that all systems are within a certain range between just perceptible and just acceptable. In Phase 2 of this project, we intend to investigate alternate glare indicator methods.

Table 3.2.5.1  
Glare Index Bin Data and Level of Dissatisfaction

Glare Index Bin	Degree of Discomfort
28-	Just intolerable
25-28	
22-25	Just uncomfortable
19-22	
16-19	Just acceptable
13-16	
10-13	Just perceptible
Below 10	

AKE CHARLES

SC=1.0 VIS=.8 NP=2 WMR=.30 UWALL=.05

TOTAL OCC HRS AT CORNELL GLARE INDEX, REF PT 1

HOUR	1AM	2	3	4	5	6	7	8	9	10	11	12	1PM	2	3	4	5	6	7	8	9	10	11	12	TOTAL	PCT	
28-	0	0	0	0	0	0	0	0	0	0	0	0	0	0	0	0	0	0	0	0	0	0	0	0	0	0	
25-	0	0	0	0	0	0	0	0	0	0	0	0	0	0	0	0	0	0	0	0	0	0	0	0	0	0	
22-	0	0	0	0	0	0	0	0	0	0	0	0	0	0	0	0	0	0	0	0	0	0	0	0	0	0	
19-	0	0	0	0	0	0	0	0	0	0	0	0	0	0	0	0	0	0	0	0	0	0	0	0	0	0	
16-	0	0	0	0	0	0	0	0	0	0	0	0	0	0	0	0	0	0	0	0	0	0	0	0	0	0	
13-	0	0	0	0	0	0	0	0	0	0	0	0	0	0	0	0	0	0	0	0	0	0	0	0	0	0	
10-13	0	0	0	0	0	0	0	0	0	0	0	0	0	0	0	0	0	0	0	0	0	0	0	0	0	0	
BELOW 10	0	0	0	0	0	0	0	251	251	251	251	251	251	251	251	251	251	251	152	0	0	0	0	0	0	2913	100
	0	0	0	0	0	0	0	251	251	251	251	251	251	251	251	251	251	251	152	0	0	0	0	0	0	2913	100

28-	0	0	0	0	0	0	0	0	0	0	0	0	0	0	0	0	0	0	0	0	0	0	0	0	0	0	
25-	0	0	0	0	0	0	0	0	0	0	0	0	0	0	0	0	0	0	0	0	0	0	0	0	0	0	
22-	0	0	0	0	0	0	0	0	0	0	0	0	0	0	0	0	0	0	0	0	0	0	0	0	0	0	
19-	0	0	0	0	0	0	0	0	0	0	0	0	0	0	0	0	0	0	0	0	0	0	0	0	0	0	
16-	0	0	0	0	0	0	0	0	0	0	0	0	0	0	0	0	0	0	0	0	0	0	0	0	0	0	
13-	0	0	0	0	0	0	0	0	0	0	0	0	0	0	0	0	0	0	0	0	0	0	0	0	0	0	
10-13	0	0	0	0	0	0	0	1	7	18	33	39	23	15	2	0	0	0	0	0	0	0	0	0	0	138	5
BELOW 10	0	0	0	0	0	0	0	251	250	244	233	218	212	228	236	249	251	251	152	0	0	0	0	0	0	2775	95
	0	0	0	0	0	0	0	251	251	251	251	251	251	251	251	251	251	251	152	0	0	0	0	0	0	2913	100

28-	0	0	0	0	0	0	0	0	0	0	0	0	0	0	0	0	0	0	0	0	0	0	0	0	0	0	
25-	0	0	0	0	0	0	0	0	0	0	0	0	0	0	0	0	0	0	0	0	0	0	0	0	0	0	
22-	0	0	0	0	0	0	0	0	0	0	0	0	0	0	0	0	0	0	0	0	0	0	0	0	0	0	
19-	0	0	0	0	0	0	0	0	0	0	0	0	0	0	0	0	0	0	0	0	0	0	0	0	0	0	
16-	0	0	0	0	0	0	0	0	0	0	0	0	0	0	0	0	0	0	0	0	0	0	0	0	0	0	
13-	0	0	0	0	0	0	0	0	0	0	0	0	0	0	0	0	0	0	0	0	0	0	0	0	0	0	
10-13	0	0	0	0	0	0	0	94	117	118	19	4	0	0	0	0	0	0	0	0	0	0	0	0	0	352	12
BELOW 10	0	0	0	0	0	0	0	157	134	133	232	247	251	251	251	251	251	251	152	0	0	0	0	0	0	2561	88
	0	0	0	0	0	0	0	251	251	251	251	251	251	251	251	251	251	251	152	0	0	0	0	0	0	2913	100

28-	0	0	0	0	0	0	0	0	0	0	0	0	0	0	0	0	0	0	0	0	0	0	0	0	0	0	
25-	0	0	0	0	0	0	0	0	0	0	0	0	0	0	0	0	0	0	0	0	0	0	0	0	0	0	
22-	0	0	0	0	0	0	0	0	0	0	0	0	0	0	0	0	0	0	0	0	0	0	0	0	0	0	
19-	0	0	0	0	0	0	0	0	0	0	0	0	0	0	0	0	0	0	0	0	0	0	0	0	0	0	
16-	0	0	0	0	0	0	0	0	0	0	0	0	0	0	0	0	0	0	0	0	0	0	0	0	0	0	
13-	0	0	0	0	0	0	0	0	0	0	0	0	0	0	0	0	0	0	0	0	0	0	0	0	0	0	
10-13	0	0	0	0	0	0	0	0	0	0	0	0	3	7	30	106	87	52	5	0	0	0	0	0	0	290	10
BELOW 10	0	0	0	0	0	0	0	251	251	251	251	248	244	221	138	122	152	147	0	0	0	0	0	0	0	2527	87
	0	0	0	0	0	0	0	251	251	251	251	251	251	251	251	251	251	251	152	0	0	0	0	0	0	2913	100

Table 3.2.5.2 Sample DOE-2 Bin Output Showing Glare Indices

### 3.2.6 Energy Simulation

This section of the report describes the building module that was used in the DOE-2.1C simulations and also describes the parametric set of runs that were made. Incremental changes were made to the module to facilitate a regression analysis that yielded simplified algebraic expressions for evaluating energy use and peak cooling requirements, effects due to daylighting, and thermal and visual comfort indices. Two WYEC weather profiles were used in the analysis: Madison, Wisconsin and Lake Charles, Louisiana.

The basic module consisted of four perimeter zones of identical geometry surrounding a central core zone, Figure 3.2.6.1. For modeling vertical windows, identical fenestration consisting of continuous strip windows was used in the exterior wall of each perimeter zone. In order to isolate the energy effects of interest, thermal transfers were selectively constrained. For fenestration studies, the important issue is the orientation-dependent flows through the exterior wall and window systems. For this reason, the floor and ceiling were modeled as adiabatic (i.e. no heat transfer) surfaces, which is a realistic assumption for multistory buildings. The walls at each end of the perimeter zones were also modeled as adiabatic surfaces in order to limit envelope effects to the fenestrated exterior wall. The envelope effects can thus be considered analogous to those in an individual office in a series of contiguous offices. Normal building thermal interactions included small transfers between core and perimeter. This interaction was accounted for by modeling thermal transfer through a conventional gypsum board partition wall.

The resultant load analysis was based on the use of zone coil-load comparisons. Ideally, the coil loads should somehow be independent of HVAC system type, but this was not possible because some type of system had to be simulated in order to obtain the loads. To isolate zone loads from the building system interactions, a separate single-zone system was assigned to each zone. Under these conditions, a simple constant-volume variable-temperature system was considered acceptable for determining coil loads in response to envelope design. Thus in the five-zone building, five separate single-zone constant-volume variable-temperature systems were simulated. In Phase 2 of this project, we intend to incorporate two additional HVAC systems in our analysis: a variable volume, constant-temperature system and a dual-duct fan system attached to the four perimeter zones. This will enable more general conclusions regarding the influence of fenestration on the performance of particular HVAC systems. The following paragraphs present a detailed description of the module.

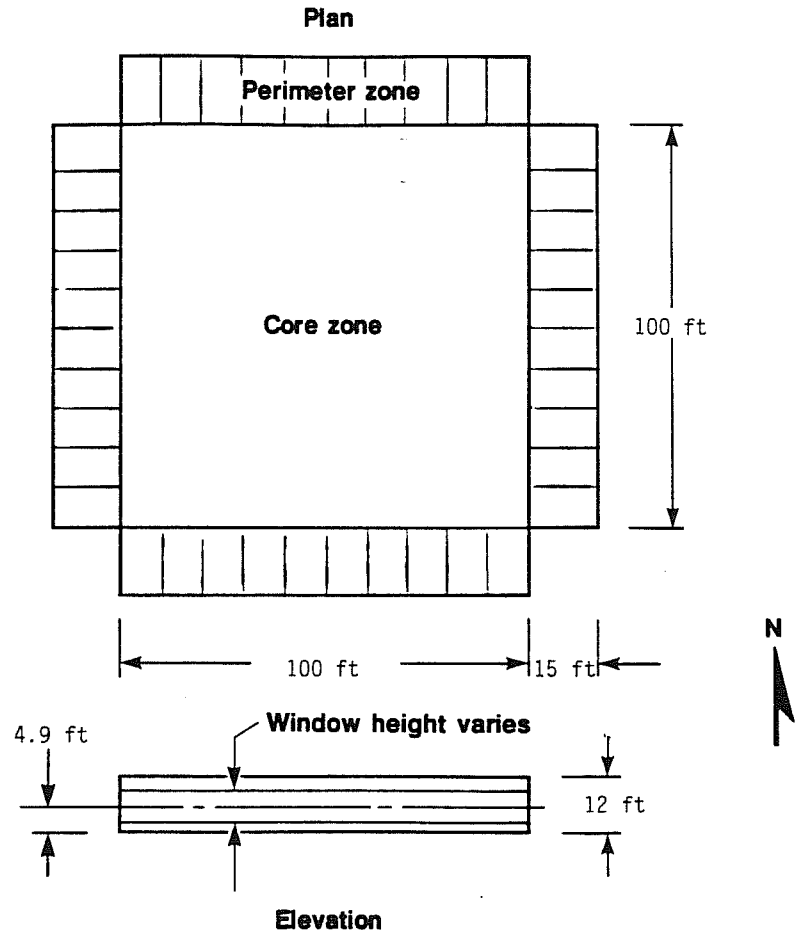


Figure 3.2.6.1. Plan of the representative office building module used in the DOE-2.1C simulations.

1. Site Conditions: Flat, unobstructed with no adjacent shading elements.
2. Architectural (see Figure 3.2.6.1):

Core zone: 100 ft x 100 ft; zone area=10,000 ft<sup>2</sup>.

Perimeter zones: Ten contiguous offices each 10 ft wide and 15 ft deep; zone area = 1500 ft<sup>2</sup>; total perimeter area = 6000 ft<sup>2</sup>.

Height: Floor to floor height of 12 ft; floor to ceiling height was 8.5 ft; plenum height was 3.5 ft. The DOE-2.1C input included the 8.5 ft conditioned space but excluded the plenum space. The exterior wall U-value was adjusted so the the UA was equivalent to that of the full 12 ft wall height. Infiltration values were similarly adjusted.

Partition walls: Stud wall with gypsum wall board on both sides. Surface visible light reflectance was 0.5.

Floors: Adiabatic surfaces consisting of carpeting over 4 in thick, 80 lb/ft<sup>3</sup> concrete slab. Surface visible light reflectance was 0.2.

Ceiling: Adiabatic surfaces consisting of acoustical tile and 4 in thick concrete slab. Surface visible light reflectance was 0.7.

Exterior wall: One hundred (100 ft) foot face of a no-mass quick wall with a U-value of 0.05 Btu/hr-ft<sup>2</sup>-F. Including the plenum wall surface area, this value changed to 0.07.

Fenestration: Continuous strip windows in the 100 ft exterior face, as seen on Figure 3.2.6.1. The glazed area was parametrically varied at 0, 15%, 30%, 45%, and 60% of the 12 ft high wall area. Four types of glazing were simulated: clear, absorptive, reflective, and low-e. Solar optical properties as well as glazing conductances were affected by these window types. In addition, thermal conductances corresponding to single, double, and triple pane windows was also a distinct parametric. Thus, the base set of window variations consisted of (5 sizes) x (4 types) x (3 U-values) or a total of 60 different window configurations.

Window management: The initial set of runs were made without an interior shading device. However, we did perform a number of simulations for an operable diffusing shade. The operable shades were deployed when the transmitted direct solar radiation exceeded 20 Btu/hr-ft<sup>2</sup>.

Exterior shading: None.

3. Electric Lighting:

Type: Fluorescent, evenly distributed.

Power density: 0.7, 1.7, 2.7 W/ft<sup>2</sup>.

Maintained level: 30, 50, 70 footcandles at each power density level.

Daylighting controls: None; Continuous dimming from full light output at 100% power to zero light at 10% power.

Daylighting control points: 5 and 10 ft in from the window, 30 in above the floor.

4. Building Operation:

Occupancy density: 100 ft<sup>2</sup>/person.

Equipment usage: 0.5 W/ft<sup>2</sup>.

Schedules (See Figure 3.2.6.2):

Occupancy: A modified version of SET standard profile number 1. The profile is shown on Figure 3.2.6.2.

Lighting: SET standard profile number 43 which is shown on Figure 3.2.6.2.

Equipment: Schedule corresponding to the occupancy schedule.

Infiltration: The infiltration schedule mirrored the fan schedule, i.e. infiltration at the specified rate when the fans were off and zero when the fans were on.

Infiltration rate: 0.6 air changes per hour.

5. HVAC System:

Type: Single-zone constant-volume variable-temperature system with economizer cycle in each zone.

Thermostat schedules:

Heating - Weekday hours 7 to 18: 72 °F; 19 to 6: 63 °F. Weekends and holidays, all hours: 63 °F.

Cooling - Weekday hours 7 to 18: 78 °F; 19 to 6: 90 °F. Weekends and holidays, all hours: 90 °F.

Fan schedules:

Weekday hours 7 to 18: on; 19 to 6: off. Weekends and holidays, all hours: off.

Night-cycle control: Fans cycle on during normally off periods when heating or cooling is required.

Humidity control: None.

Economizer limit temperature: 62 °F.

Outside air requirement: 5 ft<sup>3</sup> per minute per person.

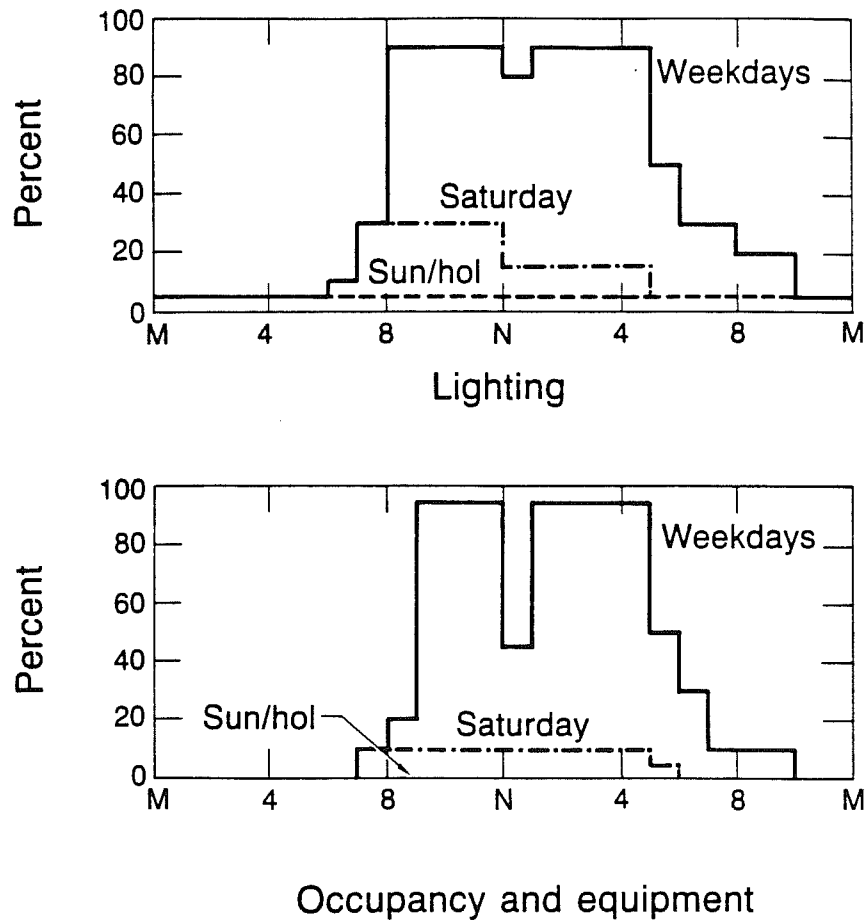


Figure 3.2.6.2. Occupancy, lighting, and equipment schedules of the modeled building.

### 3.2.7 Derivation of Performance Indices

We developed five performance indices each of which is a function of several fenestration system configuration variables. A regression analysis was performed on the DOE-2.1C parametric simulation data base and simplified algebraic expressions were derived that accurately predicted the simulation results. Multiple regression is an analytical technique for determining the best mathematical fit for a dependent variable as a function of many independent variables. The performance indices or dependent variables included three energy-related indices and two that dealt with thermal and visual comfort criteria. We envision the use of two indices: one directly related to the actual energy usage or comfort indicator and the other a non-dimensionalized index that varies between the values of 0 and 1 and represents the worst and best performers, respectively. Such a non-dimensionalizing scheme facilitates a more direct comparison of fenestration systems without regard to specific energy usage or comfort indicator amounts.

Energy-related indices are representative of annual fuel use (heating), annual electricity use (cooling, lighting, fan), and peak electrical demand. The fuel usage was obtained by applying a fixed furnace efficiency of 0.6 to the perimeter zone heating coil loads calculated by DOE-2.1C. Electricity usage and peak electric demand used a COP of 3.0 for calculating the cooling energy from the extraction rates. Such a procedure was necessary since the DOE-2.1C program does not separate the zonal energy at the plant level. The resultant regression expression used to predict these quantities was of the form:

$$\Delta E_i = \beta_{1i} \cdot U_g \cdot A_g + \beta_{2i} \cdot S_g \cdot A_g + \beta_{3i} \cdot k_d \cdot L \cdot A_f$$

where  $\Delta E$  is the incremental effect due to the fenestration system and subscript (i) refers to the particular energy-related index: fuel (therms), electricity (KWH), peak electric demand (W). The regression coefficients are denoted by  $\beta$  and the equation has three components chosen to contain the energy effects from a particular building component: conduction ( $U_g \cdot A_g$ ), solar radiation ( $S_g \cdot A_g$ ), and lighting ( $k_d \cdot L \cdot A_f$ ), where  $U_g$  is the overall conductance of the glazing,  $S_g$  is the solar heat gain coefficient,  $k_d$  is a daylighting correction term, and  $L$  is the lighting power density in watts per square meter.

We present the regression coefficients for the glazing only in Tables 3.2.7.1 through 3.2.7.3 and Tables 3.2.7.4 to 3.2.7.6 for the system using the diffusing shade for each orientation along with the multiple  $r^2$  values to indicate the goodness of fit (an  $r^2$  value of 1.0 represents a perfect fit). The configuration parameters are expressed in SI units, i.e.  $U_g$  ( $W/m^2 \cdot ^\circ C$ ),  $A_g$  ( $m^2$ ),  $L$  ( $W/m^2$ ),  $A_f$  ( $m^2$ ). An analysis of the regression terms shows

that they are reasonably physically consistent with expected building performance. When climate variables are not a factor, the regression coefficients are fairly constant over the range of climate types, i.e.  $\beta_3$  for electricity consumption and electrical peak. The regression coefficients for the solar gain and lighting terms in the fuel equation are both negative because they lower the heating load. For the electrical energy and peak terms,  $\beta_2$  rises with increasing solar gain. Thus by comparing coefficients, one can predict which loads are significant or insignificant. Non-dimensional indices are obtained by using the following equation:

$$I_{\Delta E_i} = 1.0 - [(\Delta E_i - \Delta E_{i_{\min}})/(\Delta E_{i_{\max}} - \Delta E_{i_{\min}})]$$

where  $\Delta E_{i_{\max}}$  and  $\Delta E_{i_{\min}}$  are the maximum and minimum values of the incremental energy quantities that result from the spectrum of fenestration systems analyzed.

The quantity (k) is the daylighting factor which is an exponential and varies between 0 and 1. It also was determined by a regression analysis and was found to be a function of visible transmittance ( $\tau\nu$ ), desired lighting level (C), and effective aperture ( $A_e$ ) which is the product of window-to-wall ratio and visible transmittance. Tables 3.2.7.7 and 3.2.7.8 show the regression coefficients used in the following expression:

$$k = 1.0 - [\phi_{1i} + \phi_{2i} (C/\tau\nu)] [1 - e^{(\phi_{3i} + \phi_{4i}C) A_e}]$$

where  $\phi$  are the regression coefficients. We found that there was no increase in the correlation ( $r^2$ ) by using distinct coefficients for each orientation. This is due to the general nature of the above expression in that it contains several configuration dependent terms ( $\tau\nu$ , C,  $A_e$ ), rather than just  $A_e$  which is normally used to predict the daylighting effect. In any case, the  $r^2$  values are satisfactory.

In section 3.2.4, we presented a normalized thermal comfort index which was calculated using the following:

$$I_{TC} = TC_n = 1.0 - \{ [(1-TC)/(1-TC_{\min})] [A_g/A_{g_{\max}}] \}$$

The DOE-2.1C calculated value of TC was predicted by using the newly developed solar heat gain coefficient,  $S_g$  (see Section 3.2.3) since this is a good measure of the amount of transmitted solar radiation and the TC index was generated using such bin data (see Section 3.2.4). An exponential was derived so that at a solar heat gain of zero, the index was at its maximum or most comfortable level of 1.0, and at large values of solar heat gain,

the index was at its lowest level or most uncomfortable, i.e.:

$$TC = \alpha_1 e^{\alpha_2 S_g}$$

Tables 3.2.7.9 and 3.2.7.10 show the regression coefficients, which are orientation-dependent.

The weighted annual glare indices (see Section 3.2.5) for the DOE-2.1C simulation runs were correlated with the effective aperture. This seems reasonable since the glare index is a function of luminance and solid angle values which are indirectly related to glazing transmittance and area. The following exponential expression was derived which yields the lowest or best glare index at zero effective aperture and its highest or worst index at large aperture values:

$$G = \delta_1 [ 1. - e^{\delta_2 A_e} ]$$

The coefficients are shown in Tables 3.2.7.11 and 3.2.7.12. The normalized glare index was calculated in a manner similar to the energy-related indices:

$$I_G = G_n = 1.0 - [ (G - G_{\min}) / (G_{\max} - G_{\min}) ]$$

We have shown the feasibility of condensing DOE-2 results to relatively simple, compact expressions, i.e. indices that dictate performance versus glazing properties. Other forms of equations might also be used to achieve the same results. However, the intent has been to define the process and not necessarily to derive an exact form. Also, although we did not perform DOE-2 simulations for the fenestration system that used the venetian blind, we feel that results similar to those above would be obtained from a simplification of a DOE-2 data base. There is the possibility that a non-linear incremental energy expression would be required. However, this complication does not present any difficulty for future design tool development.

Table 3.2.7.1

Regression Coefficients: Fuel in Therms (Heating)  
for Glazing-Only System (SI Units)

	Madison	Lake Charles
$\beta_1$	N	.519
	S	.319
	E	.318
	W	.365
$\beta_2$	N	-6.272
	S	-13.351
	E	-12.662
	W	-13.238
$\beta_3$	N	-0.0539
	S	-0.0343
	E	-0.0422
	W	-0.0406
$r^2$	.986	.973

Table 3.2.7.2

Regression Coefficients: Electric in KWH (Cooling+Lighting+Fan)  
for Glazing-Only System (SI Units)

	Madison	Lake Charles
$\beta_1$	N	2.302
	S	-.364
	E	.740
	W	1.038
$\beta_2$	N	114.934
	S	358.993
	E	360.203
	W	412.375
$\beta_3$	N	3.040
	S	3.233
	E	3.209
	W	3.160
$r^2$	.998	.998

Table 3.2.7.3

Regression Coefficients: Peak Electric in Watts (Cooling+Lighting+Fan)  
for Glazing-Only System (SI Units)

	Madison	Lake Charles
$\beta_1$	N	2.673
	S	.904
	E	2.155
	W	1.208
$\beta_2$	N	59.834
	S	256.569
	E	279.599
	W	279.174
$\beta_3$	N	1.282
	S	1.288
	E	1.269
	W	1.264
$r^2$	.998	.995

Table 3.2.7.4

Regression Coefficients: Fuel in Therms (Heating)  
for Glazing With Diffusing Shade (SI Units)

	Madison	Lake Charles
$\beta_1$	N	3.475
	S	3.279
	E	3.553
	W	3.587
$\beta_2$	N	-7.680
	S	-12.956
	E	-12.615
	W	-13.290
$\beta_3$	N	-.0540
	S	-.0408
	E	-.0492
	W	-.0468
$r^2$	.990	.975

Table 3.2.7.5

Regression Coefficients: Electric in KWH (Cooling+Lighting+Fan)  
for Glazing With Diffusing Shade (SI Units)

	Madison	Lake Charles
$\beta_1$	N	20.558
	S	6.747
	E	5.734
	W	4.625
$\beta_2$	N	12.368
	S	203.307
	E	225.700
	W	269.901
$\beta_3$	N	3.040
	S	3.188
	E	3.115
	W	3.202
$r^2$	.987	.993

Table 3.2.7.6

Regression Coefficients: Peak Electric in Watts (Cooling+Lighting+Fan)  
for Glazing With Diffusing Shade (SI Units)

	Madison	Lake Charles
$\beta_1$	N	2.092
	S	1.625
	E	1.316
	W	1.589
$\beta_2$	N	71.697
	S	171.707
	E	185.650
	W	191.522
$\beta_3$	N	1.283
	S	1.288
	E	1.287
	W	1.284
$r^2$	.995	.994

Table 3.2.7.7

Regression Coefficients: Daylighting (Lighting Correction Factor)  
for Glazing-Only System

	Madison	Lake Charles
$\phi_1$	.737	.737
$\phi_2$	-.000317	-.000263
$\phi_3$	-20.818	-27.521
$\phi_4$	.201	.266
$r^2$	.975	.981

Table 3.2.7.8

Regression Coefficients: Daylighting (Lighting Correction Factor)  
for Glazing With Diffusing Shade

	Madison	Lake Charles
$\phi_1$	.747	.757
$\phi_2$	-.000261	-.00033
$\phi_3$	-22.234	-28.149
$\phi_4$	.218	.271
$r^2$	.966	.975

Table 3.2.7.9  
 Regression Coefficients: Thermal Comfort Index  
 for Glazing-Only System

		Madison	Lake Charles
$\alpha_1$	N	1.0	1.0
	S	.981	.975
	E	.972	.961
	W	.965	.978
$\alpha_2$	N	0.0	0.0
	S	-.198	-.144
	E	-.123	-.097
	W	-.111	-.133
$r^2$		.868	.864

Table 3.2.7.10  
 Regression Coefficients: Thermal Comfort Index  
 for Glazing With Diffusing Shade

		Madison	Lake Charles
$\alpha_1$	N	1.0	1.0
	S	.968	.964
	E	.963	.961
	W	.948	.960
$\alpha_2$	N	0.0	0.0
	S	-.160	-.112
	E	-.095	-.083
	W	-.057	-.086
$r^2$		.708	.810

Table 3.2.7.11

Regression Coefficients: Visual Comfort Index  
for Glazing-Only System

	Madison	Lake Charles
$\delta_1$	12.798	13.075
$\delta_2$	-10.975	-13.203
$r^2$	.997	.998

Table 3.2.7.12

Regression Coefficients: Visual Comfort Index  
for Glazing With Diffusing Shade

	Madison	Lake Charles
$\epsilon_1$	12.001	12.495
$\epsilon_2$	-13.249	-14.580
$r^2$	.997	.998

### 3.2.8 Derivation of Figure of Merit

The final step in our task to evaluate the performance of fenestration systems and to establish a ranking procedure is to develop a "figure of merit" that combines all the previous index values into one number. The user can then directly compare the relative performance of the options being considered. We propose a procedure that gives the user the option of "customizing" the figures of merit for specific applications by assigning a weighting factor to each index. The figure of merit,  $F$ , would thus be derived from:

$$F = \sum w_i I_i$$

where  $w_i$  represents the weighting factors assigned to the performance indices,  $I_i$  (fuel, electric, peak electric, thermal and visual comfort). By making the sum of the weighting factors be equal to one, since the indices are expressed as values between zero and one, we also set the value of the figure of merit between zero and one. The best performer is the system with the highest figure of merit. This methodology is untested, of course, and awaits the evaluation of users. Other types of index value limits and types of weighting can be used, but, this simple technique illustrates the concept.

The procedure's versatility can be observed by considering an example. We desire to compare the performance of four glazings, two sizes, with and without daylighting and with and without diffusing shading for an east-facing perimeter zone fenestration system in Madison, WI. First we present the calculated performance indices, then show a series of "figures of merit" for various weighting schemes. The perimeter zone corresponds to the model described in Section 3.2.6. Important characteristics used in our evaluation are as follows:

1. Glazing types: Clear, bronze-tinted, reflective, low-E (all double pane)
2. Shading area: Diffusing shade
3. Window area:  $50 \text{ m}^2$  ( $540 \text{ ft}^2$ ) and  $25 \text{ m}^2$  ( $270 \text{ ft}^2$ )
4. Lighting power density:  $18.3 \text{ W/m}^2$  ( $1.7 \text{ W/ft}^2$ )
5. Lighting level: 538 lux (50 fc)

The resultant performance indices are shown in Figures 3.2.8.1 through 3.2.8.4 for the configuration without the shade and in Figures 3.2.8.5 through 3.2.8.8 with the shade. We present on a dual scale the actual energy and comfort levels as well as the nondimensional values between zero and one. The maximum and minimum values were determined by the defining best and worst performers for all module configurations used in the study. This includes variations due to orientation, window size, window type, use of daylighting, lighting power density and lighting level. Such a procedure would be used for each climate location.

The energy-related index values in Figures 3.2.8.1 to 3.2.8.3 and 3.2.8.5 to 3.2.8.7 are inversely related to usage or electrical peak demand quantities: an index of one is best, corresponding to least MWh or KW. Comfort indices in Figure 3.2.8.4 are proportional to the calculated annual average comfort levels. In viewing the indicated comfort values, one should note the extremely small range variation. Thermal comfort varies between a low of 84.7 % satisfaction level and an upper value of 95 %. The annual average IES glare index varies between the value zero, which occurs for no window and 12.74, which as indicated in section 3.2.5, is a degree of discomfort that is just perceptible. For both comfort indices, therefore, the performance range is quite small. We plan to refine this methodology in Phase 2 and develop comfort related indices which potentially may be more indicative of a comparative performance appraisal.

There is not much variation in the fuel use index among the different glazings analyzed. This is also true for configurations utilizing daylighting and the diffusing shade. The best performer for heating is the low-E unit followed by clear glazing. Madison is a heating-dominated location; one would therefore expect glazing conductance to be important. There are distinct differences, however, among glazings, daylighting, and shade management when considering cooling energy and peak demand. The diffusing shade tends to mitigate the observed variations between glazing types as would be expected since the overall radiation transmitted has decreased for all systems.

Figures 3.2.8.9 and 3.2.8.10 show results that use equal weighting for the performance indicators. A 20 % weighting factor was applied to each of the five indices. This type of weighting tempers the observed effect of daylighting apparent in the indices themselves. Figures 3.2.8.11 and 3.2.8.12 show evenly distributed weighting for only the energy-related indices. Here, the fuel index variation with glazing type is somewhat opposite to the electric and peak variation, resulting in an almost constant figure of merit for each condition for the glazing types analyzed. Figures 3.2.8.13 and 3.2.8.16 are cost-based weighting results. The three energy related indices have been weighted by maintaining a fixed ratio of the cost of electricity to gas (\$0.07/KWh for electricity and \$0.60/therm for gas results in a ratio of 3.5) and then varying the magnitude of the peak demand index between two extremes (10 % and 70 %). Since fuel costs are lowest, the figures of merit tend to approach the electric index and peak index values respectively for the figures.

# Fuel Index

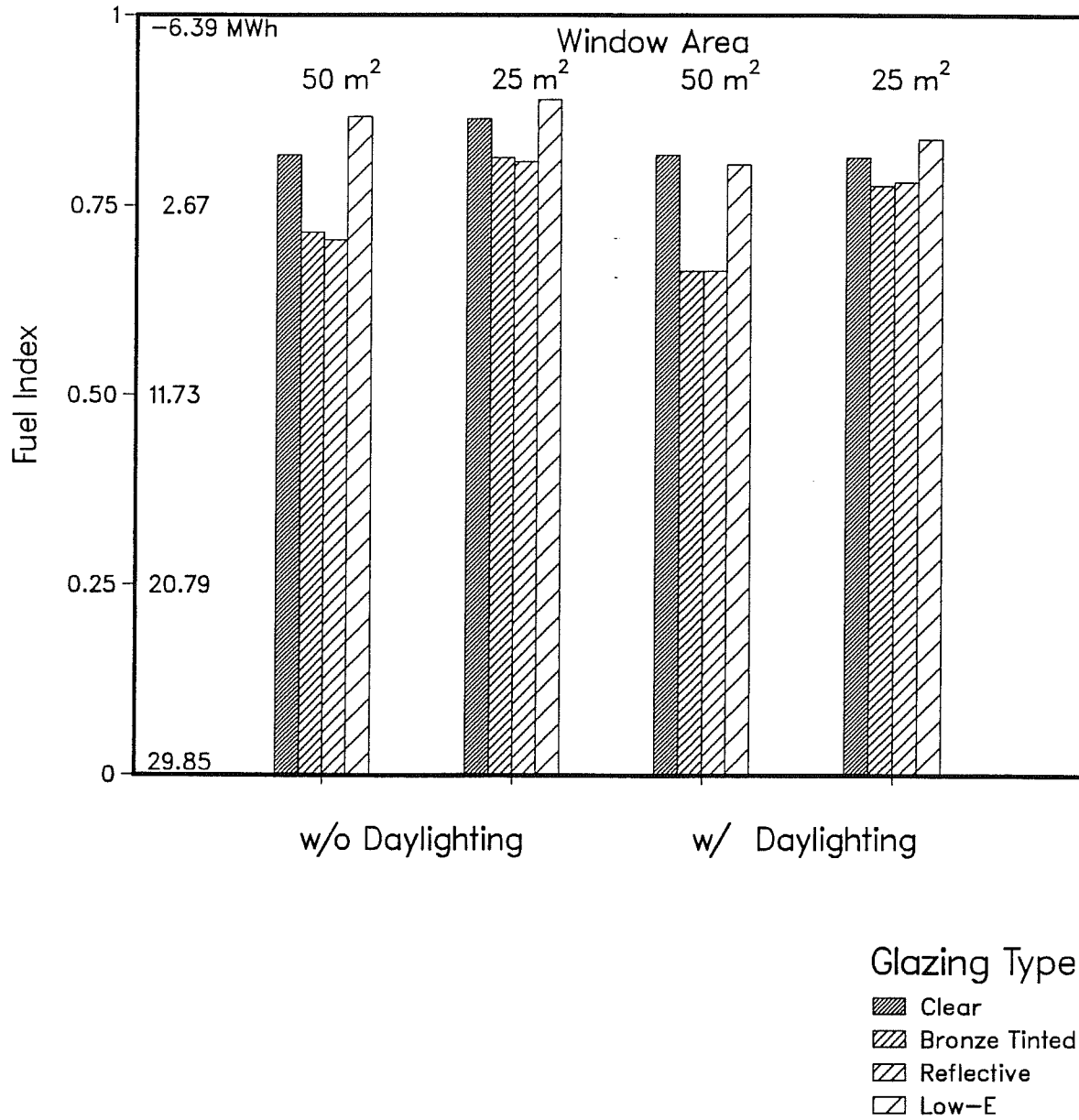


Figure 3.2.8.1. Fenestration performance indices for annual fuel consumption for an office building module in Madison, WI, without a diffusing shade.

## Electric Index

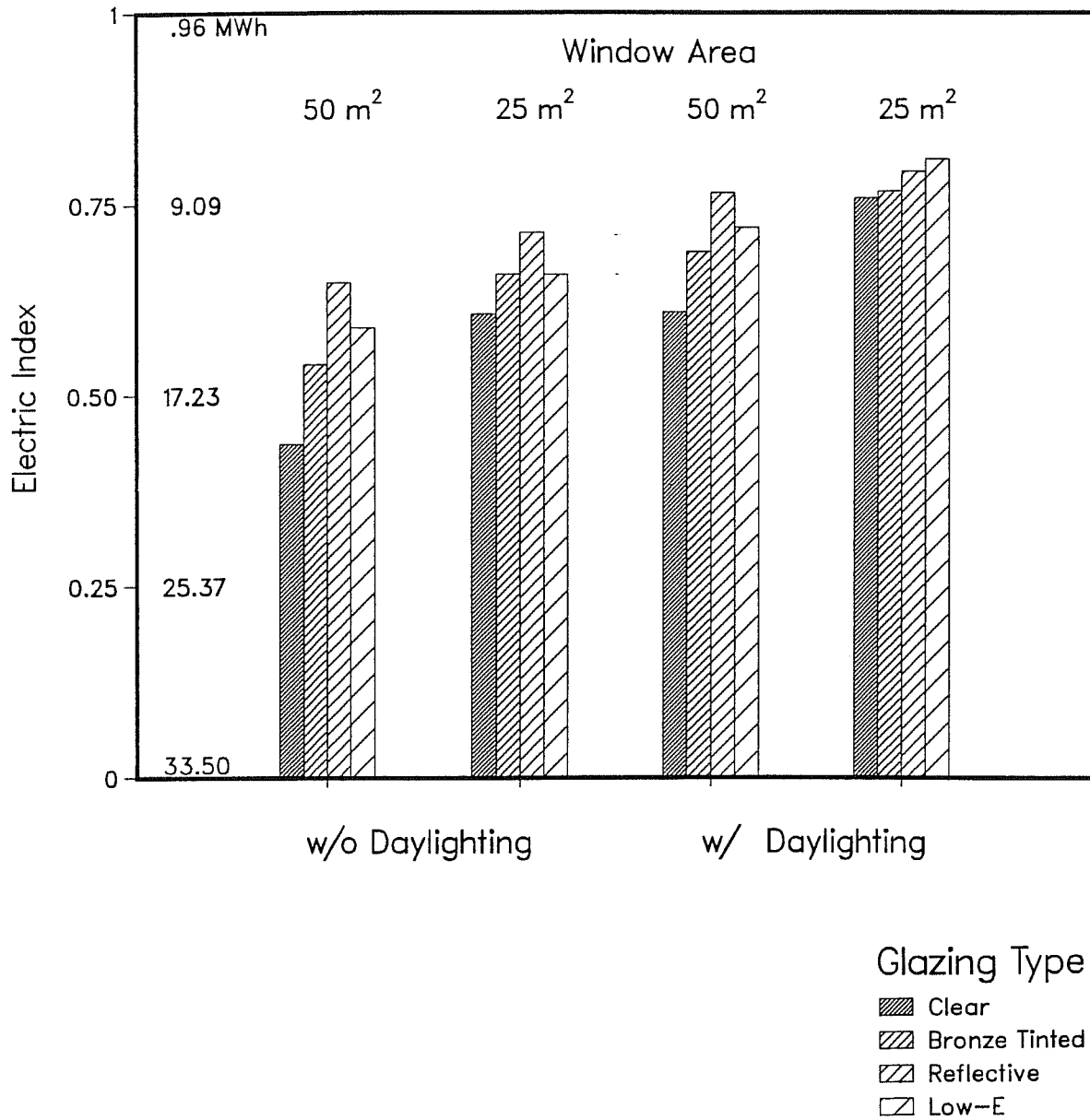


Figure 3.2.8.2. Fenestration performance indices for annual electric consumption for an office building module in Madison, WI, without a diffusing shade.

## Peak Electric Index

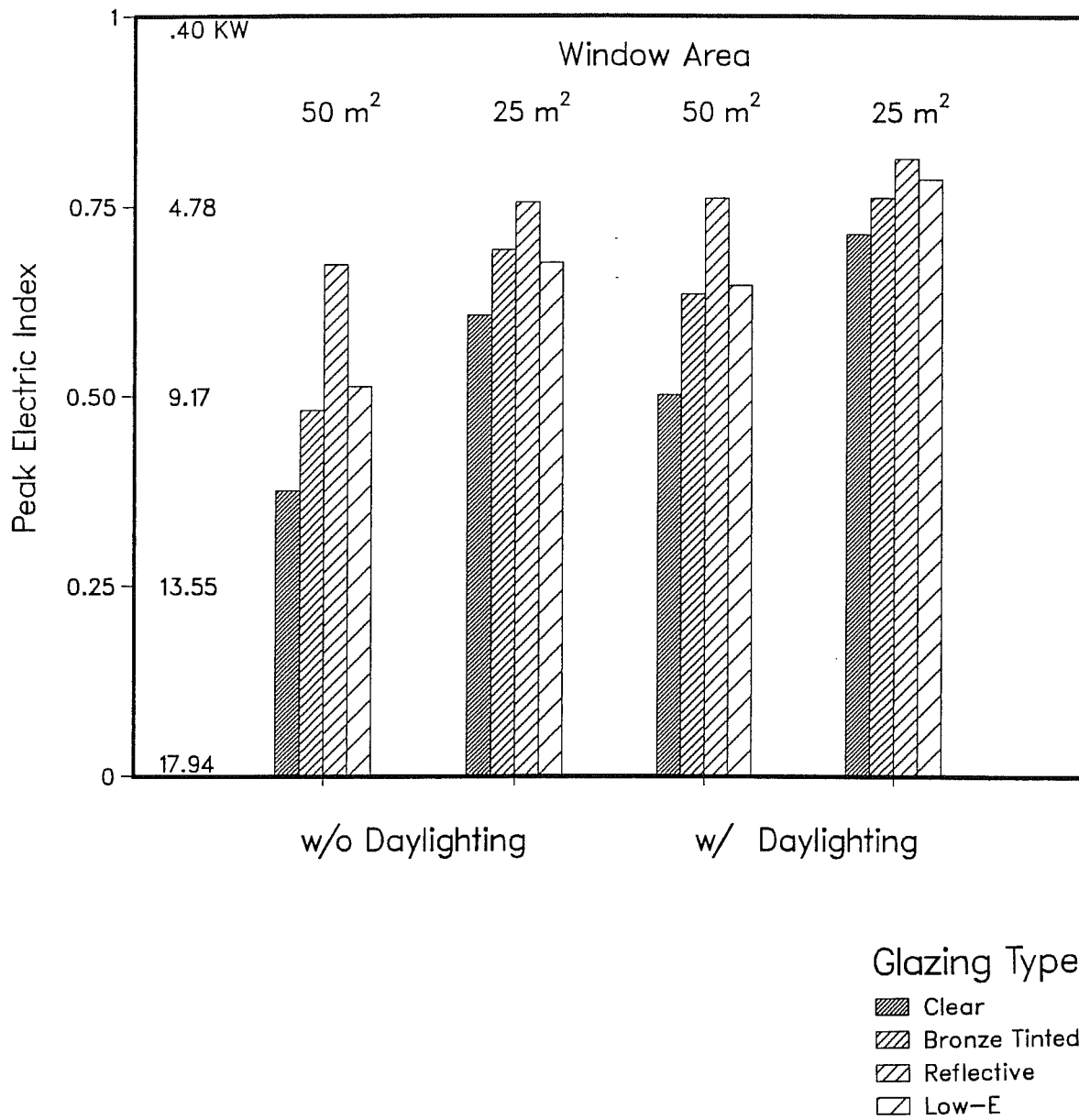


Figure 3.2.8.3. Fenestration performance indices for peak electrical demand for an office building module in Madison, WI, without a diffusing shade.

## Comfort Indices

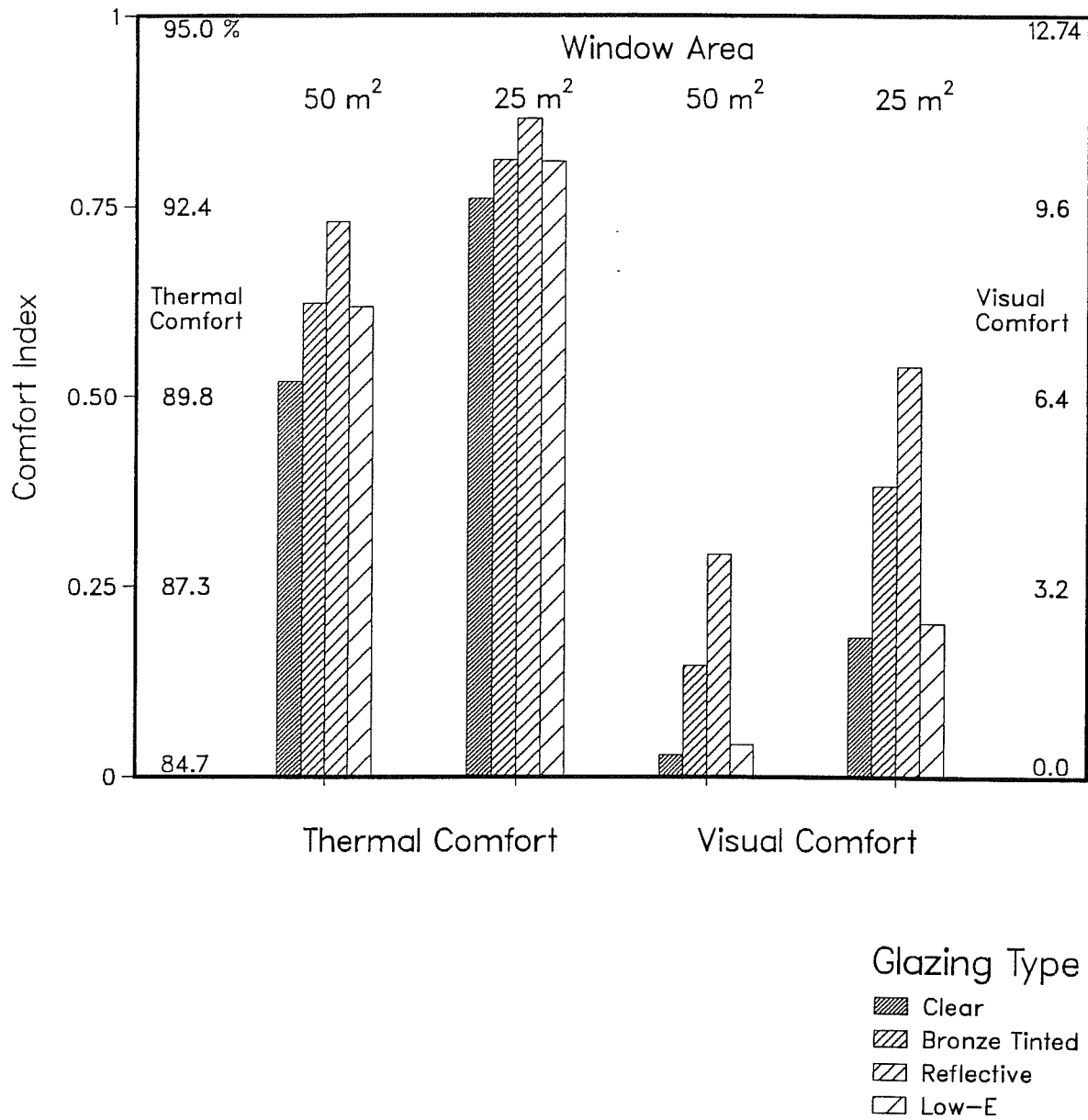


Figure 3.2.8.4. Fenestration performance indices for thermal and visual comfort for an office building module in Madison, WI, without a diffusing shade.

## Fuel Index With Diffusing Shade

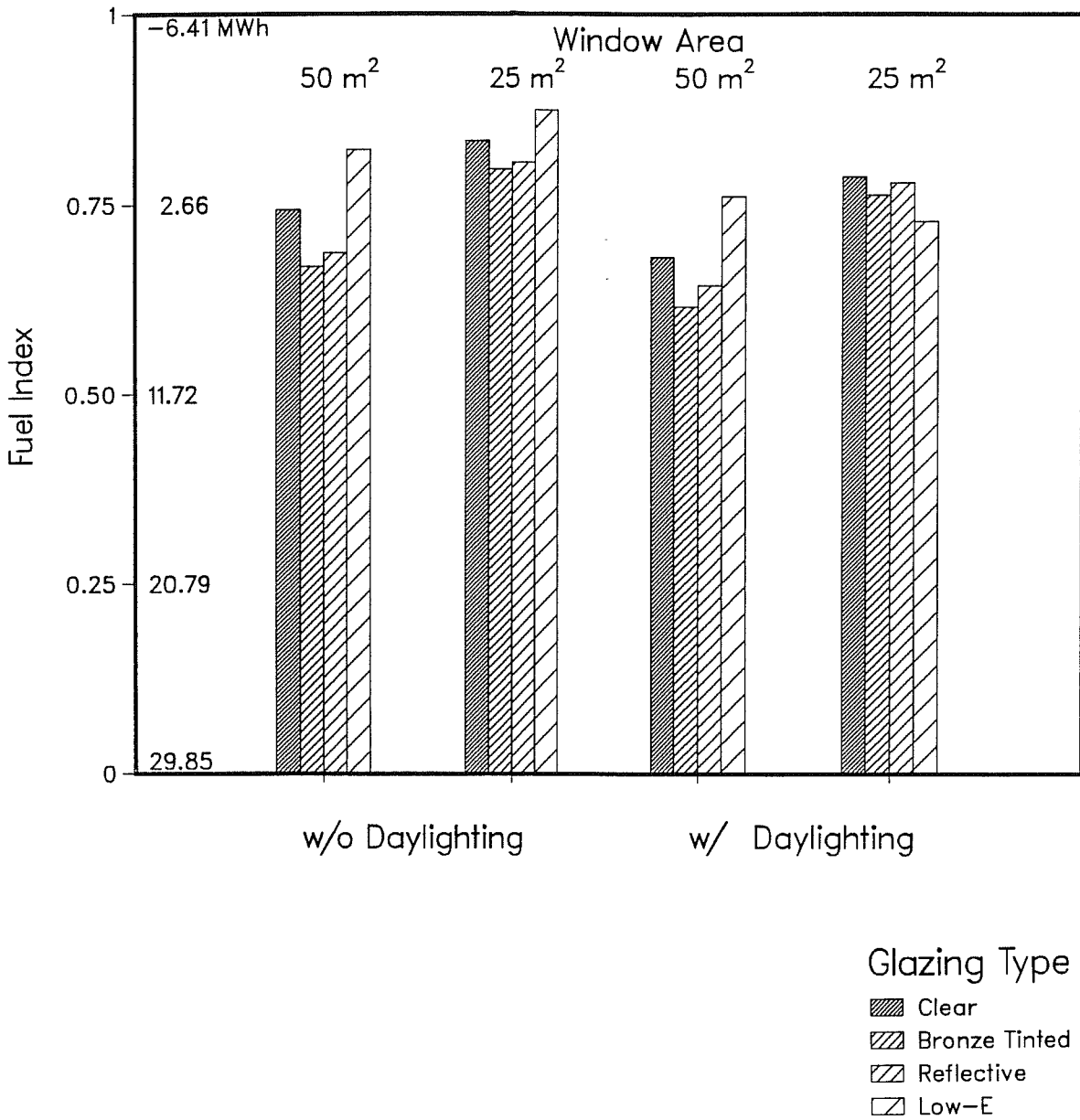


Figure 3.2.8.5 Fenestration performance indices for annual fuel consumption for an office building module in Madison, WI, with a diffusing shade.

### Electric Index With Diffusing Shade

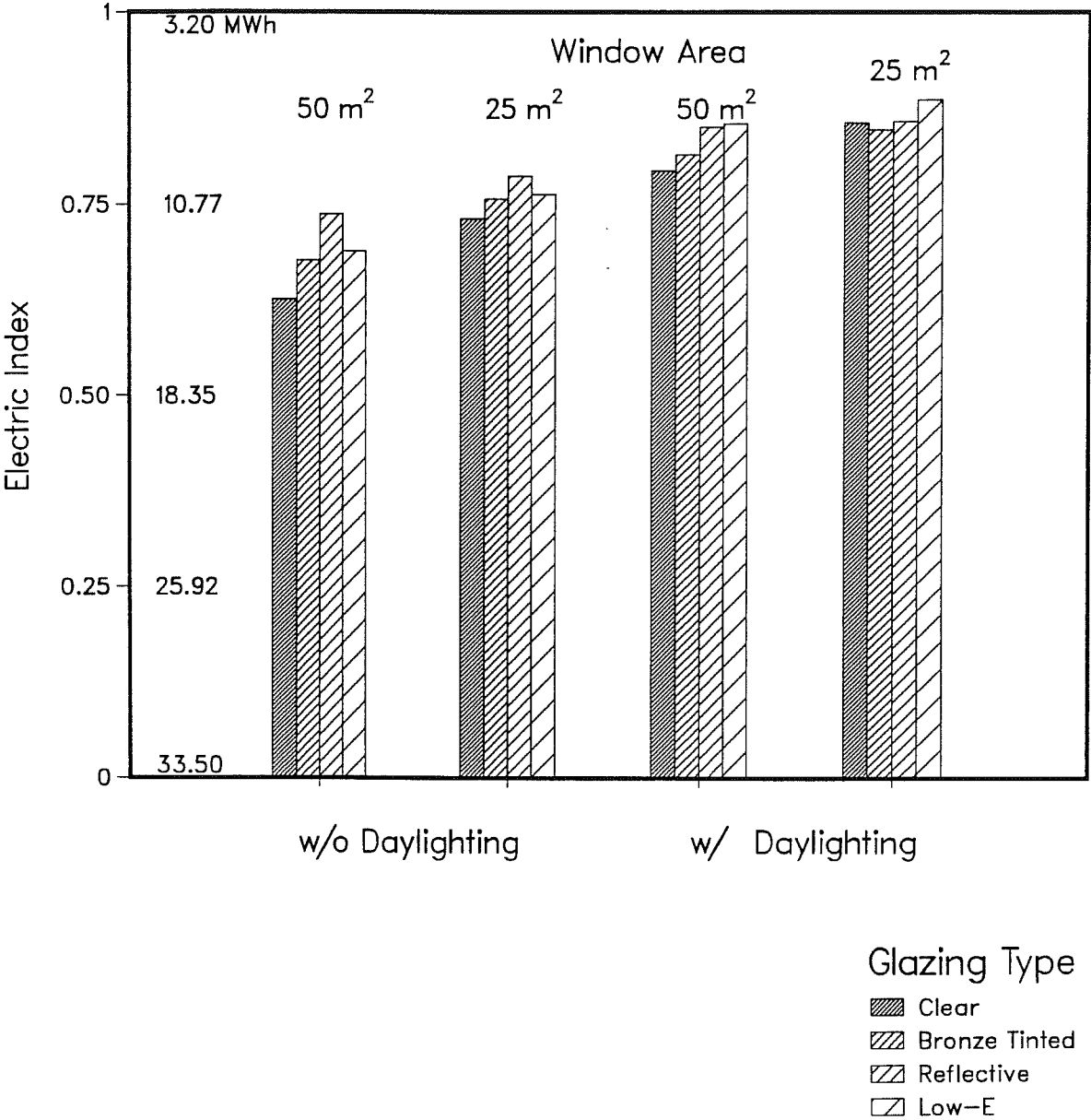


Figure 3.2.8.6 Fenestration performance indices for annual electric consumption for an office building module in Madison, WI, with a diffusing shade.

### Peak Electric Index With Diffusing Shade

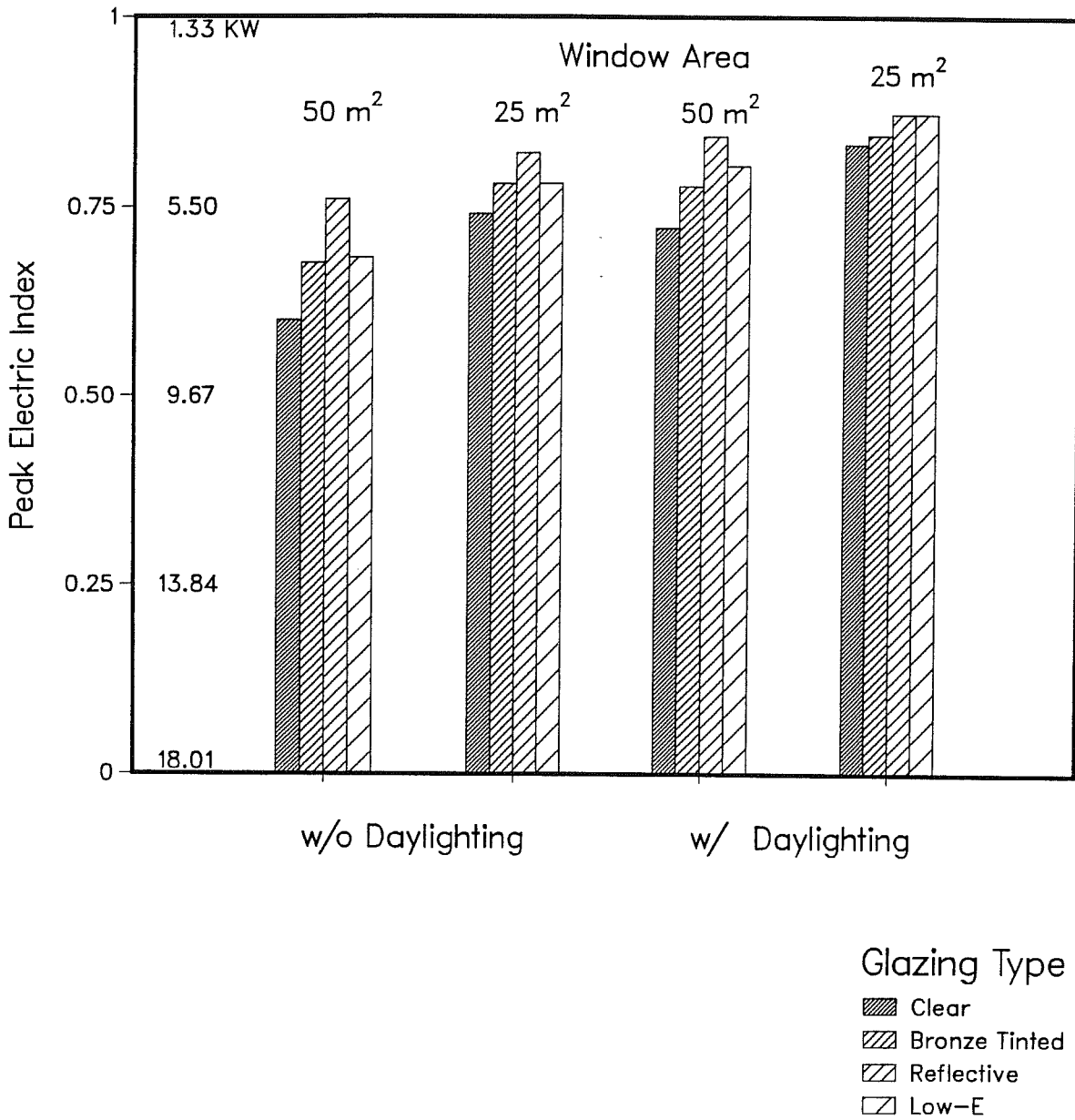


Figure 3.2.8.7. Fenestration performance indices for peak electrical demand for an office building module in Madison, WI, with a diffusing shade.

## Comfort Indices With Diffusing Shade

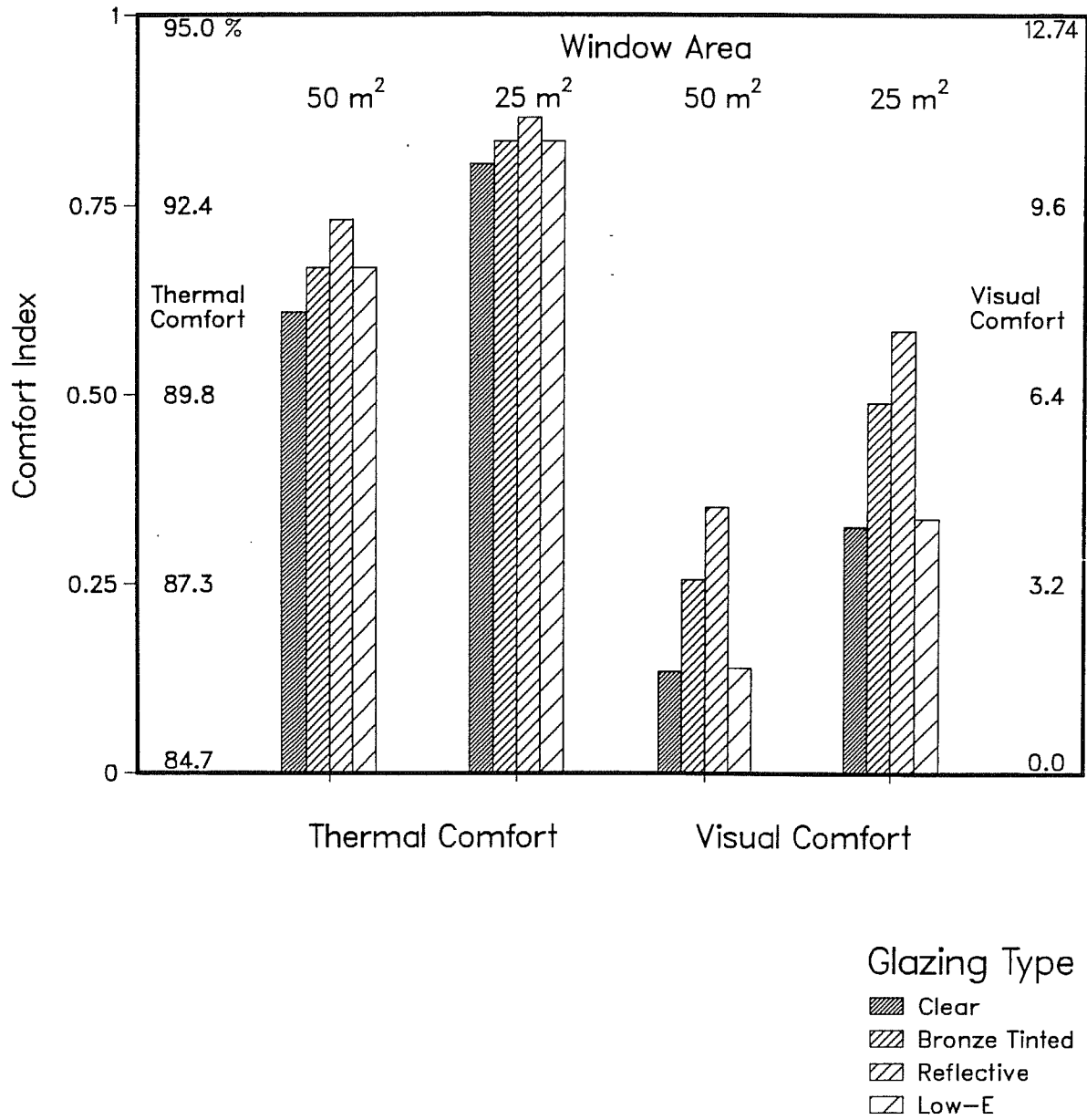


Figure 3.2.8.8. Fenestration performance indices for thermal and visual comfort for an office building module in Madison, WI, with a diffusing shade.

Distribution: 20% All Indices

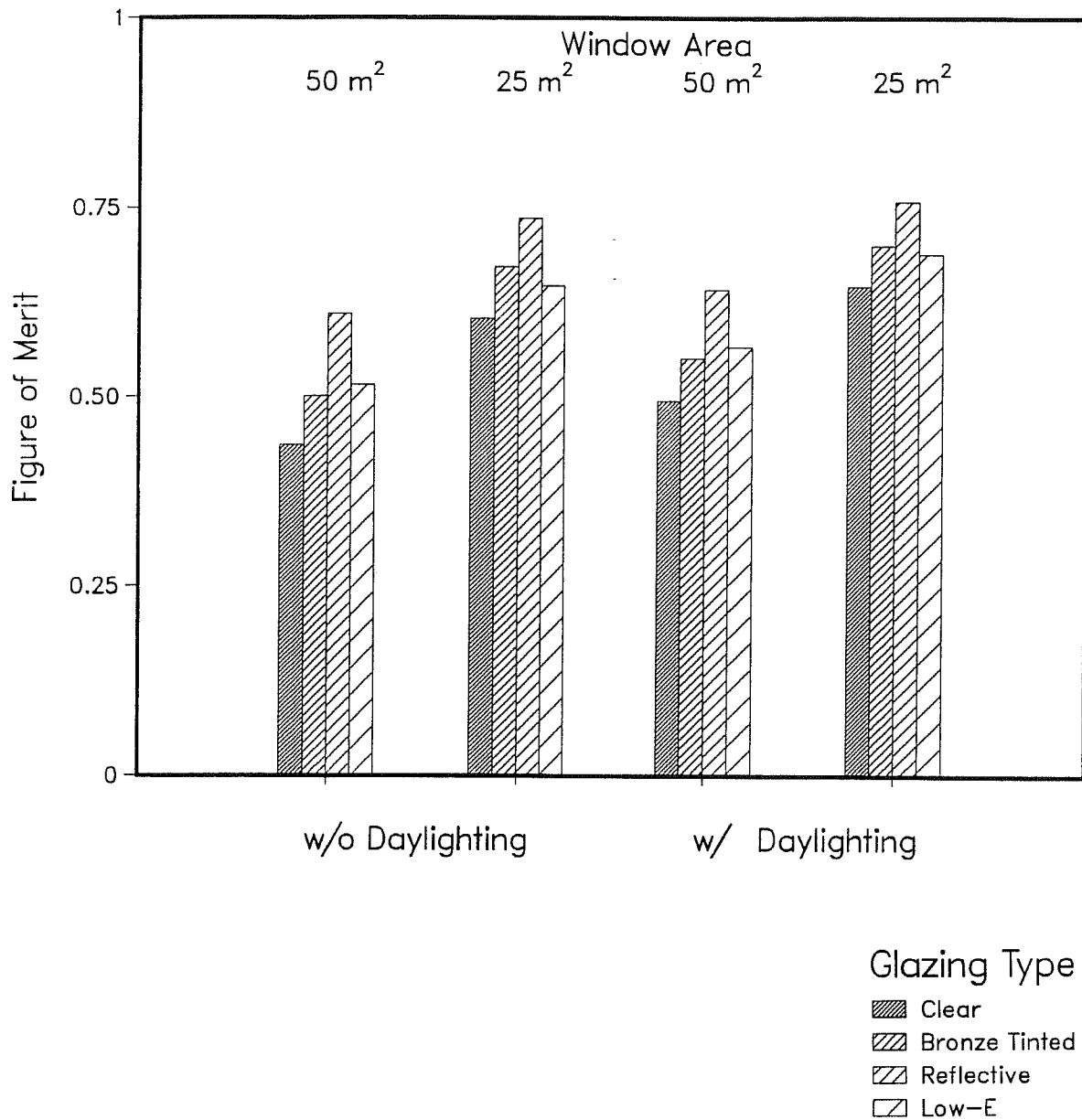


Figure 3.2.8.9. Example of the use of the figure of merit for comparing fenestration system performance, using equally weighted performance indices (20% each) for an office building module in Madison, WI, without a diffusing shade.

Distribution: 20% All Indices With Diffusing Shade

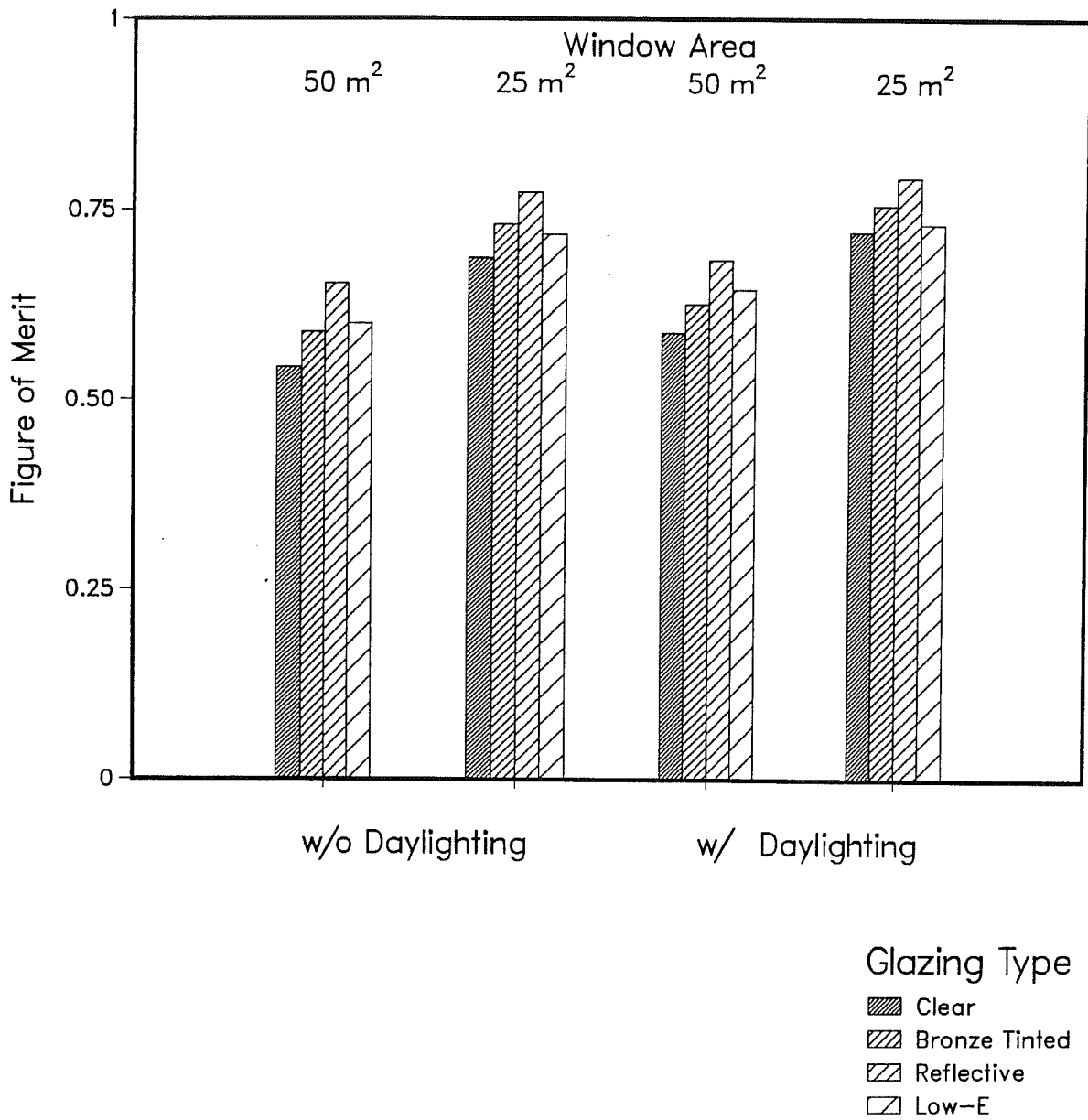


Figure 3.2.8.10. Example of the use of the figure of merit for comparing fenestration system performance, using equally weighted performance indices (20% each) for an office building module in Madison, WI, with a diffusing shade.

Distribution: Fuel=33.3%, Elec=33.3%, Peak=33.3%, Comfort=0%

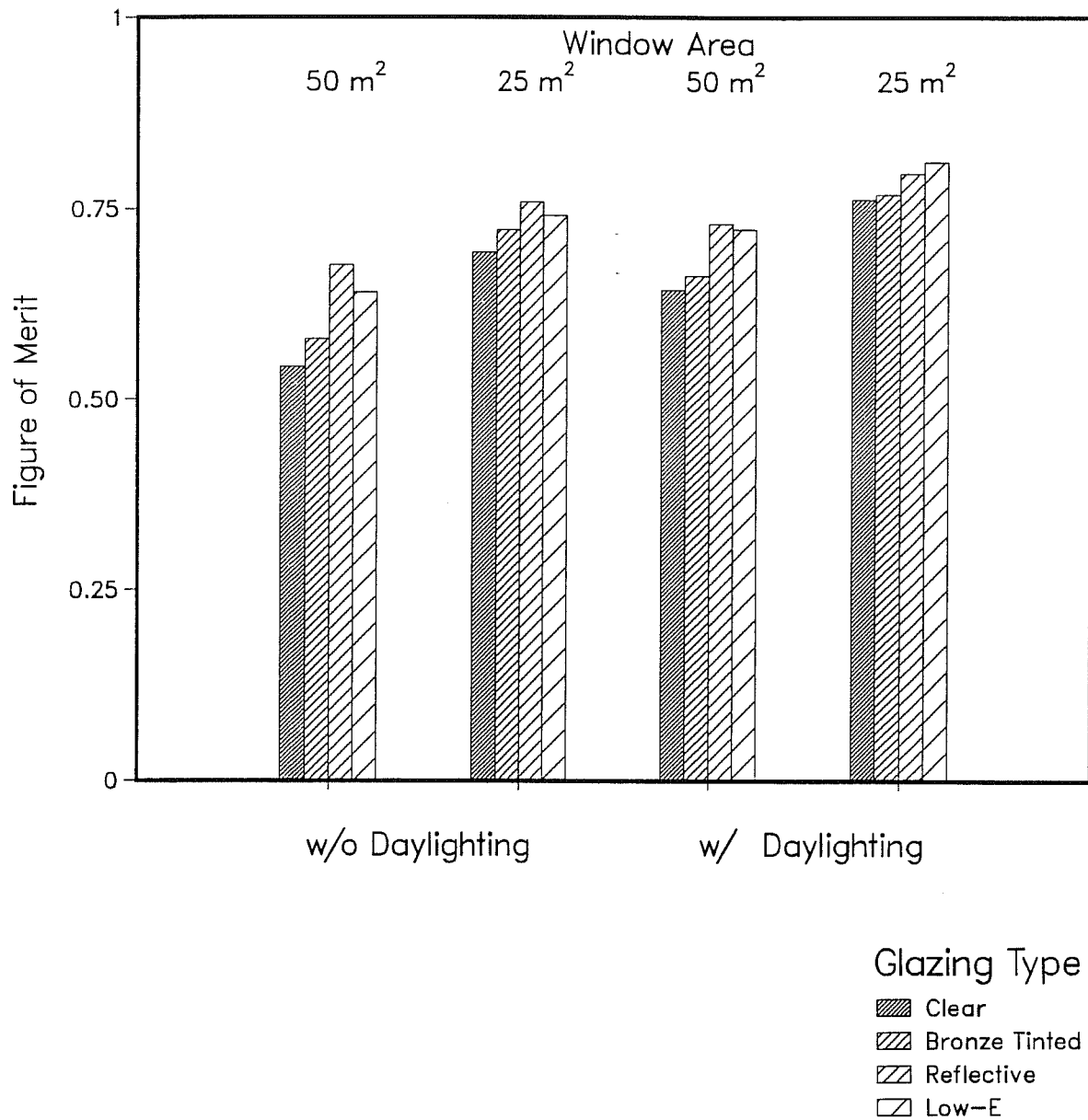


Figure 3.2.8.11. Example of the use of the figure of merit for comparing fenestration system performance, using only the three energy-related performance indices, equally weighted (33.3% each) for an office building module in Madison, WI, without a diffusing shade.

Distribution: Fuel=33.3%, Elec=33.3%, Peak=33.3%, Comfort=0%  
 With Diffusing Shade

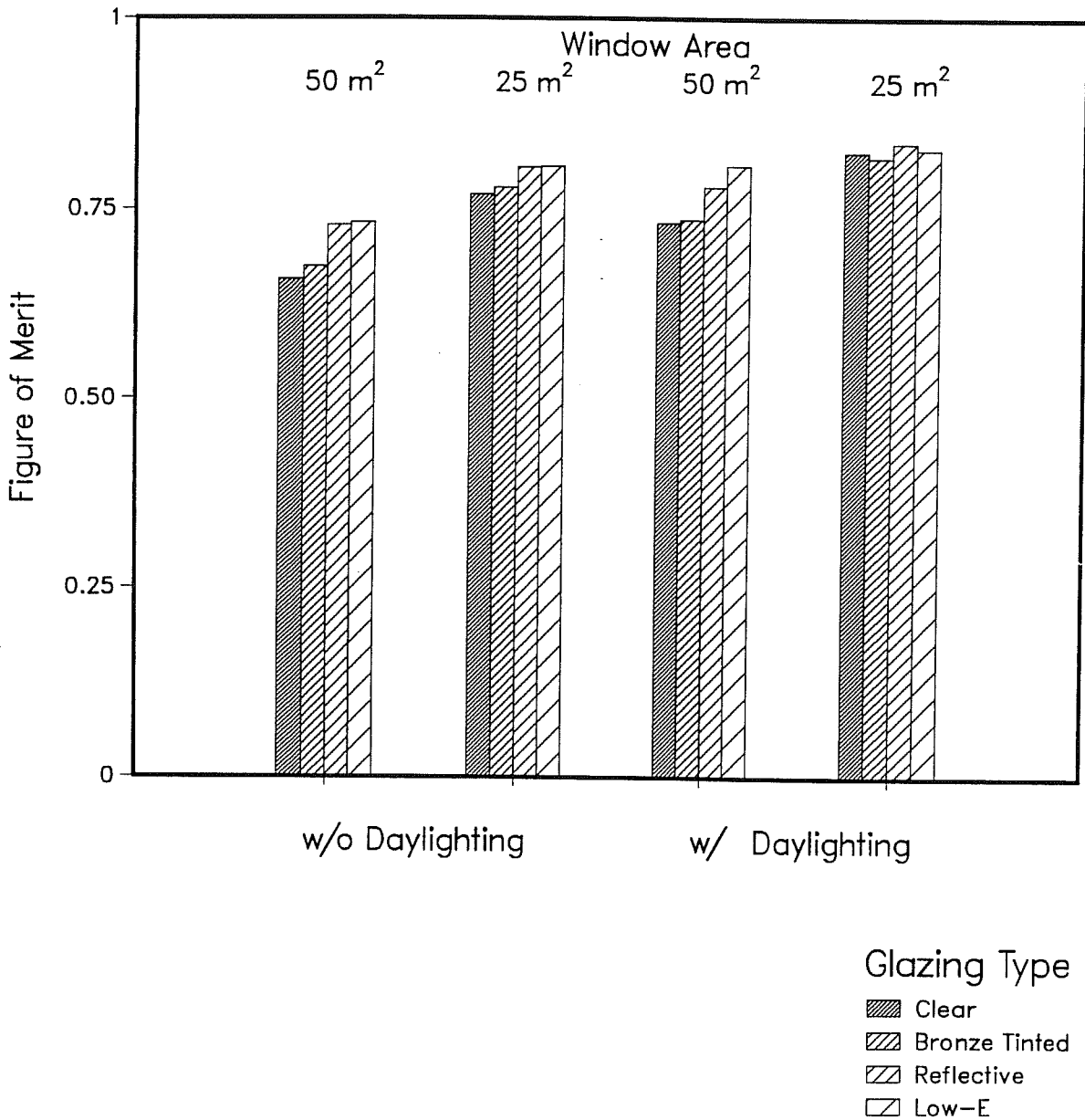


Figure 3.2.8.12. Example of the use of the figure of merit for comparing fenestration system performance, using only the three energy-related performance indices, equally weighted (33.3% each) for an office building module in Madison, WI, with a diffusing shade.

Distribution: Fuel=20%, Elec=70%, Peak=10%, Comfort=0%

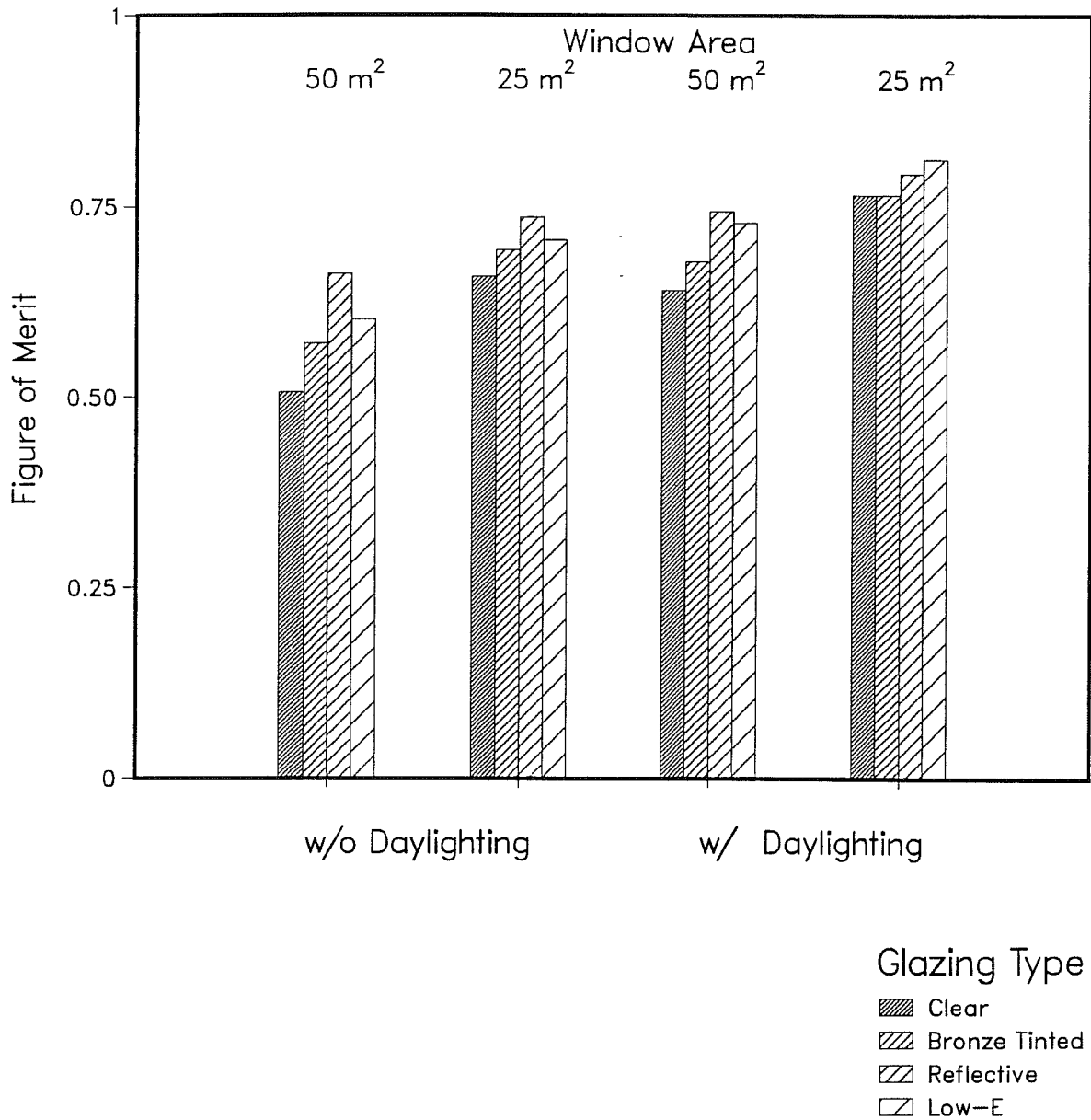


Figure 3.2.8.13. Example of the use of the figure of merit for comparing fenestration system performance, using a cost-based distribution which weights the three energy-related performance indices by relative costs (20% fuel, 70% electricity, 10% peak electrical demand) for an office building module in Madison, WI, without a diffusing shade.

Distribution: Fuel=20%, Elec=70%, Peak=10%, Comfort=0%  
 With Diffusing Shade

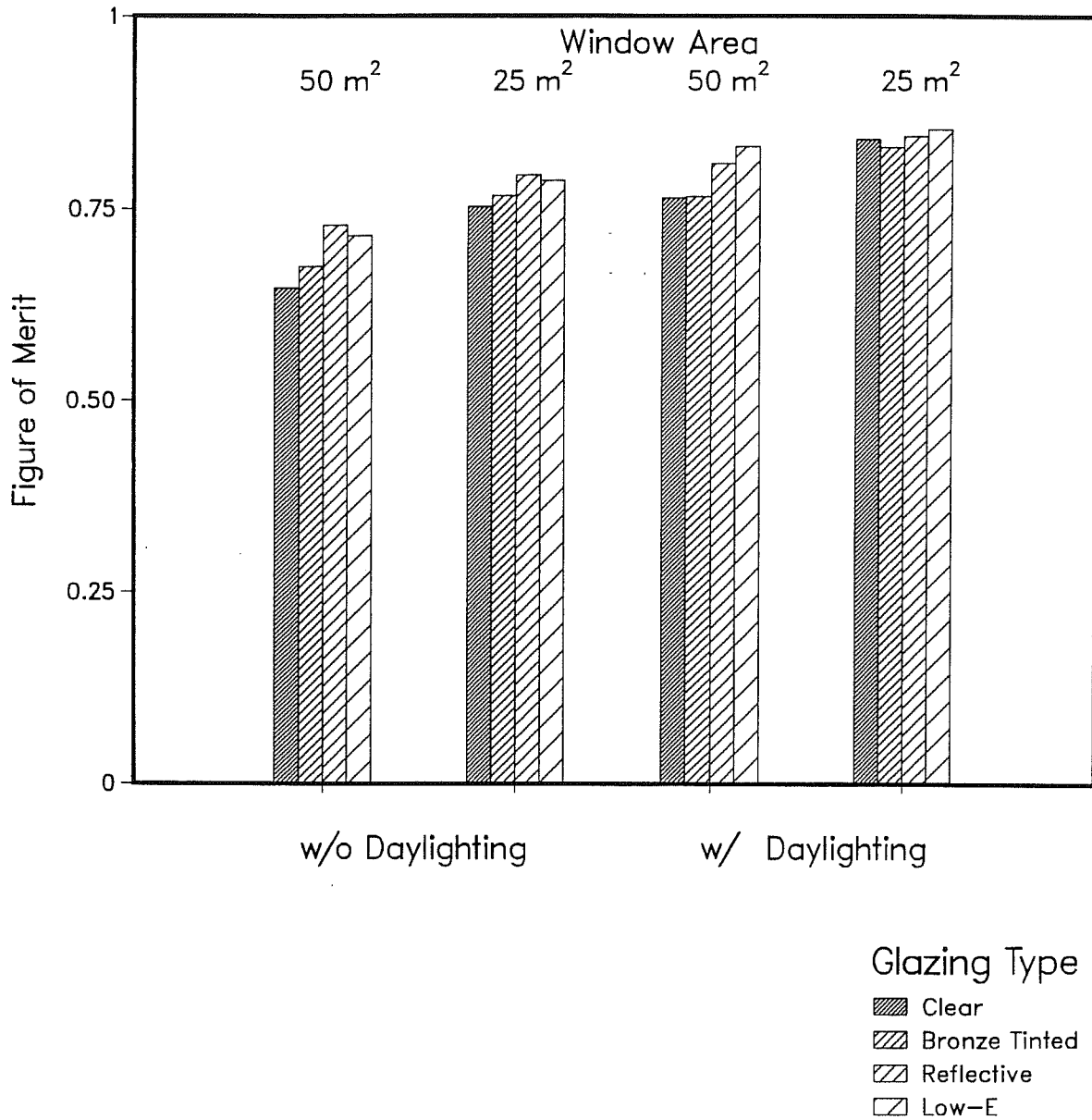


Figure 3.2.8.14. Example of the use of the figure of merit for comparing fenestration system performance, using a cost-based distribution which weights the three energy-related performance indices by relative costs (20% fuel, 70% electricity, 10% peak electrical demand) for an office building module in Madison, WI, with a diffusing shade.

Distribution: Fuel=7%, Elec=23%, Peak=70%, Comfort=0%

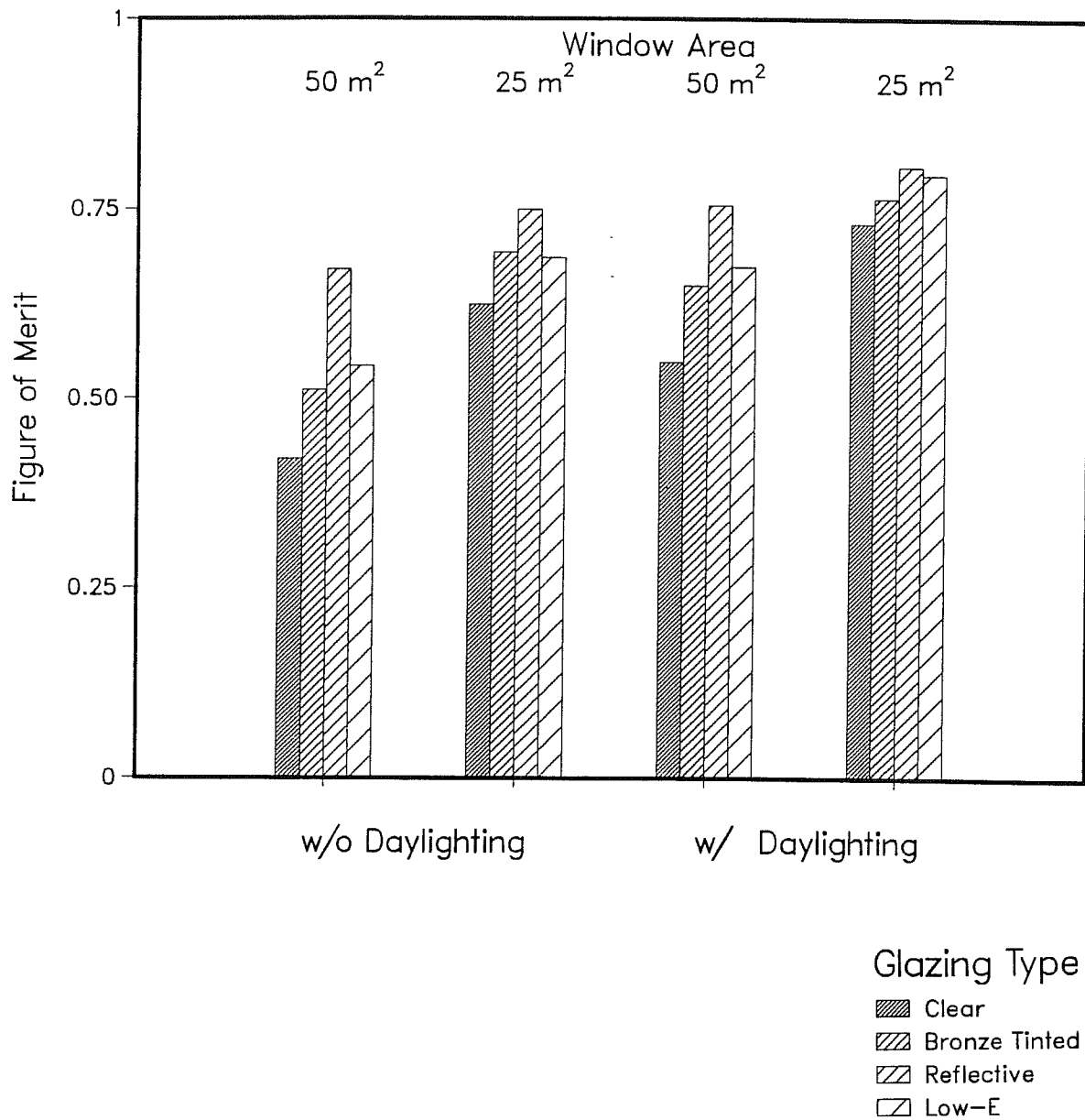


Figure 3.2.8.15. Example of the use of the figure of merit for comparing fenestration system performance, showing a different energy-cost-based distribution (7% fuel, 23% electricity, 70% peak electrical demand) for an office building module in Madison, WI, without a diffusing shade.

Distribution: Fuel=7%, Elec=23%, Peak=70%, Comfort=0%  
 With Diffusing Shade

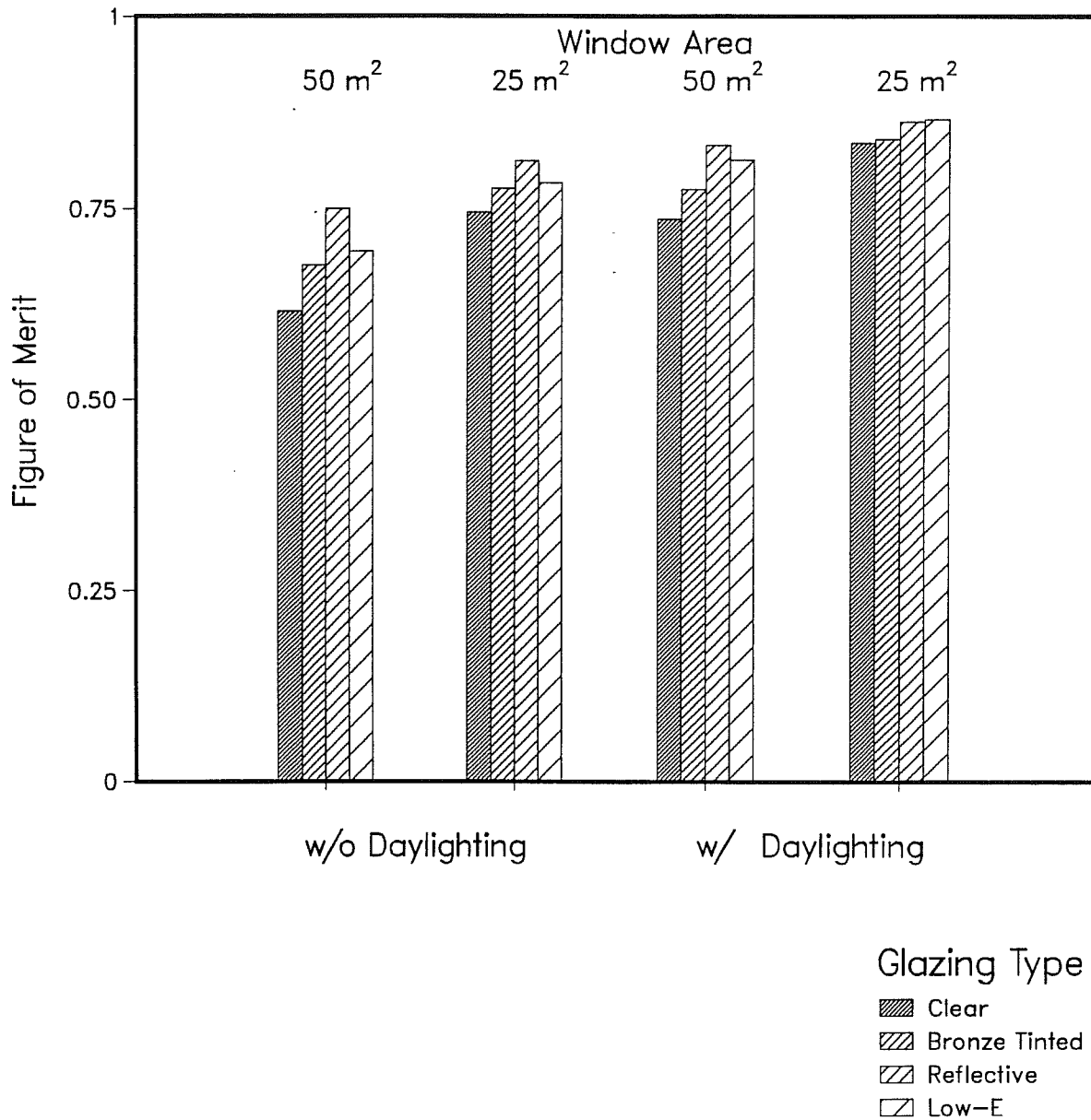


Figure 3.2.8.16. Example of the use of the figure of merit for comparing fenestration system performance, showing a different energy-cost-based distribution (7% fuel, 23% electricity, 70% peak electrical demand) for an office building module in Madison, WI, with a diffusing shade.

#### **4. Prototype Micro-Computer Design Tool**

We developed a demonstration version of a micro-computer based fenestration performance analysis computer program. The model used a program called DEMO from Software Garden, Inc. to simulate the actual interface between the user and the computer. Appendix B presents a portion of the screens that define the prototype tool.

#### **5. Phase 2 Recommendations**

Phase 2 of this project will begin with a workshop to describe the performance indices and the prototypical design tool developed in Phase 1 to representative users and to help them develop a working knowledge of the approach for various applications (e.g. new building design, retrofit, etc.). Their comments, concerns, and suggestions will be recorded and evaluated. Based on this evaluation, the definitions of performance indices, their method of calculation, and weighting functions used to generate figures of merit will be refined and revised as needed. Performance data will then be calculated for a large number of fenestration products in general use and for several new systems now entering the market. This will include conventional systems as well as complex operable shading systems, for example. These results will then be placed in a computerized data base.

It may also be desirable, if adequate resources are available, to conduct limited field measurements in an occupied building and/or in the Mobile Window Thermal Test (MOWITT) facility to establish an empirical link to the calculated data bases. Depending on the advice of the LRI review panel and other participants, one or more workbooks or other documents would be developed for use by specific groups. This will be done in consultation and collaboration with the sponsors, and with appropriate groups such as IES, ASHRAE, AIA, BTECC, DOE, or others.

A computer program will be written for a widely available microcomputer to access this data base and to apply various weighting functions. This program will evolve from the prototype developed in Phase 1 and evaluated at the workshop.

## 6. Summary and Conclusions

Building designers, utility auditors, and others are constantly required to compare and evaluate the performance of alternative fenestration systems in new and existing buildings. Frequently, the fenestration options vary radically, as when low-E coatings are compared with exterior shading devices. For this process to properly address the energy-related impacts of fenestration, one must be able to quantify the energy performance for all the different systems considered in a systematic and reproducible way. The objective of this study was to develop several numerical indicators for comparing fenestration system performance on the basis of annual energy consumption, peak electrical demand, illumination performance, and thermal and visual comfort. These indicators are to be used as guides in evaluating and selecting alternative fenestration products and systems for use in various building types and climates.

The project consists of two phases: In Phase 1, which is reported upon in this document, we developed the basic methodology for determining the performance indicators and tested the techniques for a few sample fenestration systems; Phase 2 will support the measurement and analysis tasks required to construct a large data base of indices for most of the common generic fenestration systems. In addition, we will develop a micro-computer based design tool to embody the projects' results.

We utilized various experimental devices to measure the solar optical properties and daylight transmittance/distribution functions of the sample systems since the performance of several classes of fenestration products cannot readily be characterized using conventional analysis techniques. The integrating sphere and the luminance/radiance scanner were instrumented, calibrated, and used in our experimental work. In addition, several data reduction computer programs were written that converted the raw data generated from the scanner and sphere into expressions that the DOE-2 program used to simulate transmission characteristics.

A major revision was made to the DOE-2 energy analysis simulation program incorporating these latest algorithms for calculating solar transmission and optical properties. The algorithms use the same approach as previous DOE-2 methodology, however, the polynomial coefficients that define a systems performance were changed and made more accurate. In conjunction with these revisions to DOE-2, we also introduced a number of bin type reports that tabulated U-value, solar heat gain, visible transmittance, etc. over the course of the year for each hour of the day. These reports were used in our performance evaluation of the different fenestration systems.

A methodology was developed that defined the relationship between fenestration characteristics, direct solar radiation, and comfort so that annual thermal and visual comfort indices could be calculated. In the case of thermal comfort, the index was represented by the summed product of the percent hours at a particular solar radiation level and percent dissatisfaction determined by the increase in mean radiant temperature within the space. The visual comfort index was represented by the number of occupied hours during the year during which glare as represented by a glare index was above a value deemed to be uncomfortable.

Numerous DOE-2 parametric runs were completed for the prototype configuration in Madison and Lake Charles and multiple regression coefficients obtained and used in developing performance indicators. An overall fenestration performance "figure of merit" was defined from the calculated performance indicators and a user defined weighting function.

Phase 1 objectives have been attained. We have shown that the techniques developed to evaluate and categorize fenestration system performance do work and that the basic figure of merit concept has been proven. Remaining tasks associated with Phase 2 includes field testing and user reaction evaluation, completion of a data base containing results for many fenestration systems, and development and creation of a working micro-computer design tool.

## 7. References

Johnson, R.; Sullivan, R.; Nozaki, S.; Selkowitz, S.; Conner, C.; and Arasteh, D. 1983. "Building Envelope Thermal and Daylighting Analysis in Support of Recommendations to Upgrade ASHRAE/IES Standard 90, Final Report." Lawrence Berkeley Laboratory, Report LBL-16770.

Papamichael, K.M. and Winkelmann, F. 1986. "Solar-Optical Properties of Multilayer Fenestration Systems." Lawrence Berkeley Laboratory, Report LBL-

Rubin, M.; Arasteh, D.; and Hartman, J. 1986. "WINDOW: A Computer Program for Calculating U-Values and Shading Coefficients of Windows." Lawrence Berkeley Laboratory Report, LBL-20212.

Selkowitz, S.; Kim, J.J.; Navvab, M.; and Winkelmann, F. 1982. "The DOE-2 and SUPERLITE Daylighting Programs." Proceedings of the 7th National Passive Solar Conference, Knoxville, TN.

Simulation Research Group. 1985. "DOE-2 Supplement: Version 2.1C." Lawrence Berkeley Laboratory, Report LBL-8706, Rev. 4 Suppl.

Spitzglas, M. 1986. "A New Bidirectional Scanner for Testing Building Fenestration Systems." Lawrence Berkeley Laboratory, Report LBL-21353 (to be published).



# APPENDIX A

## Thermal Comfort Analysis

This portion of the report presents a detailed analysis of the thermal comfort issues relevant to perimeter zones in commercial office buildings. It contains the background information supporting the discussion in section 3.2.4 of the report.

### 1. Historical Summary

Empirical data related to thermal comfort dates from the 1920s. At that time, ASHRAE-sponsored research led to the development of an Effective Temperature Scale (ET\*) in which the combined effects of dry-bulb and wet-bulb temperatures and air movement were correlated to the thermal sensations of warmth and coldness. The ET\* scale was revised in the 1960s to better account for the effects of humidity and has been used as a basis for the evaluation of comfort. ANSI/ASHRAE Standard 55-1981 (Thermal Environmental Conditions for Human Occupancy, Ref. 1) is the standard by which thermal environments are judged. It specifies conditions in which 80% or more of the occupants are comfortable.

The criteria defined in the standard reflects an evolution of many factors, particularly those related to human subject response data. Figure A.1 shows the acceptable ranges of operative temperatures and humidities in the standard for persons clothed in typical summer and winter clothing, during light, mainly sedentary activity. The operative temperature for the purpose of this report can be considered the mean of the air and mean radiant temperatures. The following coordinates of the comfort zones have been extracted from the standard. The relationship between effective temperature and comfort criteria is clearly illustrated by Figure A.1.

Winter: Operative temperature= 19.5-23°C (67.1-73.4°F) at 16.7°C (62°F) dew point temperature (.0012 humidity ratio) and 20.2-24.6°C (68.4-76.35°F) at 1.7°C (35°F) dew point (.00043 humidity ratio). The slanting side boundaries correspond to 20 and 23.6°C (68 and 74.5°F) effective temperature (ET\*) lines.

Summer: Operative temperatures=22.6-26°C (72.7-78.8°F) at 16.7°C (62°F) dew point temperature (.0012 humidity ratio) and 23.3-27.2°C (74 and 80.9°F) at 1.7°C (35°F) dew point (.00043 humidity ratio). The slanting side boundaries correspond to 22.8 and 26.1°C (73 and 79°F) effective temperature] (ET\*) lines.

Analytical and experimental results used in the ASHRAE standard and in recommended procedures for evaluating thermal comfort as specified in ASHRAE

Fundamentals (Ref. 2) are based in varying degrees on three fundamental models of the thermal response of the human body: the Fanger model, the Pierce two-node model, and the Kansas State University two-node model. A very compact and informative presentation of each is given in Ref. 3, which describes the mathematical and physiological basis of each technique, and compares the thermal sensation predictions.

"...These models are similar in that they all perform an energy balance on the body and, from the energy-exchange mechanisms and various physiological considerations, predict the thermal sensation and comfort response. The Fanger model uses heat transfer deviations from a neutral state where comfort is experienced to quantify the perceived thermal comfort. The Pierce model was developed for sedentary situations and converts a given environment to a standard one that would produce the equivalent thermal strain. The thermal sensation is then predicted from correlations that were obtained from experiments involving a large number of human subjects. The KSU model is physiologically similar to that of the Pierce, except that it predicts thermal sensation from changes in the thermal conductance between the core and the skin in cool environments and from changes in skin wettedness in warm environments..."(Ref. 4).

The resulting comparisons shown in Ref. 3 indicate that the Fanger model is more sensitive to temperature, while the Pierce and KSU models are more sensitive to humidity. Fanger's model is also more sensitive to metabolic rate or activity level. Thermally neutral sensations for all three are about the same for several environments, but as conditions deviate from neutral, the Pierce and KSU models are more accurate. The Effective Temperatures (ET\*) used in the ASHRAE Standard and Fundamentals were derived from the Pierce and KSU data. However, Fanger's results are used extensively in each to define comfort for varying levels of activity, clothing, and the four environmental parameters of air temperature, humidity, mean radiant temperature, and air velocity. These variables directly influence thermal sensation and represent the primary indices through which comfort is determined.

Recent work by Fanger on asymmetric thermal radiation is also used in the ASHRAE standard. In general, Fanger's results are more conservative than the others and his methodology has been prepared in the form of tables and charts which are very easy to use. For these reasons, Fanger's model was used to predict comfort in this study.

## 2. Fanger's Comfort Model

Fanger's thermal comfort model (Ref. 5) consists of a steady-state heat balance on the human body equating heat production to heat dissipation, assuming no heat storage. Metabolic rate is balanced by respiration, skin diffusion, and evaporative heat losses as well as the heat conducted between the skin and the outer surface of clothing. The latter quantity also equals the dissipated radiative and convective losses at the surface. Using the resulting balance equation and defining comfort criteria to be based on skin temperature and evaporative heat loss as a function of activity level (metabolic rate), Fanger derived the comfort equation that, when solved, yields the environmental (air temperature, mean radiant temperature, air velocity, and humidity) and personal (activity level, type of clothing) factors that are a necessary condition for optimal comfort.

For conditions that are not optimal in the sense that the comfort equation is not satisfied, Fanger derived an index, from numerous experiments on human subjects, designated the Predicted Mean Vote (PMV) that gives an indication of the thermal sensation for any combination of the above parameters. The PMV uses the sensation response scale developed by ASHRAE, with a slight change in numerical indicators (see Table A.1). Use of the methodology was facilitated by the generation of tables and charts so that one could very simply determine the PMV for most conditions without resorting to solutions of complicated mathematical expressions. Table A.2 presents a sample of the PMV table for a sedentary individual or slightly active individual. Values are shown for many different clothing levels and air velocities. Air temperature is assumed the same as the mean radiant temperature and relative humidity is fixed at 50%.

In conjunction with PMV, which gives an indication of the degree of comfort or discomfort, the Predicted Percentage of Dissatisfied (PPD) is also usually ascertained. Figure A.2 shows the relationship between PMV and PPD. It is symmetrical about the optimal thermal comfort point,  $PMV=0$ . As can be seen from the figure, there is always at least a dissatisfaction level of 5% even under optimal conditions.

The general procedure for using Fanger's methods in assessing the thermal environment in a space is to select a network of points to define contours of PMV values. This requires knowing or ascertaining the previously mentioned four environmental variables and two personal variables. As an example relevant to the LRI study, consider the commercial building perimeter zone module shown in Figure A.3. It is desired in this example to show the PMV distribution throughout the space under conditions close to optimal, i.e.,  $PMV=0$ . A description of the model and the assumptions used are as follows:

- a. The space is 3.05 m (10 ft) wide by 4.57 m (15 ft) deep and 2.59 m (8.5 ft) high. It has one external wall and window, a partition adjacent to a core zone in which heat transfer is permitted, and four other surfaces (ceiling and floor, right and left wall) that are adiabatic. Window-to-wall ratio is 0.59 (using ceiling height).
- b. The activity level is set to 1.2 met (69.8 W/m<sup>2</sup> 22.1 Btu/h-ft<sup>2</sup>, 60 kcal/h-m<sup>2</sup>) corresponding to a person doing sedentary or slightly active office work. Clothing (clo) value is set to 1.0 (0.155 m<sup>2</sup>-°K/W, 0.88 ft<sup>2</sup>-°F/Btu), which is near the recommended value used for winter (0.9, light clothes). A typical summer value would be 0.5 clo.
- c. Relative humidity is fixed at 50% and the air velocity is 0.15 m/s (30 fpm).
- d. The room temperature and all surface temperatures except for the window are assumed to be at 22°C (71.6°F). This value coincides to a PMV of zero as seen on Table A.2 under the assumed conditions. For an operative temperature near the air temperature, these conditions are also at the midpoint of the winter comfort criteria. In order to observe the effect on mean radiant temperature, an extreme winter condition for the glass surface temperature will be assumed, i.e., 0°C (32°F).

The distribution within the space is defined by grids every .76 m (2.5 ft) along the length and width as seen on Figure A.3. Since the air temperature is assumed the same at all points in the space, the first step is to calculate the mean radiant temperature at the center of each grid using the respective surface temperatures and appropriate solid angle factors between the surfaces and points. The MRT or mean radiant temperature is defined as:

$$\text{MRT} = \sum_{i=1}^{\text{NS}} T_i \cdot \Phi_{p-i} \quad (1)$$

This is done using the angle factors,  $\Phi_i$ , supplied with the ASHRAE standard, which have been extracted from Fanger's text (Ref. 5). They represent the mean value angle factors between a seated person (or standing if using the appropriate figure) and a vertical rectangle above or below the person's center when the person is rotated around a vertical axis. Fanger also supplies, although the standard does not, orientation-dependent angle factors that relate to the specific direction the person is facing.

The PMV values in Table A.2 are valid for the situation in which the air temperature equals the MRT. In the example, the MRT is not equal to the air temperature because of the influence of the window. Thus, the MRTs must be calculated by using equation 1. Once this is done, Fanger supplies a change in PMV with MRT as a function of activity level, clothing, and air velocity. For the conditions stated above, the observed value is ( $\Delta\text{PMV}/\Delta\text{MRT}=0.12$ ) (Ref. 5). One should note that this is a very small number. Thus for a significant change to be seen in either PMV or PPD, the MRT at a particular point would also be required to change significantly.

Table A.3 presents the necessary data for a determining comfort for this example. Only results for points A1-A6 and B1-B6 are shown since the space is symmetrical about its center. One will note immediately the small effect of the glazing surface because of its temperature. However, even if the glass temperature was not zero, the small angle factor values would significantly reduce its effect. The angle factors for the remaining surface in the space were easily determined by subtracting the glass values from 1.0.

The calculated MRT, differential MRT, and differential PMV all indicate a very inconsequential effect arising from the glass surface temperature. The ( $\Delta\text{PMV}$ ) values vary from a low of -.05 at the far end of the room to a high of -.174 at the point closest to the window. This quantity denotes an increase of only a few percent in PPD as seen on Figure A.2. If the model's window-to-wall ratio was 1.0 (all glass) at  $0^{\circ}\text{C}$  ( $32^{\circ}\text{F}$ ), the largest ( $\Delta\text{PMV}$ ) value would be -.486 which translates into a much more significant increase in PPD. The determining factor for comfort in the example was the assumption of uniform temperature throughout the space at the optimum comfort condition,  $\text{PMV}=0$ . One could make the argument that the room air temperature would not necessarily be the same at all locations; however, for a conditioned space, the variation would not be very large.

This example has presented a typical case of the use of Fanger's comfort methodology. Recent work by Fanger and others (Refs. 7, 8, 10), however, deals with the problem of asymmetric radiation represented by the introduction of radiant temperature asymmetry and plane radiant temperature rather than just the mean radiant temperature. The next section of the report deals with these matters.

### 3. Asymmetric Thermal Radiation

Of particular importance in the office environment are the effects on thermal comfort arising from asymmetric thermal radiation. Thermal radiation, in this context, not only includes that due to longwave low-temperature sources such as cold or warm

surfaces (walls and windows) or radiators, but also high-intensity sources such as infrared heaters and direct solar radiation. The literature is mixed in its treatment of each of these, with an early emphasis on high-intensity sources. Lately, however, the concentration has been on longwave sources. In either case, concepts other than mean radiant temperature and predicted mean vote are used to evaluate comfort. For low-temperature sources, Radiant Temperature Asymmetry has been introduced. The Effective Radiant Field has been used for high-intensity sources.

ANSI/ASHRAE Standard 55-1981 specifies that the radiant temperature asymmetry in the vertical direction must be less than  $5^{\circ}\text{K}$  ( $9^{\circ}\text{F}$ ) and in the horizontal direction less than  $10^{\circ}\text{K}$  ( $18^{\circ}\text{F}$ ). Although not explicitly stated in the standard, these limits are for low-temperature sources (see Refs. 7 and 8) and refer to warm ceilings and cool walls, respectively. The concept of Radiant Temperature Asymmetry was first introduced by McIntyre in Ref. 9 and expanded by Fanger for heated ceilings (Ref. D.7) and for cooled ceilings and heated and cooled walls (Ref. 8).

Radiant temperature asymmetry "...is defined as the difference between the plane radiant temperature of two opposite sides of a small plane element. Plane Radiant Temperature is then defined as the uniform temperature of an enclosure where the irradiance on one side of a small plane element is the same as in the non-uniform actual environment. The plane radiant temperature is a parameter which describes the radiation in one direction. The mean radiant temperature (MRT) describes the radiation from all surrounding surfaces, which influences the radiant exchange between the human body and the environment. Mean radiant temperature is therefore defined in relation to the human body while plane radiant temperature and radiant temperature asymmetry are defined in relation to a small plane element.." (Ref. 10).

For the purposes of the ASHRAE standard, the small plane element is located 0.6 m (2 ft) above the floor, corresponding to the position of a seated individual. Solid angle factors are given in the standard for both parallel and perpendicular plane element-surface relationships. As was the case in the previous example, comfort is ascertained by defining the temperature distribution within the space. The temperatures of concern, however, are the plane radiant temperatures and radiant temperature asymmetries.

The standard is only applicable to cold vertical surfaces and warm horizontal surfaces because Fanger's studies relative to warm verticals and cold horizontals (Refs. 7, 8, 11) indicated that individuals are less sensitive to this type environment. This can be seen in Figure A.4, which was extracted from Ref. 1. The four types of asymmetries are presented as a function of level of dissatisfaction. A 10% dissatisfaction level for warm verticals and cold horizontals coincides with approximately a  $30^{\circ}\text{C}$  ( $54^{\circ}\text{F}$ ) and  $20^{\circ}\text{C}$

(36°F) asymmetry, respectively. Such large values are unlikely in most environments.

Table A.4 presents the breakdown of angle factors and temperatures for the same configuration as in the previous example. The radiant temperature asymmetries ( $\Delta T_{pr}$ ) vary from a low of 1.078°C (1.94°F) far from the window to a high of 4.29°C (7.72°F) close to the window, values that are within the 10°C (18°F) Standard 55 horizontal limit. Essentially no one would find such a situation uncomfortable. For an all-glazing surface corresponding to a window-to-wall ratio of 1.0, the radiant temperature asymmetry near the window would be 10.34°C (18.61°F). This value corresponds to approximately a 10% dissatisfaction level as can be seen on Figure A.4. Thus it is seen that only in an extremely cold environment with an all-wall window will comfort be a problem for low-temperature radiant sources.

Experimental testing on comfort resulting from high-intensity sources has been concerned with subject response to infrared heating devices (Refs. 2, 5, 12, 13). Unlike the case of the longwave sources above, which were evaluated for their asymmetric characteristics, no such studies have been found in the literature that dealt with high-intensity sources in the same manner. Rather, the analyses relied on mean radiant temperature, operative temperature, and a parameter called the Effective Radiant Field or ERF (Ref. 12). ASHRAE Fundamentals defines the operative temperature for comfort in the presence of radiant heating as follows:

$$T_o = T_a + ERF/h \quad \text{or} \quad MRT = T_a + ERF/h_r \quad (2)$$

where  $T_o$  is the operative temperature, ( $T$ ) is the ambient air temperature, ( $h_r$ ) is the radiative exchange coefficient of the human body surface, and ( $h$ ) is the combined radiative and convective coefficient. (This relationship was derived from work reported in Ref. 12.) The ratio ( $ERF/h$ ) is a measure of the radiant field and as used in the equations represents the ERF for comfort. Such a condition manifests itself in radiant fields being defined for colder than normal situations in which an infrared or other type heater is being used for local heating in a cold environment. Arens in Ref. 14, for example, has defined lines of comfort on a psychometric chart in which radiant heating was used for low space temperatures and increased air velocity was used for high temperatures. Since this LRI study is concerned with solar radiation as a high-intensity source under typical office environmental conditions, these studies do not yield adequate information on comfort in such surroundings.

Some indication of discomfort can be obtained from the information displayed in Figure A.5 from Fanger's original work (Ref. 5). The mean radiant temperature of an unirradiated person has been revised to account for the effect of a high-intensity source.

Lines of constant MRT differences have been superimposed on the original figure. Since the source is a high-temperature beam, the radiant exchange is essentially independent of the temperature of the surroundings, and therefore the curves are valid for most configurations. It is very easy to see from Figure A.5 why direct solar radiation through a window and incident on a person might be considered uncomfortable at times. The absorbed radiation as shown on the figure is a function of  $f_p$ , the projected area factor, which for a seated person facing the sun at a solar altitude of 30-45° equals 0.30;  $(\alpha_{ir})$ , the mean absorptance of the skin-clothing combination, which is about 0.6; and  $(q_{ir})$ , the incident solar radiation, which at times could equal magnitudes on the order of 800 W/m<sup>2</sup> (254 Btu/hr-ft<sup>2</sup>, 687 kcal/hr-m<sup>2</sup>). The product of these three variables equals 144 W/m<sup>2</sup> (46 Btu/hr-m<sup>2</sup>, 124 kcal/hr-m<sup>2</sup>). For a condition in which the mean radiant temperature for an unirradiated person equals a room air temperature of 22°C (71.6°F), this translates (according to Figure A.5) into a mean radiant temperature for an irradiated person of about 43°C (109°F). This change in MRT may be even greater since the surrounding room surface temperatures also would be affected by the shortwave source. Such a condition would, of course, cause dissatisfaction.

Accepting that in most geographic locations there will generally be a finite number of hours when office building occupants will be uncomfortable because of high-intensity radiation, it would be useful to know the number of hours at certain solar intensity levels to determine expected discomfort during the year. Also, with the use of operable shading devices that intercept direct solar radiation, one could ascertain the effect of the device. The original LRI proposal suggested a similar approach as a method of isolating glare discomfort. Data bases currently in existence generally have monthly average daily summed or peak solar data (Ref. 15), which do not fulfill the requirements of a comfort index.

#### 4. BLAST Annual Results

Ref. 4 presents a recent study by the Solar Group at LBL. Although the work is still incomplete, it does provide useful information relative to the LRI thermal comfort situation. Revisions were made to the BLAST energy analysis program that enabled the calculation of comfort parameters using the Pierce two node-model previously discussed (Refs. 16 and 17). Particular characteristics of the study are listed below:

- a. The model consisted of a single-story office building of five conditioned zones: four perimeter zones of floor area 118.4 m<sup>2</sup> (1275 ft<sup>2</sup>) and a core zone of area 455.2 m<sup>2</sup> (4900 ft<sup>2</sup>) for a total area of 929 m<sup>2</sup> (10000 ft<sup>2</sup>). Window-to-wall ratio for each

perimeter was 0.292.

b. The activity level was set to 1 met ( $58.2 \text{ W/m}^2$ ,  $18.4 \text{ Btu/h-ft}^2$ ), which corresponds to sedentary activity. Clothing value was varied according to the season: winter (Nov 15-Mar 31) 1 clo; summer (Jun 15-Sep 14) 0.5 clo; and swing (Apr 1-Jun 14 and Sep 15-Nov14) 0.75 clo.

c. Relative humidity was assumed fixed at 50%, because the structure of BLAST does not permit the calculation of humidity prior to the comfort calculations.

d. Air velocity was assumed to be 0.076 m/s (15 fpm) except when cooling was required. The velocity was then varied as a linear function between the limits of 0.076 m/s (15 fpm) and 0.2 m/s (40 fpm). This high value corresponded to the peak cooling demand.

e. Radiant flux incident on a human body from both direct and diffuse solar radiation and internal lights was included as part of the model. The total radiation was divided by floor area to obtain the amount incident on the occupants. The following characteristics were assumed: angle of incidence  $45^\circ$ ; long-wave absorptivity 0.95; short-wave absorptivity 0.67; total body area  $1.87 \text{ m}^2$  ( $19.4 \text{ ft}^2$ ); projected body area exposed to beam sunlight  $0.41 \text{ m}^2$  ( $4.4 \text{ ft}^2$ ); and projected body area exposed to diffuse sunlight  $0.64 \text{ m}^2$  ( $6.9 \text{ ft}^2$ ). The distribution of the radiation by floor area was done because the BLAST modifications did not include geometric data or algorithms so that solid angle factors could be calculated. The MRT in this instance would tend to be lower than if calculated using realistic position information.

f. The mean air and mean radiant temperatures for each zone were calculated hourly and used in conjunction with the physiological equations governing comfort to generate discomfort indices corresponding to PMV and PPD. Whole-building values were determined by a weighted floor area average.

g. Configuration parameters investigated were glazing type (clear and reflective); thermostat control (air temperature versus air and mean radiant temperature); thermostat deadband limits; daylighting from skylights; and geographic location (Atlanta, Los Angeles, New York).

Figure A.6 presents a sample of the results for Atlanta comparing clear and reflective glazing in the south zone. These results are presented here to show, at least for the data available in Ref. 4, a worst case scenario, i.e., clear glazing for a south orientation in Atlanta yields a 10-25% dissatisfaction level on the warm side for about 32% of

the occupied hours and a 25-50% level for 5% of the occupied hours. The remaining 63% of the occupied hours were within the 10% comfort region. Reflective glazing PPD values are all within the comfort zone. For the whole building, Figure A.7 indicates that for clear glazing, about 13% of the occupied hours are in the 10-25% warm discomfort region, while the remaining hours are comfortable.

A climate comparison is shown in Figure A.8, in which results from Atlanta, Los Angeles, and New York are compared for the whole building. The only cool discomfort occurs in New York where approximately 4% of the occupied hours have a 10-25% discomfort level. Los Angeles has the same 13% occupied hours' warm discomfort as Atlanta; New York is about 8%.

Although the authors of Ref. 4 indicate that the above results represent serious discomfort, we disagree to some extent. With the exception of the 10-25% discomfort level prevalent 32% of the time for the south zone in Atlanta, none of the results seem to represent especially uncomfortable conditions. Also, the use of reflective glazing eliminates this warm discomfort entirely, as probably would the use of a shade-management scheme with clear glazing. The possibility exists that the discomfort levels above would increase if geometric position information had been used or if the total radiation had been divided by window area rather than floor area to define the amount of incident radiation on occupants. In either case, the MRT values would have been larger and thus the comfort distribution somewhat different than that obtained. Of particular importance with respect to the LRI study is the fact that useful annual information is contained in Ref. 4.

## **5. Thermal Comfort Related to High-Intensity Direct Solar Radiation**

A correlation was made between the magnitude of direct solar radiation coming through a window and the percentage of people dissatisfied (PPD), in accordance with Fanger's procedures described above. This was accomplished after experimental tests were conducted using two instruments that evaluate different aspects of thermal comfort: Bruel and Kjaer's Indoor Climate Analyzer and Thermal Comfort Meter.

The indoor climate analyzer consists of five devices that measure air temperature, air velocity, air humidity, radiant temperature asymmetry, and surface temperature. No direct indication is given of level of comfort; however, with the help of data from past Fanger experiments, this information can be obtained from Figure A.4.

The thermal comfort meter is a device which for dialed-in values of clothing, activity level, and vapor pressure (humidity) uses a transducer to thermally simulate a human being to define levels of comfort/discomfort. Fanger's Predicted Mean Vote

(PMV) and Percent People Dissatisfied (PPD), as well as the operative and equivalent temperatures are determined by the instrument. The operative temperature is the mean of the air and mean radiant temperatures for zero air velocity; the equivalent temperature is the same as operative temperature except that air velocity is considered in its calculation.

Fourteen measuring sessions were conducted at about 9 a.m. or at 6 p.m. The selected times corresponded to satisfactory levels of direct solar radiation in the available work spaces. Immediately apparent after the first session was the large magnitude of the radiant temperature asymmetry under the influence of direct solar radiation. The radiant temperature asymmetry transducer read "overrange" in almost all instances. This situation exists when the plane radiant temperatures in the two opposite directions exceed 50 °C (90 °F). The room-side plane radiant temperature was typically on the order of 22-24 °C (72-75 °F), implying a window-side temperature greater than 74 °C (165 °F). The asymmetric criteria established by Fanger for warm walls stops at 35 °C (95 °F) corresponding to a 10% dissatisfaction level. Fanger's experiments were conducted for longwave sources and not for a shortwave high-temperature source such as the sun; therefore, the results are not too surprising.

Readings from the thermal comfort meter were more encouraging although confusing. We were able to correlate a few data point readings with the information contained in Figure A.5. Solar radiation was measured by an Epply pyranometer. The mean radiant temperature under the influence of the irradiation was determined using the measured operative temperature from the comfort meter and air temperature from the climate analyzer. The unirradiated MRT was assumed to equal the room temperature.

Table A.5 presents the test conditions that were averaged to yield a data point comparable to the information contained on Figure A.5. Also shown in the table is one other data point corresponding to a much lower value of solar radiation and other unused data that do not fit expected trends, i.e., either the amount of solar radiation is too high or too low for the corresponding operative temperature. The solar data shown is for a direction normal to the source. Averaging was done because of the different response times of the comfort meter and pyranometer. The comfort meter does not respond instantaneously as does the pyranometer and thus there was some lag. Generally, we waited until some sense of stability appeared on the comfort meter, and then recorded the operative temperature, air temperature, and incident horizontal, vertical, and normal solar radiation. Individual temperature data points gave 1-2 °C (1.8-3.6 °F) variations for very small changes in solar radiation. Using each independently would have resulted in unrealistic scattering.

Satisfied that Figure A.5 could be used to predict an irradiated MRT given an unirradiated MRT and an amount of irradiation, and also because the plane radiant temperatures could not be used to determine comfort levels, we proceeded to use a portion of Fanger's original methodology in the following manner:

$$\frac{\Delta PMV}{\Delta q} = \frac{\Delta PMV}{\Delta MRT} \frac{\Delta MRT}{\Delta \alpha \cdot f \cdot q} \frac{\Delta \alpha \cdot f \cdot q}{\Delta q} \quad (3)$$

This expression explains how the predicted mean vote can be obtained from a change in solar radiation. The  $(\Delta PMV/\Delta MRT)$  term was obtained from Fanger's original text for varying values of activity, clothing, and air-velocity. For the typical office conditions of concern in this report, the value was 0.12. The term  $(\Delta MRT/\Delta \alpha f q)$  was obtained from Figure A.5 using the intersection of the  $(\Delta MRT)$  and  $(\Delta \alpha f q)$  lines at a particular thermally neutral temperature. The mean absorptance for the human body is  $(\alpha)$ ,  $(f)$  is the projected area factor, and  $(q)$  is the incident solar radiation. Assuming thermal neutrality at an indoor air temperature and unirradiated MRT of 24.4 °C (75 °F), we cross-plotted the two parameters with the result that the curve was very nearly linear, with the value  $\Delta MRT/\Delta \alpha f q$  equal to 0.19.

The last term  $(\Delta \alpha f q/\Delta q)$  is simply  $(\alpha \times f)$  or 0.18, assuming  $\alpha=0.6$  and  $f=0.3$ . Figure A.9 shows the variation of projected area factors for seated persons as a function of source azimuth and altitude (Fanger's 1970 text). The value 0.3 is rather conservative and corresponds to a person facing the sun at an altitude of 45°. The largest value is 0.33 and that occurs for a 30° azimuth condition at a 15° altitude angle. Substitution of the above information into equation 3 yields the following solution values:

$$\begin{aligned} (\Delta PMV/\Delta q) &= 0.004 \text{ per kcal/hr-m}^2 \\ &= 0.0035 \text{ per W/m}^2 \\ &= 0.011 \text{ per Btu/hr-ft}^2 \end{aligned}$$

Percent level of dissatisfaction (PPD) is obtained from the relationship between PPD and PMV (see Figure A.2). To utilize this methodology, we tabulated solar radiation bins from DOE-2.1C and related the values to level of dissatisfaction. Solar bin data for north and south perimeter zones in Madison are presented in Table A.6. Two columns of percent dissatisfaction are shown opposite the particular solar level. The more conservative PPDs represent recommended values to be used in the LRI study. Note should be taken at this point of the fact that the solar bin data presented in the

DOE-2.1C report relate to the amount of transmitted solar radiation perpendicular to the window. This results in an additional safety factor since the solar values on Figure A.5 are normal to the source.

A comfort index was derived from these results using the following formulation:

$$TC = \sum_{i=1}^{NB} X_i (1. - PPD_i) \quad (4)$$

where X is the percent hours at a solar level divided by 100 and PPD is the percent dissatisfied at that level divided by 100. Index (i) represents a summation over the ten bins (NB). For the north and south zone data in Table A.6 and using the conservative PPDs, the index is:

$$\text{North} \quad TC = (.97)(.95) + (.03)(.95) = 0.95$$

$$\text{South} \quad TC = (.58)(.95) + (.13)(.90) + (.15)(.80) + (.09)(.60) + (.04)(.50) = 0.86$$

The highest or best index value for thermal comfort would be 0.95 since there is always at least a 5% level of dissatisfaction. The lowest or worst index would be 0.0 for the case where 100% of the occupied hours have a solar radiation greater than  $473 \text{ W/m}^2$  ( $150 \text{ Btu/hr-ft}^2$ ). This would occur for the largest window and the index would proportionally increase as the window size decreases. The value of the TC index for both east and west zones is 0.90.

## 6. Thermal Comfort Related to a Low-Temperature Cold-Window Source

The example presented in Table A.4 was redone using outside air temperature bin data from DOE-2.1C runs in Madison, WI. Rather than assuming a glass temperature equal to  $0^\circ\text{C}$  ( $32^\circ\text{F}$ ), as in the earlier example, we used outside air temperature as the glass surface temperature. The assumption here is that the glass temperature would not be lower than the air temperature and that this represents a worst-case scenario. The bins and calculated radiant temperature asymmetries and resultant dissatisfaction levels are shown in Table A.7 for position B5, which represents the largest value of asymmetry.

Again, for the whole facade window, the 5% level is exceeded, whereas the standard-size window is well within this limit. Based on these results and with the understanding that the LRI configuration will not include windows of a size larger than a window-to-wall ratio of 0.59 (0.50 if including ceiling height), we will ignore cold windows

as a source of discomfort in our standard set of parametric runs. If, however, we analyze larger windows, we can use the outdoor temperature bin data in a manner similar to the above example to generate comfort levels.

## 7. Conclusions

This Appendix has documented the thermal comfort aspects of the LRI fenestration performance indices project. A cursory discussion of the historical development of thermal comfort was presented as well as the procedures used in performing a comfort analysis using the methods of P.O. Fanger. Specific examples examined the variations in human satisfaction level using both mean radiant temperature and radiant temperature asymmetry. General conclusions reached are as follows:

- a. If the assumption is made that an HVAC system or other active or passive system is available for maintaining a comfortable environment under most conditions, then thermal comfort in commercial office buildings is an issue only in terms of asymmetric radiation effects.
- b. ANSI/ASHRAE Standard 55-1981 specifies limits to acceptable radiant temperature asymmetry. The limits are  $5^{\circ}\text{C}$  ( $9^{\circ}\text{F}$ ) in the vertical direction and  $10^{\circ}\text{C}$  ( $18^{\circ}\text{F}$ ) in the horizontal direction due to low temperature and longwave sources such as cold windows and warm heated ceilings. These numbers correspond to a 10% level of dissatisfaction. For windows of area less than 60% of the wall, it appears that discomfort due to a cold window is not a problem. Only with the extreme of a large (all facade), cold window will any significant amount of discomfort be experienced. Although past research has indicated that warm walls do not affect comfort, we feel that additional research is warranted to evaluate the use of heat-absorbing glass in warm environments.
- c. For high-intensity radiant sources, it is recommended that solar radiation bin data be generated for a number of weather locations. The data would consist of the number of hours at particular radiation levels for various solar altitudes and azimuths. From such information, one could ascertain the effects on mean radiant temperatures in perimeter-zone spaces.
- d. Results from an annual thermal comfort analysis performed by the Solar Group at LBL using BLAST indicate that for locations such as Atlanta, Los Angeles, and New York, the most serious discomfort occurs for south-facing, clear glazing on sunny days. Such a condition in Atlanta, yields a 10-25% dissatisfaction level

during 32% of the occupancy hours. However, implementation of a shade-management strategy or changing to a more reflective glazing eliminates the discomfort. A more accurate model characterizing occupant position than the one used in the study might lead to higher values of mean radiant temperature and therefore higher levels of dissatisfaction.

## 8. References

1. ANSI/ASHRAE Standard 55-1981, p.5. 1981. "Thermal environmental conditions for human occupancy." Standard is available from ASHRAE, 1791 Tullie Circle, N.E., Atlanta, GA. 30329.
2. ASHRAE Fundamentals. 1985. ASHRAE. Atlanta, GA.
3. Berglund, L. 1978. "Mathematical models for predicting the thermal response of building occupants." ASHRAE Transactions AT-78-7A No.1.
4. Courtier, J.P., Kammerud, R., and Place, J.W. 1985. "Thermal Comfort of building occupants: a preliminary impact assessment of passive strategies." Unpublished LBL Report No. 19496, Berkeley, CA.
5. Fanger, P.O. 1970. Thermal Comfort. McGraw-Hill. New York, NY.
6. Johnson, R., Sullivan, R., Nozaki, S., Selkowitz, S., Conner, C., and Arasteh, D. 1983. "Building envelope thermal and daylighting analysis in support of recommendations to upgrade ASHRAE/IES standard 90 - final report." LBL Report No. 16770, Berkeley, CA.
7. Fanger, P.O., Banhidi, L., Olesen, B.W., and Langkilde, G. 1980. "Comfort limits for heated ceilings." ASHRAE Transactions, 86 (2) 141-156.
8. Fanger, P.O., Ipsen, B.M., Langkilde, G., Olesen, B.W., Christensen, K., and Tanabe, S. 1985. "Comfort limits for asymmetric thermal radiation." *Energy and Buildings*, 8 (1985) 225-236.
9. McIntyre, D.A. 1974. "The thermal radiation field." *Building Science*, 9 (1974) 247-262.
10. Olesen, B.W. 1985. "Local thermal discomfort." *Bruel and Kjaer Technical Note 1-1985*. Naerum, Denmark.
11. Fanger, P.O. 1986. "Radiation and discomfort." *ASHRAE Journal*, February (1986) 33-34.
12. Gagge, A.P., Rapp, G.M., and Hardy, J.D. 1967. "The effective radiant field and operative temperature necessary for comfort with radiant heating." ASHRAE

Transactions 73 (1) I.2.1.

13. Berglund, L.G. and Gagge, A.P. 1979. "Thermal comfort and radiant heat." Third National Passive Solar Conference Proceedings 260-265.
14. Arens, E., Gonzalez, R., and Berglund, L. 1986. "Thermal comfort under an extended range of environmental conditions." ASHRAE Transactions, 92 (1).
15. Olsen, A.R., Moreno, S., Deringer, J., and Watson, C.R. 1984. "Weather data for simplified energy calculation methods." PNL Report No. 5143.
16. Courtier, J.P. 1985. "Thermal comfort post-processing methodology." Technical Note 39, Lawrence Berkeley Laboratory, Berkeley, CA.
17. Courtier, J.P. 1984. "Description and utilization of the thermal comfort routine in BLAST." Technical Note 38, Lawrence Berkeley Laboratory, Berkeley, CA.

## 9. Bibliography

Berglund, L.G. 1979. "Thermal acceptability." ASHRAE Transactions DE-29-9 No.4 825-834.

Fanger, P.O. 1978. "Future research needs concerning the human response to indoor environments." ASHRAE Transactions AT-78-7A No.3.

Fanger, P.O. and Valbjorn, O. 1979. "Indoor climate." Proceedings of the First International Indoor Climate Symposium. Danish Building Research Institute, Copenhagen, Denmark.

Madsen, T.L. 1980. "Definition and measurement of local thermal discomfort parameters." ASHRAE Transactions, 86 (2) 23-33.

McNall, P.E. and Biddison, R.E. 1970. "Thermal and comfort sensations of sedentary persons exposed to asymmetric radiant fields." ASHRAE Transactions, III.2.1-III.2.14.

Olesen, B.W., Mortensen, E., Thorshauge, J., and Berg-Munch, B. 1980. "Thermal comfort in a room heated by different methods." ASHRAE Transactions, 86 (2) 34-48.

Olesen, B.W. 1982. "Thermal comfort." Bruel and Kjaer Technical Note 2-1982. Naerum, Denmark.

Rapp, G.M. and Gagge, A.P. 1967. "Configuration factors and comfort design in radiant beam heating of man by high temperature infrared sources." ASHRAE Transactions,

III.1.1-III.1.17.

Rohes, F.H., Laviana, J.E., Runbai, W., and Wruck, R. 1985. "The human response to temperature drifts in a simulated office Environment." ASHRAE Transactions 91 (1).

Rohes, F.H., Hayter, R.B., and Milliken, G. 1975. "Effective temperature (ET\*) as a predictor of thermal comfort." ASHRAE Transactions, 81 (2) 148-156.

Sherman, M. 1985. "A simplified model of thermal comfort." Energy and Buildings 8 (1985) 37-50.

Wray, W.O. 1979. "A simple procedure for assessing thermal comfort in passive solar heated buildings." LA-UR-79-1337, Los Alamos, NM.

Table A.1  
Thermal Sensation Measuring Scale

-3	cold
-2	cool
-1	slightly cool
0	neutral
1	slightly warm
2	warm
3	hot

Table A.2  
 Example of Fanger's Predicted Mean Vote  
 Activity level 1 met ( $58.3 \text{ W/m}^2$ ); Relative humidity 50%;  
 Air temperature equal MRT.

Activity Level 60 kcal/m<sup>2</sup>hr

Clothing clo	Ambient Temp. °C	Relative Velocity (m/s)									
		<0.10	0.10	0.15	0.20	0.30	0.40	0.50	1.00	1.50	
0	25.	-1.33	-1.33	-1.59	-1.92						
	26.	-0.83	-0.83	-1.11	-1.40						
	27.	-0.33	-0.33	-0.63	-0.88						
	28.	0.15	0.12	-0.14	-0.36						
	29.	0.63	0.56	0.35	0.17						
	30.	1.10	1.01	0.84	0.69						
	31.	1.57	1.47	1.34	1.24						
32.	2.03	1.93	1.85	1.78							
0.25	23.	-1.18	-1.18	-1.39	-1.61	-1.97	-2.25				
	24.	-0.79	-0.79	-1.02	-1.22	-1.54	-1.80	-2.01			
	25.	-0.42	-0.42	-0.64	-0.83	-1.11	-1.34	-1.54	-2.21		
	26.	-0.04	-0.07	-0.27	-0.43	-0.68	-0.89	-1.06	-1.65	-2.04	
	27.	0.33	0.29	0.11	-0.03	-0.25	-0.43	-0.58	-1.09	-1.43	
	28.	0.71	0.64	0.49	0.37	0.18	0.03	-0.10	-0.54	-0.82	
	29.	1.07	0.99	0.87	0.77	0.61	0.49	0.39	0.02	-0.22	
	30.	1.43	1.35	1.25	1.17	1.05	0.95	0.87	0.58	0.39	
	0.50	18.	-2.01	-2.01	-2.17	-2.38	-2.70				
		20.	-1.41	-1.41	-1.58	-1.76	-2.04	-2.25	-2.42		
22.		-0.79	-0.79	-0.97	-1.13	-1.36	-1.54	-1.69	-2.17	-2.46	
24.		-0.17	-0.20	-0.36	-0.48	-0.68	-0.83	-0.95	-1.35	-1.59	
26.		0.44	0.39	0.26	0.16	0.01	-0.11	-0.21	-0.52	-0.71	
28.		1.05	0.98	0.88	0.81	0.70	0.61	0.54	0.31	0.16	
30.		1.64	1.57	1.51	1.46	1.39	1.33	1.29	1.14	1.04	
32.	2.25	2.20	2.17	2.15	2.11	2.09	2.07	1.99	1.95		
0.75	16.	-1.77	-1.77	-1.91	-2.07	-2.31	-2.49				
	18.	-1.27	-1.27	-1.42	-1.56	-1.77	-1.93	-2.05	-2.45		
	20.	-0.77	-0.77	-0.92	-1.04	-1.23	-1.36	-1.47	-1.82	-2.02	
	22.	-0.25	-0.27	-0.40	-0.51	-0.66	-0.78	-0.87	-1.17	-1.34	
	24.	0.27	0.23	0.12	0.03	-0.10	-0.19	-0.27	-0.51	-0.65	
	26.	0.78	0.73	0.64	0.57	0.47	0.40	0.34	0.14	0.03	
	28.	1.29	1.23	1.17	1.12	1.04	0.99	0.94	0.80	0.72	
30.	1.80	1.74	1.70	1.67	1.62	1.58	1.55	1.46	1.41		
1.00	16.	-1.18	-1.18	-1.31	-1.43	-1.59	-1.72	-1.82	-2.12	-2.29	
	18.	-0.75	-0.75	-0.88	-0.98	-1.13	-1.24	-1.33	-1.59	-1.75	
	20.	-0.32	-0.33	-0.45	-0.54	-0.67	-0.76	-0.83	-1.07	-1.20	
	22.	0.13	0.10	0.00	-0.07	-0.18	-0.26	-0.32	-0.52	-0.64	
	24.	0.58	0.54	0.46	0.40	0.31	0.24	0.19	0.02	-0.07	
	26.	1.03	0.98	0.91	0.86	0.79	0.74	0.70	0.57	0.50	
	28.	1.47	1.42	1.37	1.34	1.28	1.24	1.21	1.12	1.06	
30.	1.91	1.86	1.83	1.81	1.78	1.75	1.73	1.67	1.63		
1.25	14.	-1.12	-1.12	-1.24	-1.34	-1.48	-1.58	-1.66	-1.90	-2.04	
	16.	-0.74	-0.75	-0.86	-0.95	-1.07	-1.16	-1.23	-1.45	-1.57	
	18.	-0.36	-0.38	-0.48	-0.55	-0.66	-0.74	-0.81	-1.00	-1.11	
	20.	0.02	-0.01	-0.10	-0.16	-0.26	-0.33	-0.38	-0.55	-0.64	
	22.	0.42	0.38	0.31	0.25	0.17	0.11	0.07	-0.08	-0.16	
	24.	0.81	0.77	0.71	0.66	0.60	0.55	0.51	0.39	0.33	
	26.	1.21	1.16	1.11	1.08	1.03	0.99	0.96	0.87	0.82	
28.	1.60	1.56	1.52	1.50	1.46	1.43	1.41	1.34	1.30		
1.50	12.	-1.09	-1.09	-1.19	-1.27	-1.39	-1.48	-1.55	-1.75	-1.86	
	14.	-0.75	-0.75	-0.85	-0.93	-1.03	-1.11	-1.17	-1.35	-1.45	
	16.	-0.41	-0.42	-0.51	-0.58	-0.67	-0.74	-0.79	-0.96	-1.05	
	18.	-0.06	-0.09	-0.17	-0.22	-0.31	-0.37	-0.42	-0.56	-0.64	
	20.	0.28	0.25	0.18	0.13	0.05	0.00	-0.04	-0.16	-0.23	
	22.	0.63	0.60	0.54	0.50	0.44	0.39	0.36	0.25	0.19	
	24.	0.99	0.95	0.91	0.87	0.82	0.78	0.76	0.67	0.62	
26.	1.35	1.31	1.27	1.24	1.20	1.18	1.15	1.08	1.05		

\* Reproduced by permission from Thermal Comfort by P.O. Fanger, McGraw-Hill, New York, NY, c. 1970, p. 116 (Ref. 5).

Table A. 3  
 Tabulated Data for the Example Showing Fanger's Methodology  
 Activity level 1.2 met ( $69.8 \text{ W/m}^2$ ); Clothing level 1.0 clo;  
 Relative humidity 50%; Air velocity 0.15 m/s.

Point	$\Phi_{p-g}$	$\Phi_{p-w}$	$T_g \Phi_{p-g}$	$T_w \Phi_{p-w}$	MRT	$\Delta\text{MRT}$	$\Delta\text{PMV}$
A1	.019	.981	0.0	21.582	21.582	-.418	-.050
A2	.022	.978	0.0	21.516	21.516	-.484	-.058
A3	.034	.966	0.0	21.252	21.252	-.748	-.090
A4	.037	.963	0.0	21.186	21.186	-.814	-.098
A5	.054	.946	0.0	20.812	20.812	-1.188	-.143
A6	.045	.955	0.0	21.010	21.010	-.990	-.119
B1	.020	.980	0.0	21.560	21.560	-.440	-.053
B2	.031	.969	0.0	21.318	21.318	-.682	-.082
B3	.035	.965	0.0	21.230	21.230	-.770	-.092
B4	.050	.950	0.0	20.900	20.900	-1.100	-.132
B5	.066	.934	0.0	20.548	20.548	-1.452	-.174
B6	.059	.941	0.0	20.702	20.702	-1.298	-.156

Table A.4  
 Tabulated Data for the Example on Asymmetric Radiation  
 Activity level 1.2 met ( $69.8 \text{ W/m}^2$ ); Clothing level 1.0 clo;  
 Relative humidity 50%; Air velocity 0.15 m/s.

Point	$\Phi_{e-g}$	$\Phi_{e-w}$	$T_{pr1}$	$T_g \Phi_{e-g}$	$T_w \Phi_{e-w}$	$T_{pr2}$	$\Delta T_{pr}$
A1	.054	.946	22.000	0.0	20.812	20.812	-1.188
A2	.066	.934	22.000	0.0	20.548	20.548	-1.452
A3	.095	.905	22.000	0.0	19.910	19.910	-2.090
A4	.125	.875	22.000	0.0	19.250	19.250	-2.750
A5	.136	.864	22.000	0.0	19.008	19.008	-2.992
A6	.125	.875	22.000	0.0	19.250	19.250	-2.750
B1	.049	.951	22.000	0.0	20.992	20.922	-1.078
B2	.072	.928	22.000	0.0	20.416	20.416	-1.548
B3	.117	.883	22.000	0.0	19.426	19.426	-2.574
B4	.162	.838	22.000	0.0	18.436	18.436	-3.564
B5	.195	.805	22.000	0.0	17.710	17.710	-4.290
B6	.162	.838	22.000	0.0	18.436	18.436	-3.564

Table A.5  
Comfort Meter and Pyranometer Readings

Date	Time	Room Temp °C (°F)	Oper Temp °C (°F)	MRT °C (°F)	Solar Radiation W/m <sup>2</sup> (Btu/hr-ft <sup>2</sup> )
Averaged Data					
5/8 (Th)	8:45am	21.5 (70.7)	30.0 (86.0)	38.5 (101.3)	562 (178)
5/8 (Th)	9:05am	21.5 (70.7)	31.3 (88.3)	41.1 (105.9)	588 (186)
5/10(Sat)	9:10am	25.4 (77.7)	29.6 (85.3)	33.8 ( 92.8)	588 (186)
5/10(Sat)	9:20am	23.0 (73.4)	31.8 (89.2)	40.6 (105.1)	603 (191)
5/29(Th)	9:20am	21.0 (69.8)	30.2 (86.4)	39.4 (102.9)	577 (183)
5/29(Th)	9:25am	21.0 (69.8)	31.1 (88.0)	41.2 (106.2)	596 (189)
5/29(Th)	9:30am	21.0 (69.8)	31.5 (88.7)	42.0 (107.6)	598 (190)
Average	—	22.0 (71.6)	30.8 (87.4)	39.5 (103.1)	589 (187)
Additional Data Point					
5/9 (Fri)	6:45pm	27.6 (81.7)	30.3 (86.5)	33.0 ( 91.4)	198 (63)
Unused Data					
4/26 (Sat)	8:30am	22.1 (71.8)	28.7 (83.7)	35.3 ( 95.5)	728 (231)
4/26 (Sat)	5:20pm	24.1 (75.4)	28.0 (82.4)	31.9 ( 89.4)	481 (153)
4/27 (Sun)	8:45am	22.3 (72.1)	26.3 (79.3)	30.3 ( 86.5)	642 (204)
5/9 (Fri)	6:15pm	26.1 (79.0)	26.5 (79.7)	26.9 ( 80.4)	0.0 (0.0)
5/9 (Fri)	6:30pm	28.9 (84.0)	32.1 (89.8)	35.3 ( 95.5)	438 (139)

Table A.6  
Percent Occupied Hours and Percent People Dissatisfied at  
a Particular Solar Bin Level

Solar Bin W/m <sup>2</sup> (Btu/hr-ft <sup>2</sup> )	Percent Occupied Hours	Percent Dissatisfied	Percent Dissatisfied *
North Zone			
567- (180- )	0	>76	100
473-567(150-180)	0	59-76	100
378-473(120-150)	0	43-59	70
284-378( 90-120)	0	28-43	50
189-284( 60-90 )	0	16-28	40
95-189( 30-60 )	0	7-16	20
63-95 ( 20-30 )	0	6- 7	10
32-63 ( 10-20 )	0	5- 6	10
3-32 ( 1-10 )	3	5	5
Less Than 3(1)	97	5	5
South Zone			
567- (180- )	0	>76	100
473-567(150-180)	0	59-76	100
378-473(120-150)	0	43-59	70
284-378( 90-120)	4	28-43	50
189-284( 60-90 )	9	16-28	40
95-189( 30-60 )	15	7-16	20
63-95 ( 20-30 )	5	6- 7	10
32-63 ( 10-20 )	8	5- 6	10
3-32 ( 1-10 )	20	5	5
Less Than 3(1)	38	5	5

Note: ( \* ) Conservative PPD value

Table A.7  
 Low temperature Bin Data and Resultant Radiant  
 Temperature Asymmetries and Percent Dissatisfied

Temperature Bin °C(°F)	Radiant Temperature Asymmetry °C(°F)	Percent Dissatisfied
Window to Wall Ratio = 0.59		
1.66 to 4.44(35-40)	4.01-3.58(7.22-6.44)	< 1
-1.11 to 1.66(30-35)	4.55-4.01(8.19-7.22)	< 1
-3.89 to -1.11(25-30)	5.09-4.55(9.16-8.19)	< 1
-6.67 to -3.88(20-25)	5.63-5.09(10.1-9.16)	< 1
-9.44 to -6.67(15-20)	6.18-5.63(11.1-10.1)	< 1
-12.22 to -9.44(10-15)	6.72-6.18(12.1-11.1)	< 2
-15.00 to -12.22( 5-10)	7.26-6.72(13.1-12.1)	< 2
-17.78 to -15.00( 0- 5)	7.80-7.26(14.0-13.1)	< 2
Less Than-17.78 (0)	7.80(14.0)	< 2
Window to Wall Ratio = 1.0		
1.66 to 4.44(35-40)	9.97- 8.89(17.94-16.00)	5 - 3
-1.11 to 1.66(30-35)	11.32- 9.97(20.40-17.94)	6 - 5
-3.89 to -1.11(25-30)	12.66-11.32(22.79-20.38)	10 - 6
-6.67 to -3.89(20-25)	14.01-12.66(25.22-22.79)	15 -10
-9.44 to -6.67(15-20)	15.36-14.01(27.65-25.22)	20 -15
-12.22 to -9.44(10-15)	16.71-15.36(30.07-27.65)	28 -20
-15.00 to -12.22( 5-10)	18.05-16.71(32.49-30.07)	36 -28
-17.78 to -15.00( 0- 5)	19.40-18.05(33.12-32.49)	>40 -36
Less Than -17.78 (0)	19.40(33.12)	>40

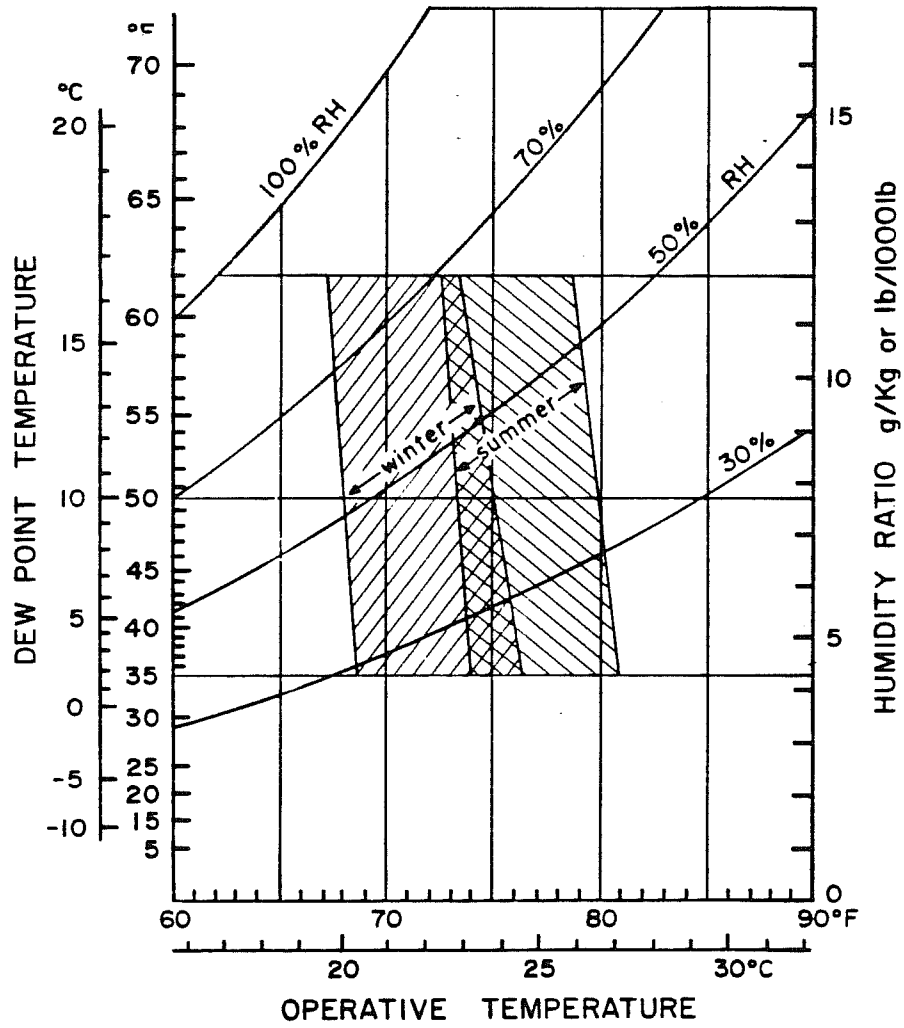


Figure A.1 Acceptable ranges of operative temperature and humidity for persons clothed in typical summer and winter clothing, at light, mainly sedentary, activity. Reprinted by permission of ASHRAE, Atlanta, GA (Ref. 1).

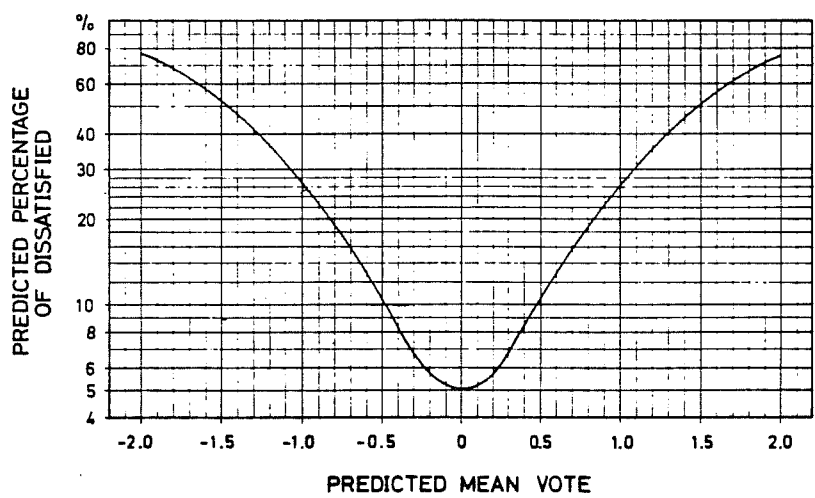


Figure A.2 Predicted percentage of dissatisfied (PPD) as a function of predicted mean vote (PMV). Reproduced from Thermal Comfort , by P.O. Fanger, McGraw-Hill, New York, NY, c. 1970, p.131 (Ref. 5).

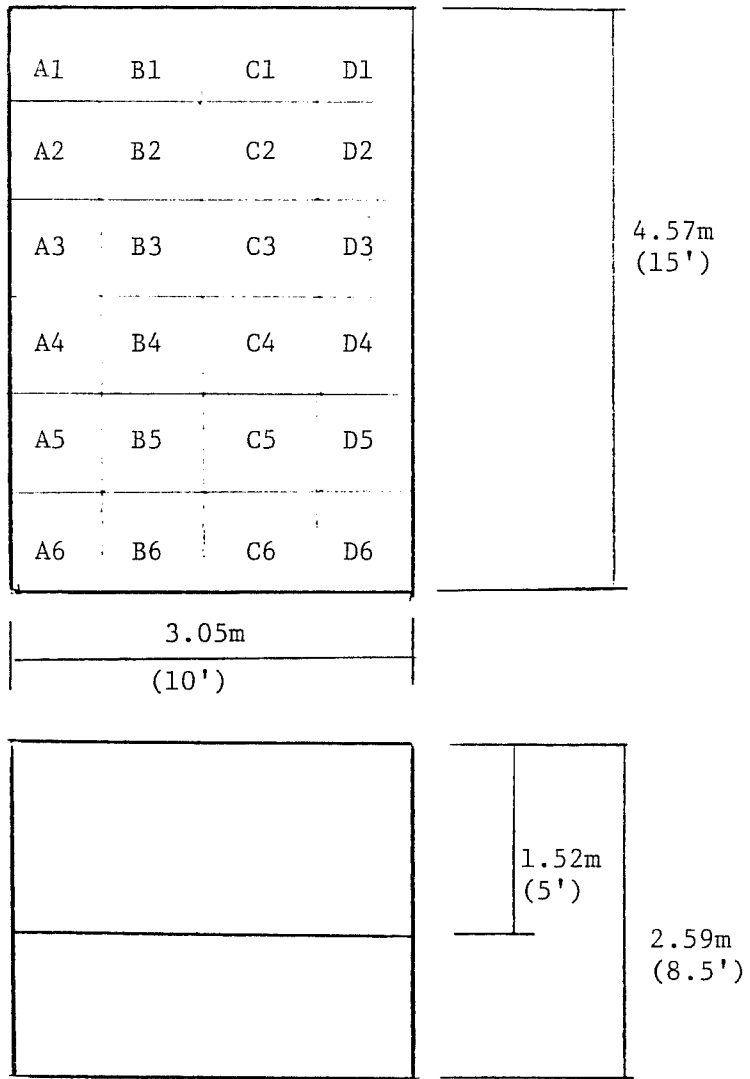


Figure A.3 Commercial office building module (Ref. 6).

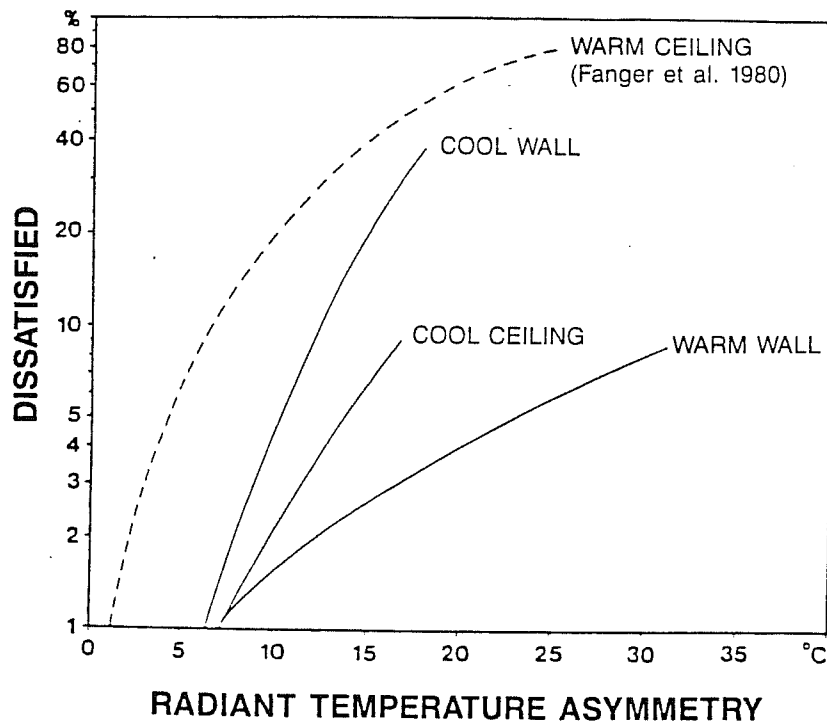
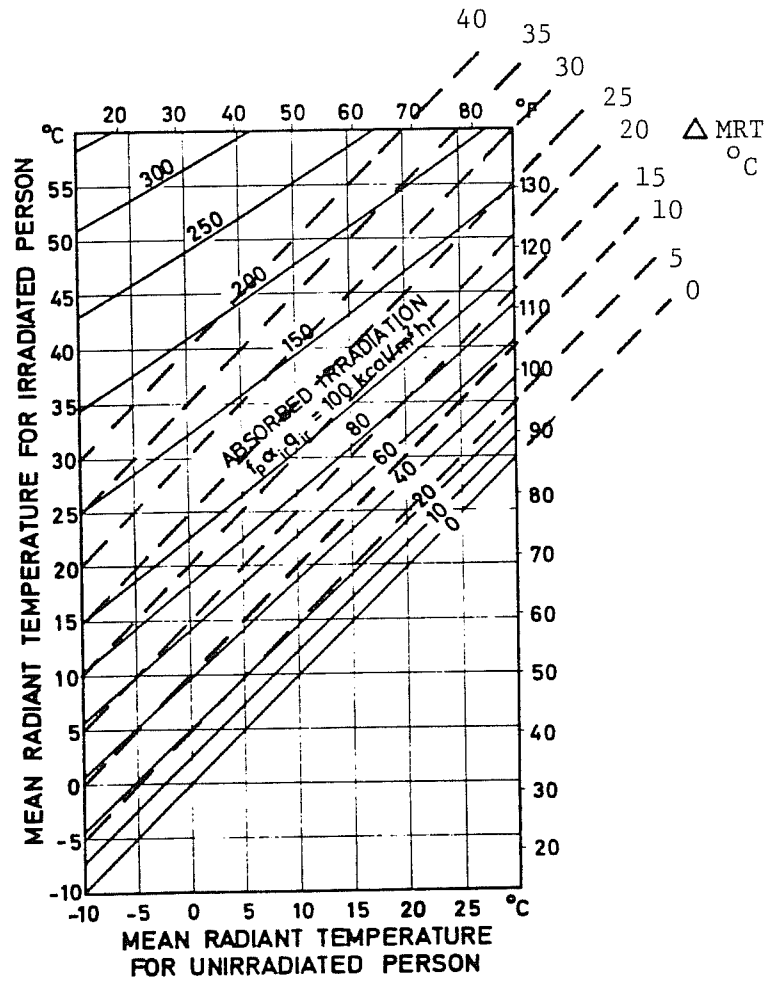


Figure A.4 Percentage of people expressing discomfort due to asymmetric radiation. Reproduced by permission from ASHRAE Journal, Feb (1986): 33-34 (Ref. 11).



$$1 \text{ kcal/hr-m}^2 \times 1.162 = 1 \text{ W/m}^2$$

$$1 \text{ W/m}^2 \times 0.3172 = 1 \text{ Btu/hr-ft}^2$$

$$1 \text{ kcal/hr-m}^2 \times 0.368 = 1 \text{ Btu/hr-ft}^2$$

Figure A.5 Diagram used to determine mean radiant temperature for a person exposed to irradiation from a high-intensity radiant source. Reproduced by permission from Thermal Comfort, by P.O. Fanger, McGraw-Hill, New York, NY, c. 1970, p. 150, (Ref. 5).

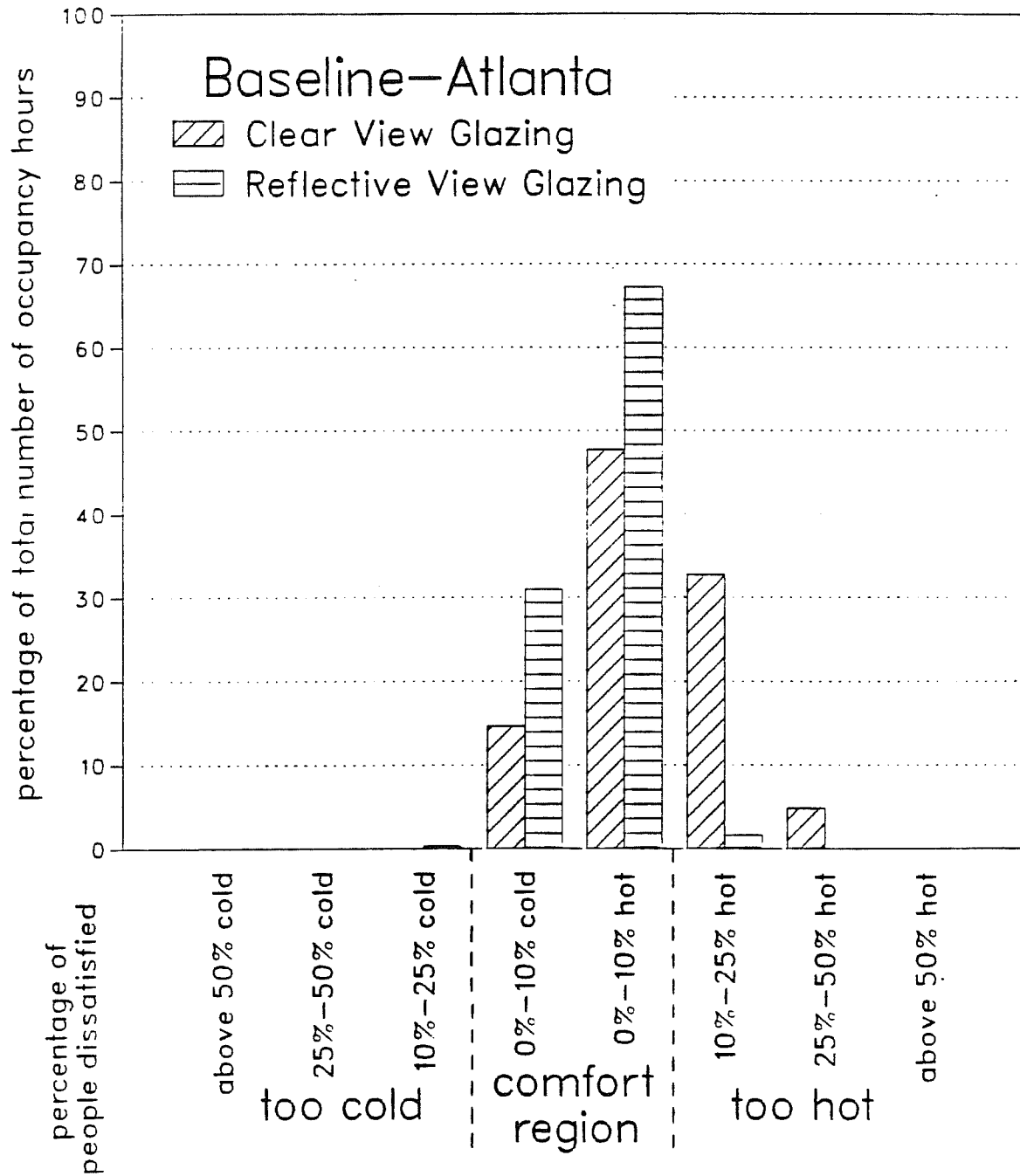


Figure A.6 Bin report of thermal comfort conditions using BLAST: comparison of clear and reflective glazing for a south zone (Ref. 4).

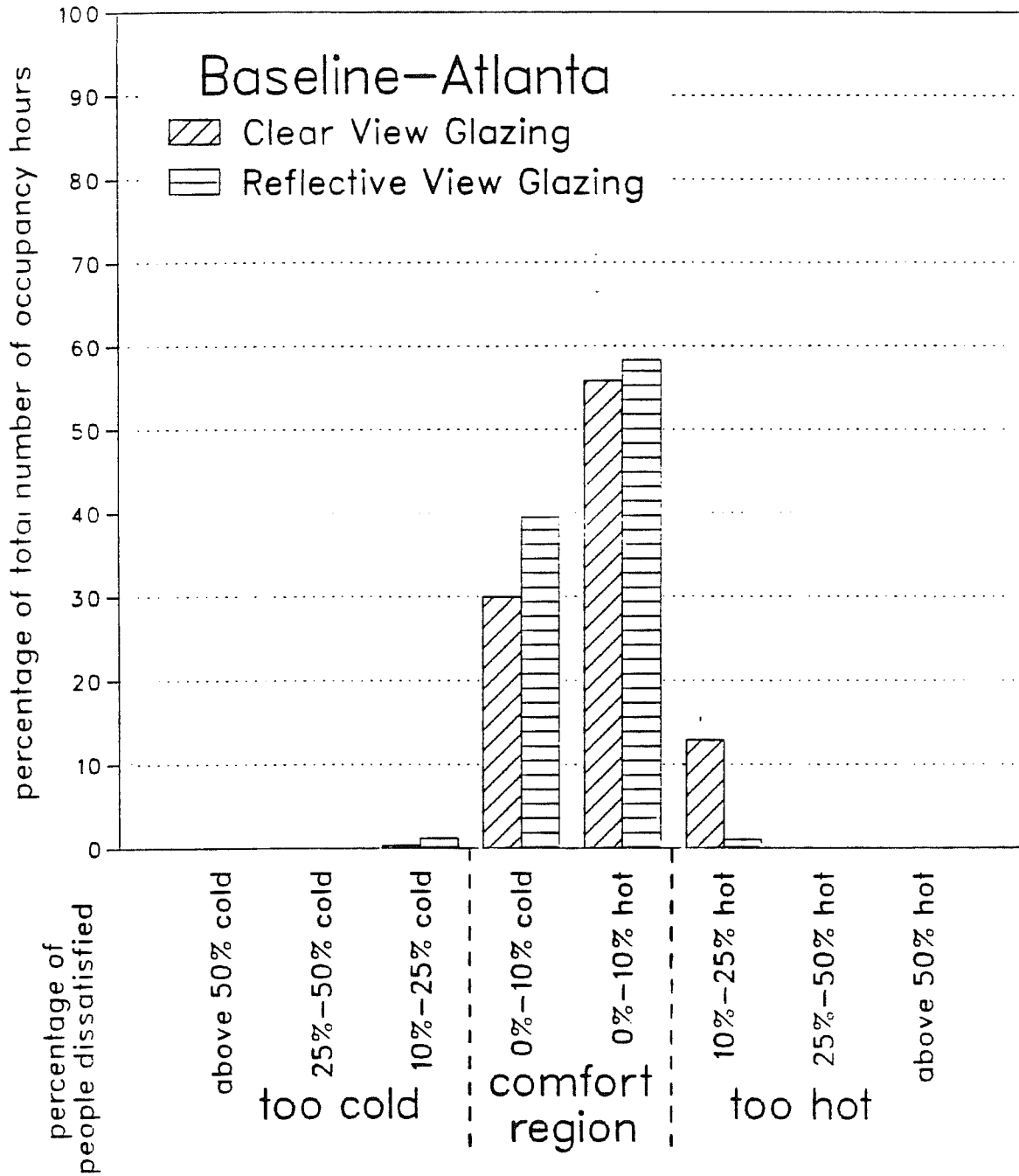


Figure A.7 Bin report of thermal comfort conditions using BLAST: comparison of clear and reflective glazing for total building (Ref. 4).

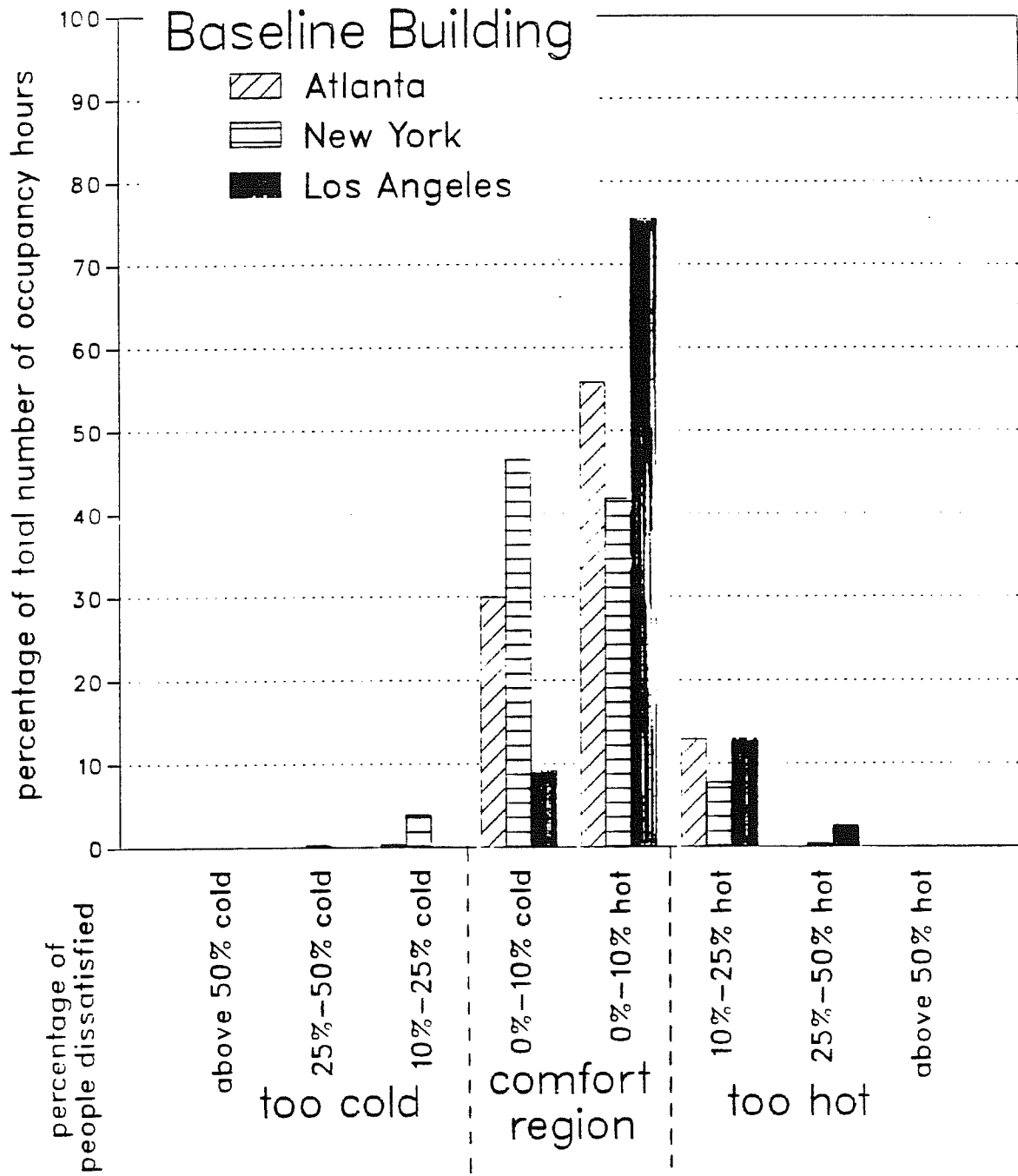


Figure A.8 Bin report of thermal comfort using BLAST: climate comparison of clear glazing for the total building (Ref. 4).

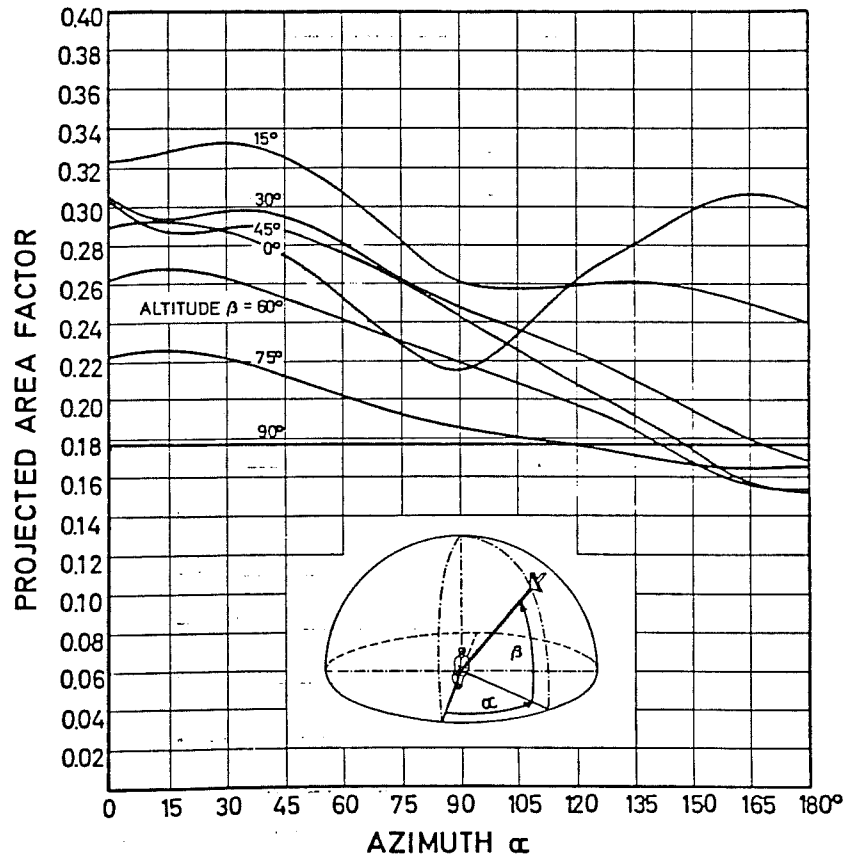


Figure A.9 Diagram used for determination of the projected area factor of a seated person as a function of source azimuth and altitude. Reproduced from Thermal Comfort, P.O. Fanger, McGraw-Hill, 1970.

## **APPENDIX B.**

### **Prototype Micro-Computer Design Tool**

The following pages are reproductions of several screens that define the method of performance of a prototype fenestration performance design tool. This program is a demonstration model and uses another computer program called DEMO from Software Garden, Inc. to simulate the actual interface between the user and the computer. Performance indicators for annual energy consumption, peak electrical demand, and thermal and visual comfort are presented as a function of geographic location, building type, orientation, and fenestration system. These indicators are then combined into a single figure of merit that can be used for evaluating and ranking alternative designs. This tool was created to give possible users insight into the functional nature of the actual program which remains to be created.



F e n e s t r a t i o n   P e r f o r m a n c e  
A n a l y s i s   P r o g r a m

This program was developed by Lawrence Berkeley Laboratory and the Florida Solar Energy Center through support provided by the Electric Power Research Institute and the New York State Energy Research and Development Administration. Project Management was provided by the Lighting Research Institute.

Any key to continue

This program is a demonstration model of a proposed commercial building fenestration performance design tool. Performance indicators for annual energy consumption, peak electrical demand, illumination quality, and thermal and visual comfort are presented as a function of geographic location, building type, orientation, and fenestration system. These indicators are then combined into a single figure of merit that can be used for evaluating and ranking alternative designs.

This is a demonstration package. Program flow will proceed only for certain selected options, namely: Madison, WI., office type building, and south orientation. These are default values and are always present unless revised.

Any key to continue

Run Options selected for analysis will be shown in this area.

---

MENU ITEMS AND OTHER INSTRUCTIONS  
WILL BE SHOWN IN THIS AREA

Any key to continue

---

Keyboard actions required will be shown in this area.

---

Main Menu
1. Load Past Runs
2. Run
3. Optimize
4. Save Run Info
5. Default Set
6. Quit

Options:

Load Past Runs - Loads past analysis runs for observation.  
Run - Normal run stream.  
Optimize - Optimization run stream.  
Save Run Info - Save run information.  
Default Set - Sets default options for future runs.  
Quit - Terminates operation.

---

Select a number, letter, or ↑↓, then Enter(Return).

---

Run Menu
1. Geographic location
2. Building type
3. Orientation
4. Fenestration systems
5. Performance indicators
6. Weighting function

Standard runs require the definition of geographic location, building type, and orientation. The fenestration systems (maximum of 4) of interest are then defined followed by selection of various performance indicators and calculation of a weighting function, if desired.

---

Select a number, letter, or ↑↓, then Enter(Return), Home for Main Menu.

---

Run Menu
1. Geographic location
2. Building type
3. Orientation
4. Fenestration systems
5. Performance indicators
6. Weighting function

Locations
1. Atlanta
2. Boston
3. Chicago
4. Cincinnati
5. Denver
6. Honolulu
7. Lake Charles
8. Los Angeles
9. Madison
A. Miami
B. Minneapolis
C. New York
D. Phoenix

---

Select a number or ↑↓, then Enter(Return).

Madison

---

Run Menu
1. Geographic location
2. Building type
3. Orientation
4. Fenestration systems
5. Performance indicators
6. Weighting function

Building Type
1. Office
2. Retail
3. Apartment

---

Select a number, letter, or ↑↓, then Enter(Return).

Madison      Office

---

P e r i m e t e r   Z o n e   D e s c r i p t i o n

Exterior Wall Area (ft <sup>2</sup> )	1000
Floor Area (ft <sup>2</sup> )	1500
Overhead Lighting Energy (W/ft <sup>2</sup> )	1.7
Desired Lighting Level (fc)	50
Daylight Control Strategy	C

Type in Zone Sizing/Lighting characteristic values.  
Daylighting control strategies are:  
N = None      C = Continuous      S=Stepped

---

Enter(Return) upon completion of input.

Run Menu
1. Geographic location
2. Building type
3. Orientation
4. Fenestration systems
5. Performance indicators
6. Weighting function

Orientation
1. North
2. South
3. East
4. West

---

Select a number, letter, or ↑↓, then Enter(Return).

Run Menu
1. Geographic location
2. Building type
3. Orientation
4. Fenestration systems
5. Performance indicators
6. Weighting function

Fenestration systems
1. Glazing options
2. Shading devices
3. Window sizing

Note:

The fenestration systems offered for analysis consist of different combinations of glazings and shading devices. Selection of menu item 1 or 2 will permit observation of parameters that characterize a particular glazing or shading device. Window sizing is defined by menu item 3.

---

Select a number, letter, or ↑↓, then Enter(Return).

Glazing Characteristics

Thk	Width	U	SC	SHG	VIS	Ct Sur	Glazing Options
1/4	-	.957	.800	.737	.804	-	1. SP Clear
1/4	-	.963	.604	.531	.453	-	2. Bronze Tinted
1/4	-	.651	.420	.321	.297	-	3. Bronze Reflective
1/4	-	.644	.650	.613	.757	2	4. Low-e Clear
1/4	1/2	.526	.610	.598	.667	-	5. DP Clear
1/4	1/2	.533	.450	.410	.376	-	6. Bronze Tinted
1/4	1/2	.419	.305	.226	.245	-	7. Bronze Reflective
1/4	1/2	.340	.420	.418	.629	3	8. Low-e Clear
1/4	1/2	.359	.510	.481	.562	-	9. TP Clear
1/4	1/2	.362	.370	.335	.317	-	A. Bronze Tinted
1/4	1/2	.308	.210	.168	.207	-	B. Bronze Reflective
1/4	1/2	.258	.350	.311	.535	4	C. Low-e Clear

Type in a maximum of four selections:  
(e.g. 1, 5, 8, B)

PgUp or PgDn to observe options, Enter(Return) for Fenestration System Menu.

Shading Characteristics

Type in a device  
for each glazing  
selected:

- 1. Sp Clr 0
- 5. DP Clr 1
- 8. DP Lowe 0
- B. TP BRef 4

SC	SHG	VIS	Shading Devices
-	-	-	0. None
.63	.60	.85	1. Venetian blind 1
.42	.54	.61	2. blind 2
.23	.35	.52	3. blind 3
.85	.86	.90	4. Diffusing shade 1
.64	.65	.80	5. shade 2
.44	.49	.50	6. shade 3
.75	.75	.80	7. Diffusing overhang 1
.60	.62	.66	8. overhang 2
.45	.47	.50	9. overhang 3

Enter(Return) upon completion of input.

Window Sizing

Glazing	Shading	Window Area(ft2)
1.SP Clr	0.None	600
5.DP Clr	1.VenBld 1	600
8.DP Lowe	0.None	600
B.TP BRef	4.DifShd 1	600

Type in window area for each glazing selected.  
If area is the same for each type glazing, use  
the Enter(Return) key.

---

Enter(Return) upon completion of input.

Run Menu
1. Geographic location
2. Building type
3. Orientation
4. Fenestration systems
5. Performance indicators
6. Weighting function

Performance Indicators
1. Fuel
2. Electric
3. Peak electric
4. Thermal comfort
5. Visual comfort
6. All of the above

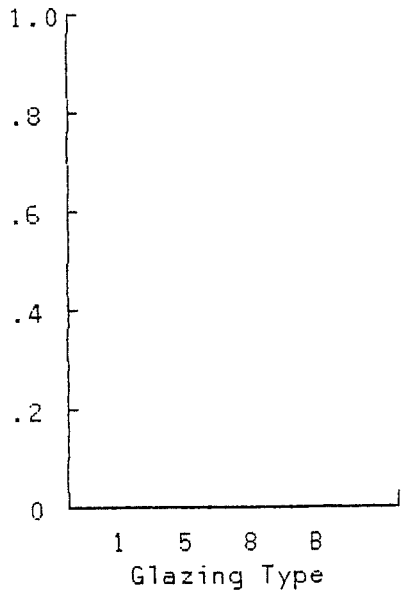
Note:

The performance indicators show the relative performance of the selected fenestration systems. An index value between 0 - 1 is used for this purpose. The value of 1 represents optimum performance.

---

Select a number, letter, or ↑↓, then Enter(Return).

Annual Fuel Index

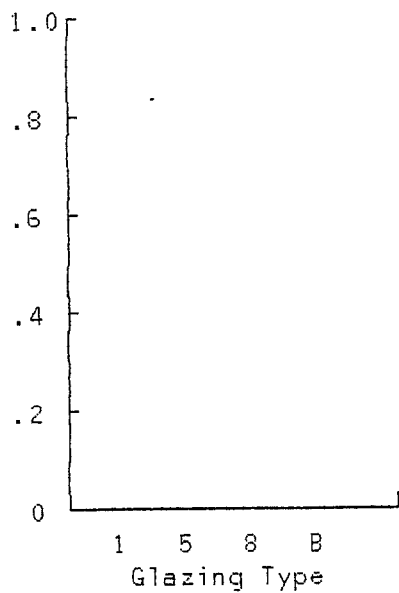


Glazing	Shading	Area	Index Value
1.SP C1r	0.None	600	.28
5.DP C1r	1.VenB1d 1	600	.86
8.DP Lowe	0.None	600	.95
B.TP BRef	4.DifShd 1	600	.64

---

PgUp or PgDn for other indices, Enter(Return) for Indicator Menu.

Annual Electric Index



Glazing	Shading	Area	Index Value
1.SP C1r	0.None	600	.08
5.DP C1r	1.VenB1d 1	600	.12
8.DP Lowe	0.None	600	.40
B.TP BRef	4.DifShd 1	600	.82

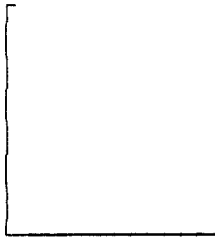
---

PgUp or PgDn for other indices, Enter(Return) for Indicator Menu.

Madison Office South Glazing(1,5,8,B) Shade(0,1,0,4)

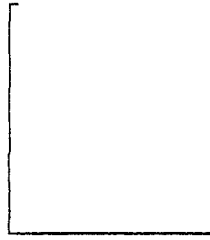
---

Fuel



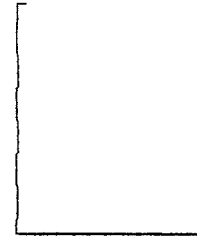
1 5 8 B

Electric



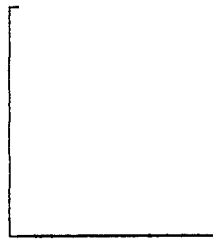
1 5 8 B

Peak



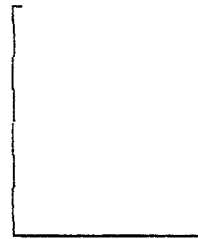
1 5 8 B

Thermal Comfort



1 5 8 B

Visual Comfort



1 5 8 B

---

PgUp or PgDn for other indices, Enter(Return) for Run Menu.

Madison Office South Glazing(1,5,8,B) Shade(0,1,0,4)

---

### W e i g h t i n g F u n c t i o n

The weighting function allows the user to independently weigh each performance indicator to determine a composite Figure of Merit, i.e.  $F = \sum(W)(I)$  where (W) is the user specified weight and (I) the particular performance indicator. For example, cost based weighting would be related to the relative cost of fuel, electricity, and peak demand. The value of (F) varies between 0 - 1 as do the values of each performance indicator. The highest value represents the best overall performance.

---

Enter(Return) to continue with weighting, ↑ for Run Menu.

Madison Office South Glazing(1,5,8,B) Shade(0,1,0,4)

---

Weighting Function		Index values			
Performance Indicator	% Weight	SP C1r	DP C1r	DP Lowe	TP BRef
Fuel	20	.28	.86	.95	.64
Electric	20	.08	.12	.40	.82
Peak electric	20	.08	.16	.42	.29
Thermal comfort	20	.85	.87	.90	.94
Visual comfort	20	.85	.87	.90	.94
Figure of Merit ▶		.43	.58	.71	.73

This table is presented as an example of evenly distributed weighting.

---

Enter(Return) to continue.

---

Madison Office South Glazing(1,5,8,B) Shade(0,1,0,4)

---

Weighting Function		Index values			
Performance Indicator	% Weight	SP C1r	DP C1r	DP Lowe	TP BRef
Fuel	30	.28	.86	.95	.64
Electric	30	.08	.12	.40	.82
Peak electric		.08	.16	.42	.29
Thermal comfort		.85	.87	.90	.94
Visual comfort		.85	.87	.90	.94
Figure of Merit ▶					

Type in weight for each performance indicator. Total must equal 100.

---

Enter(Return) upon completion of input, to Re-Do.

---

Optimization Menu
1. Geographic location
2. Building type
3. Orientation
4. Performance indicators
5. Fenestration systems

Optimization is accomplished by initially selecting the geographic location, building type, and orientation. The performance indicator (dependent variable) to be optimized is next defined, followed by the fenestration system (independent variables) that facilitates the optimization. Solution yields the four best systems.

---

Select a number, letter, or ↑↓, then Enter(Return), Home for Main Menu.

---

Optimization Menu
1. Geographic location
2. Building type
3. Orientation
4. Performance indicators
5. Fenestration systems

Locations
1. Atlanta
2. Boston
3. Chicago
4. Cincinnati
5. Denver
6. Honolulu
7. Lake Charles
8. Los Angeles
9. Madison
A. Miami
B. Minneapolis
C. New York
D. Phoenix

---

Select a number or ↑↓, then Enter(Return).

Optimization Menu
1. Geographic location
2. Building type
3. Orientation
4. Performance indicators
5. Fenestration systems

Performance Indicators
1. Fuel
2. Electric
3. Peak electric
4. Thermal comfort
5. Visual comfort
6. Simultaneous Optim

Select the performance indicator to be optimized.  
If simultaneous optimization is desired on two or more indicators, select item number 6 to perform the appropriate weighting.

---

Select a number, letter, or ↑↓, then Enter(Return).

Weighting Function	
Performance Indicator	% Weight
Fuel	50
Electric	50
Peak electric	0
Thermal comfort	0
Visual comfort	0

Type in weight for each performance indicator. Total must equal 100.

---

Enter(Return) upon completion of input.

Optimization Menu
1. Geographic location
2. Building type
3. Orientation
4. Performance indicators
5. Fenestration systems

Fenestration Systems
1. Glazing
2. Shading
3. Window area
4. Glazing/Shading
5. Glazing/Area
6. Shading/Area
7. Glazing/Shading/Area

Select the fenestration system parameters that will facilitate the optimization. The program will request information on those variables not selected.

---

Select a number or ↑↓, then Enter(Return).

Shading Characteristics

SC	SHG	VIS	Shading Devices
-	-	-	0. None
.63	.60	.85	1. Venetian blind 1
.42	.54	.61	2. blind 2
.23	.35	.52	3. blind 3
.85	.86	.90	4. Diffusing shade 1
.64	.65	.80	5. shade 2
.44	.49	.50	6. shade 3
.75	.75	.80	7. Diffusing overhang 1
.60	.62	.66	8. overhang 2
.45	.47	.50	9. overhang 3

Optimization using glazing type.  
 Type in shading device: 0  
 Type in window area:

---

Enter(Return) upon completion of input, to Re-Do.

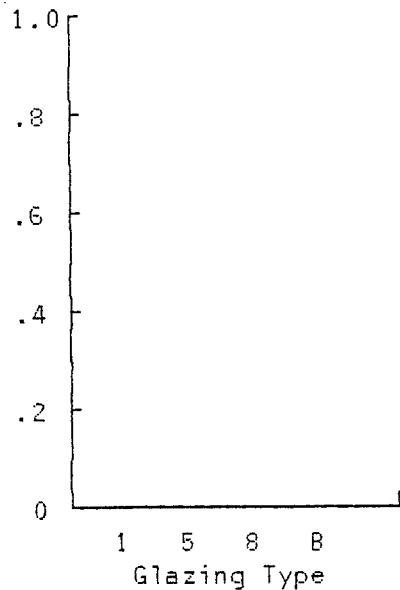
Glazing Characteristics Page 1

Thk	Width	U	SC	SHG	VIS	Ct Sur	Glazing Options
1/4	-	.957	.800	.737	.804	-	1. SP Clear
1/4	-	.963	.604	.531	.453	2	2. Bronze Tinted
1/4	-	.651	.420	.321	.297	2	3. Bronze Reflective
1/4	-	.644	.650	.613	.757	2	4. Low-e Clear
1/4	1/2	.526	.610	.598	.667	-	5. DP Clear
1/4	1/2	.533	.450	.410	.376	3	6. Bronze Tinted
1/4	1/2	.419	.305	.226	.245	3	7. Bronze Reflective
1/4	1/2	.340	.420	.418	.629	3	8. Low-e Clear
1/4	1/2	.359	.510	.481	.562	-	9. TP Clear
1/4	1/2	.362	.370	.335	.317	4	A. Bronze Tinted
1/4	1/2	.308	.210	.168	.207	4	B. Bronze Reflective
1/4	1/2	.258	.350	.311	.535	4	C. Low-e Clear

Optimization using shading device.  
 Type in glazing option:  
 Type in window area:

PgUp or PgDn for options, Enter(Return) upon completion of input, to Re-Do.

Fuel(50) Elec(50) Index



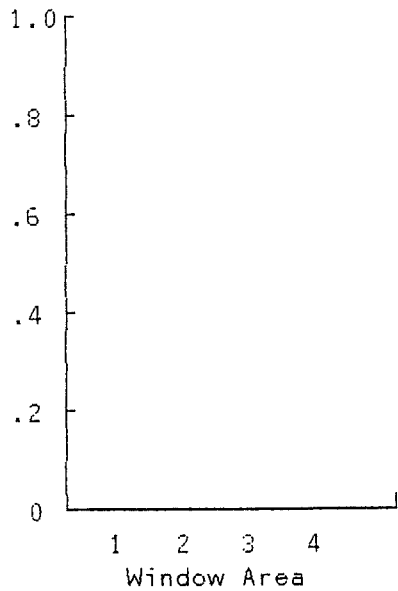
Optimization Using Glazing

Glazing	Index Value
1.SP Clr	.82
5.DP Clr	.90
8.DP Lowe	.91
B.TP BRef	.96

Shading Device: None  
 Window Area: 600 ft2

PgUp to Re-do,Enter(Return) for Optim Menu,Home for Main Menu,Ctrl-End to Stop.

Fuel(50) Elec(50) Index



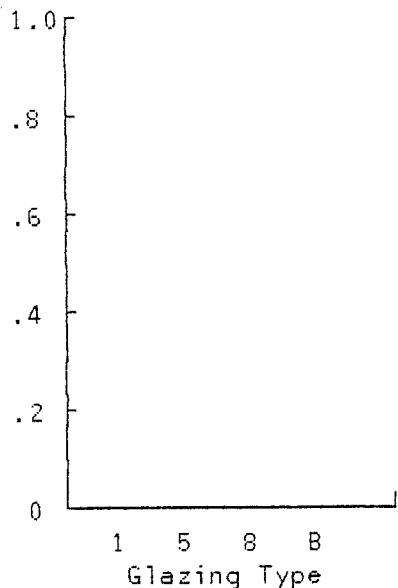
Optimization  
Using Area

Area(ft2)	Index Value
1. 425	.82
2. 450	.90
3. 475	.91
4. 500	.96

Glazing Option: DpClr  
Shading Device: None

PgUp to Re-do, Enter(Return) for Optim Menu, Home for Main Menu, Ctrl-End to Stop.

Fuel(50) Elec(50) Index



Optimization  
Using Glazing / Shading / Area

Glazing	Shading	Area	Index Value
1.SP Clr	0.None	550	.82
5.DP Clr	1.VenBld 1	575	.90
8.DP Lowe	0.None	580	.91
B.TP BRef	4.DifShd 1	585	.96

PgUp to Re-do, Enter(Return) for Optim Menu, Home for Main Menu, Ctrl-End to Stop.

L O A D

This operation allows you to load and observe past runs.

File name to load:

Type file name, Enter(Return) to load file. Home for Main Menu.

H I S T O R I C A L		S U M M A R Y			Page 1
Configuration	Run1	Run2	Run3	Run4	
Location	Madison	Madison	Madison	Madison	
Building type	Office	Office	Office	Office	
Orientation	South	South	South	South	
Fenestration system	SPClr	SPClr	DPClr	DPClr	
Areas(Window,Wall,Floor,kft)	.6,1,1.5	.6,1,1.5	.6,1,1.5	.6,1,1.5	
Overhead Lighting(W/ft2)	1.7	1.7	1.7	1.7	
Desired Lighting Level(fc)	50	50	50	50	
Daylight Control	None	None	None	None	
Performance Indicator	Index. Value - Weight (%)				
Fuel	.28-30	.15-30	.85-30	.64-30	
Electric	.10-30	.05-30	.15-30	.10-30	
Peak electric demand	.12-20	.07-20	.20-20	.15-20	
Thermal comfort	.85-10	.80-10	.90-10	.95-10	
Visual comfort	.83-10	.79-10	.88-10	.85-10	
Figure of Merit	.30	.24	.50	.34	

PgUp or PgDn for more runs, Home for Main Menu.

---

S A V E

This operation allows you to save run results.

Save in file:

---

Type file name, Enter(Return) to save file. Home for Main Menu.

---

D E F A U L T   S E T

Default set is used is set default values for future analysis when using the Run and Optimization selections in the Main Menu. Invoking this option will automatically set the default values as you proceed thru the current Run or Optimization routines.

Is this a Default Set run (Y or N):

---

Enter(Return) upon completion of input, to Re-Do.